Explorations of pulvinar circuitry in the northern greater galago (*Otolemur garnettii*)

By

Brandon Moore

Dissertation

Submitted to the Faculty of the

Graduate School of Vanderbilt University

in partial fulfillment of the requirements

for the degree of

DOCTOR OF PHILOSOPHY

in

Neuroscience

May 10, 2019

Nashville, Tennessee

Approved:

Jon H. Kaas, Ph.D.
Suzanna Herculano-Houzel, Ph.D.
Troy Hackett, Ph.D.
Karri Hoffman, Ph.D.

In loving remembrance of those long gone who shaped my scientific development:

Prof. Vivien Casagrande – You were more than my doktormutter; you were a true friend. Throughout my doctoral training process we shared many laughs, tears, and occasional moments of excited procrastination marked by spirited ranting on irrelevant and esoteric topics. May this dissertation be one that you would have been proud of.

Prof. Richard Held – You reinvigorated my love of science and sparked my interest in non-human primate research. I treasure the memories of our beer infused journal club discussions.

Dr. Val and Roger Morash – You both had sharp minds that were only rivaled by impish creativity. You were true Renaissance people whose passions inspired and challenged me whether we were solving elaborate puzzles for Mystery Hunt or preparing psychophysics stimuli.

Karissa Serrato – You were the original reason for this wild journey and are one of the forces that drive me to advance science, art, and kindness every single day.

ACKNOWLEDGEMENTS

Throughout my graduate school training, I have had the opportunity to benefit from the guidance of two talented anatomists: Prof. Vivien Casagrande and Prof. Jon Kaas. Between Prof. Casagrande's seemingly limitless knowledge of every research method and Prof. Kaas's almost superhuman ability to classify even the faintest staining tissue, I have received some of the best scientific guidance that I could have ever asked for.

I've also had the privilege of working side-by-side with some of the most wonderful, intelligent, and supportive lab mates that I could imagine. Without their tireless efforts, this dissertation would never have gotten finished. Thanks to Dr. Chia-chi Liao, Dr. Keji Li, Dr. Iwona Stepniewska, and Dr. Hui-Xin Qi. Additionally I'd like to thank my undergraduate trainees and assistants: Andrew Boal, Gabby Corona, Cesar Vargas, Sam Beloin, and Rohan Nag. Special thanks to my two lab managers Julie Mavity-Hudson and Laura Trice. Both of them were there for me whenever I needed histological staining, coverslipped slides, or solutions to any of the thousand-and-one little crises that occur every day around the lab. I'd also like to thank the animals involved in the research documented in this volume as well as the veterinary support staff of Wilson Hall that care for them; especially Mary Fertado, Dr. Troy Apple, and Dr. Carissa Jones for their assistance and expertise.

In conclusion, I'd like to thank my family and friends. Thanks to my parents for putting up with the years of stress, proofreading requests, and recondite dinner conversation. Thanks to my little sister for inspiring me with her passionate idealism and to my best friend Jessica Burris for making every day an adventure. Finally, thanks to Dr. Franklin Echevarria, Dr. Thomas Belulovich, Sarah Krell, Dr. Julianne Kreuger, and Kianoush Banaie for the years of friendship and support.

Funding for this research provided by the National Institute of Health (NIH) grants R01-EY025422, R01-EY001778 and core grants P30-EY007135, P30-HD015052. Additional support provided by Vanderbilt's Vision Research Center, Brain Institute, Electron Microscopy Core, and Departments of Psychology and Cell/Developmental Biology.

TABLE OF CONTENTS

LIST OF FIGURES

Figure **Page**

LIST OF TABLES

Table **Page**

CHAPTER 1
INTRODUCTION

The thalamus is the largest diencephalic structure and has been described as a "gateway" between the sensory periphery and cortex (Sherman, 2001). With the exception of olfaction, every instance of sensory perception is based on signals that pass through this collection of subcortical nuclei. In fact, the very act of reading this document results in sensory messages that are currently running through the reader's thalamus. This structure can be subdivided into constituent nuclei on the basis of both histological and functional properties with each nucleus classically held as being a part of the processing stream for a characteristic afferent signal type (Jones, 2007). For example, the lateral geniculate nucleus (LGN) is a part of the thalamus which primarily serves as a visual information relay between the retina and primary visual cortex (V1). The pulvinar complex contained within the thalamus stands in contrast to the LGN as one of these traditionally difficult to define areas. Much like the LGN, this complex is considered a visual thalamic area as it has vast reciprocal projections that reach throughout the visual system, however, unlike the LGN the exact role of these connections remains poorly understood. If the LGN serves as the "visual relay" of the brain then what is the pulvinar's role? Although many thalamic nuclei can be designated as cortical relay centers within the confines of this traditional paradigm (Clark, 1932, for review), the majority of thalamic activity is left unclassified (Sherman, 2007). To move toward a complete understanding of the thalamus, a more flexible functional classification paradigm must be used in which nuclei can act as more than just cortical relay centers; instead being classified by afferent and efferent projection properties.

Projections to and from the thalamus can be divided into two groups: those that drive and those that modulate. A projection is said to "drive" its target if it carries the main perceptual signal while others "modulate" this signal (Sherman and Guillery, 2006). A simplified illustration of this driver/modulator framework would be a hypothetical visually responsive neuron tuned to a specific color. A driving projection to this neuron would carry the message that light of a specific wavelength has been detected. A modulatory projection, however, would modify this main message. In the case of this hypothetical color-tuned neuron, a modulating projection could be one that gates responses based on general arousal. Although these designations are functionally defined, they have strong anatomical correlates that can be utilized for differentiation in the absence of electrophysiological recordings (Figure 1.1). The laminar location of a projection's origin or termination in cortex is the first of these anatomical properties that

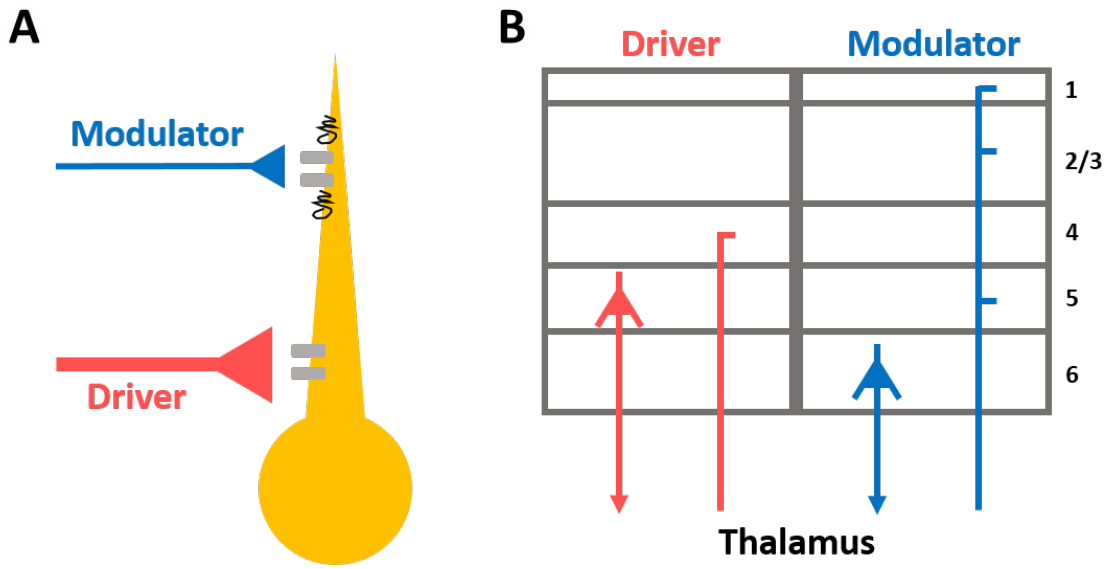

Figure 1.1: Anatomical correlates of drivers and modulators. A) Driving projections typically have large boutons that synapse on ionotropic receptors close to their target's cell body. Modulators, however, have smaller boutons that terminate on metabotropic profiles further from the cell body. B) The laminar distribution of driving and modulating projections to and from cortex. Corticothalamic driving projections originate from layer 5 while those coming from layer 6 are known to modulate thalamic activity. Thalamocortical drivers have granular terminations. Driving projections are indicated in red while modulating projections are blue.

reflect a neuron's driver/modulator designation. Corticothalamic projections originating in layer 5 are known drivers while those coming from layer 6 typically serve as modulators. Projections from the thalamus that end in cortex can be similarly segregated with drivers exhibiting granular termination sites (Marion et al., 2013). Post-synaptic receptor type can also be revealing with metabotropic receptors typically only being acted on by modulating projections (Sherman and Guillery, 1998). In addition to cortical layer information, both bouton size and position can be used as driver/modulator designation criteria with drivers typically having larger synaptic terminals that are made relatively close to the cell body of their targets compared to their smaller and more distantly terminating modulatory counterparts (Bickford, 2016).

With this driver/modulator framework in mind, thalamic nuclei can be subdivided based on their primary driving input source with higher (or second) order nuclei being driven by the cortex and first order nuclei being driven by subcortical sources (Sherman and Guillery, 2006). The LGN serves as a classic example of a first order nucleus as it relays the retina's driving input to V1. Higher order nuclei receive their driving input from cortical layer 5 and can, in turn, either drive or modulate their targets based on this input. It is important to note that these projections are of a feed-forward nature (Van Horn and

Sherman, 2004) and represent a complex but understudied set of circuitry running from cortex to thalamus back to cortex. This information processing loop is further complicated when a thalamic subdivision contains both first and higher order circuits. The pulvinar complex is one such subdivision; receiving most of its driving input from V1's layer 5 while also being driven by subcortical sources. The pulvinar's higher order visual circuit stands in stark contrast to LGN's simple relay and remains poorly understood.

First described as a cushion shaped lump of tissue resting on the dorsolateral surface of the thalamus, the pulvinar takes its name from the modernization of the Latin word for pillow (Jones, 2007). This thalamic complex stands in stark contrast to what might be implied by its namesake and remains a reputably hard structure to understand. A large proportion of pulvinar neurons are responsive to simple visual stimuli (Moore et al., 2018; Li et al., 2013) and have been proposed to play an important role in attention (Van Essen, 2005; Petersen et al., 1987) but are also implicated in more complicated information processing. The pulvinar has been depicted as relaying saccade related information between superior colliculus (SC) and cortex (Berman and Wurtz, 2011; Robinson et al., 1986; Robinson and Petersen, 1985) while also exerting a possible emotion-related effects on occulomotor control (West et al., 2011). The pulvinar additionally gates the flow of visual information within layer 1 of V1 (Purushothaman et al., 2012). Lesion studies of this thalamic complex add to the confusion by demonstrating dramatic hemineglect in some cases but barely noticeable effects in others (Wilke et al., 2010; Bender and Baizer, 1990; Bender and Butter, 1987; Leiby et al., 1982). Damage has also shown deficits in temporal discrimination/binding (Arend et al., 2008) and attentional selection (Snow et al., 2009). The pulvinar complex is implicated in a large range of functionality spanning both visual (including visuomotor) and multisensory processing, however, consensus on its functional subdivisions remains elusive with popular organization schemes proposing between 4 and 10 distinct pulvinar regions (Baldwin et al., 2017; Lyon et al., 2010; Kaas and Lyon, 2007; Gutierrez et al., 2000). The author Charlotte Brontë once mused that a ruffled mind makes a restless pillow. In kind, characterization of the thalamic pillow (pulvinar complex) remains ruffled leaving the minds of many neuroscientists quite restless.

Compared to other areas of the thalamus, the pulvinar remains poorly understood and it's proposed subdivisions lack accord. This dissertation is part of the larger effort to better understand the structure and function of this thalamic complex. More specifically, a series of tracer studies in the northern greater galago (*Otolemur garnettii*) pulvinar are described within. Galagos, like other wet-nosed strepsirrhine primates, have brains that are more phylogenetically similar to those of early primate ancestors (Figure 1.2) (Kaas and Lyon, 2007; Preuss et al., 1993; Preuss and Goldman-Rakic, 1991; Radinsky, 1975). This

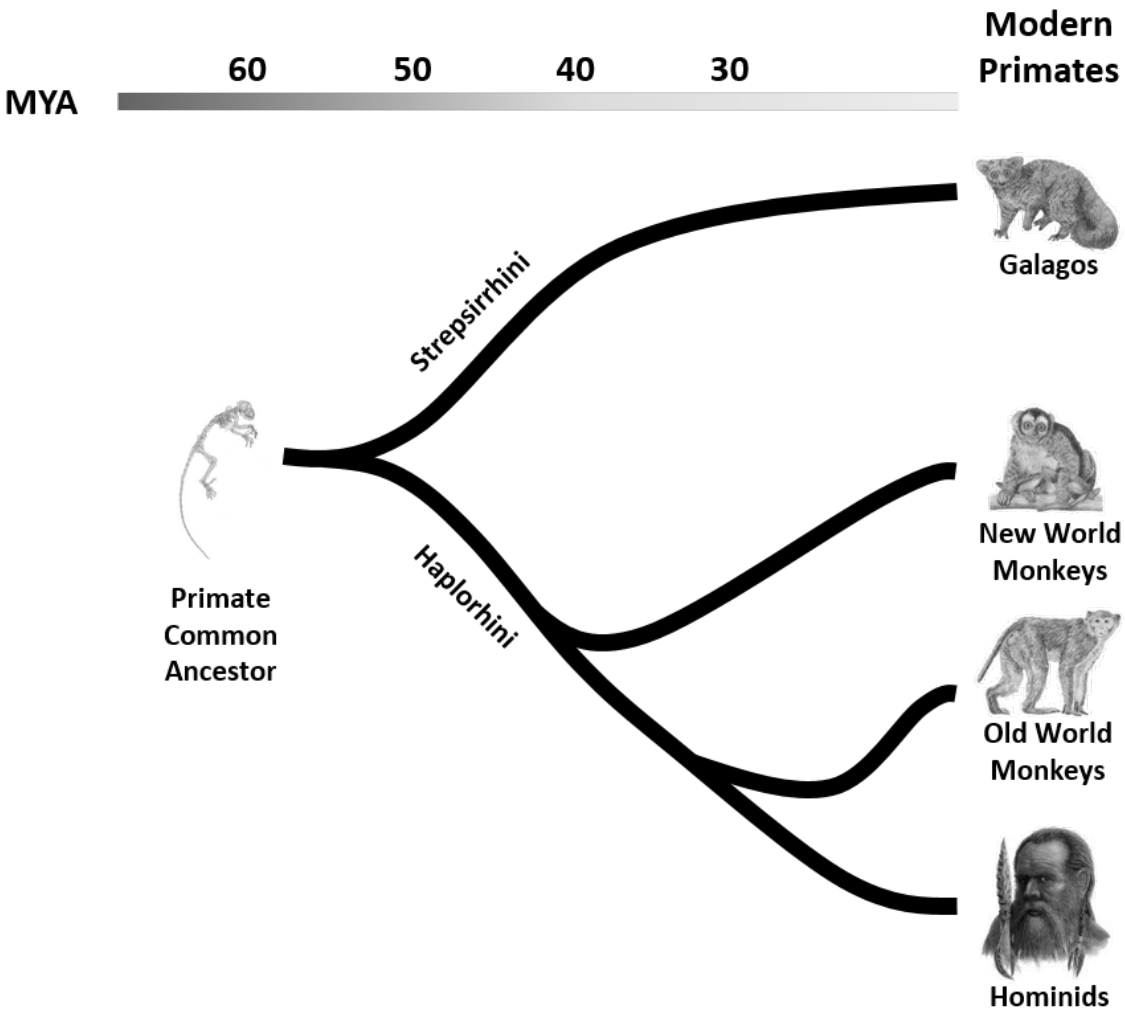

Figure 1.2: Primate cladogram. Phylogenetic tree showing relationships between primate radiations. Note the suborder split between haplorhines and strepsirrhines approximately 50mya. Unlike its dry-nosed cousins, galagos are also differentiated by their smaller brains, large olfactory bulbs, and the presence of a reflective tapetum lucidum at the back of their eyes. Primate drawings adapted from (Jameson et al., 2011).

means that advances in understanding this species could provide information on features that are common between all primates. After describing these studies, an updated model for pulvinar organization is proposed and discussed within the context of the driver/modulator framework. This model is based both on data from the aforementioned galago studies and from comparisons made to the comparatively rich macaque literature.

The next chapter (Chapter 2) reviews the connections and structure of the pulvinar complex before proposing an updated layout of its subdivisions. This review focuses primarily on macaque studies as these encompass the majority of pulvinar literature, however, comparisons with strepsirrhine primate literature are also explored. An updated model of pulvinar organization based on these reviewed anatomical and functional studies

is then presented. This model is differentiated from others in that it includes functionally distinct regions of medial pulvinar (PM) and the suspected collicular relay "shell" subdivision of lateral pulvinar (PL_s). This review concludes by proposing the pulvinar can be functionally grouped into either visual or association regions that influence cortical information processing in a parallel manner.

Galago visual pulvinar is spatially arranged in such a manner that its retinotopic maps are a seemingly dorso-ventral transposition of those observed in the macaque (Li et al., 2013; Ungerleider et al., 1983, 1984). This means that these two maps are mirrored along a central representation that separates them allowing for convenient electrophysiologically guided tracer injections at matched visuotopic locations. Chapter 3 is a published study where such injections were made (Moore et al., 2018). This study found that these two maps receive input spanning a majority of the brain's visual areas but, more interestingly, that these maps receive input from distinct populations of cells within these visually driven areas.

Felleman and Van Essen (1991) advocated for the idea of a visual processing hierarchy in which information moves up and down via feed forward or feedback projections. Sherman and Guillery (1996) extended this concept of hierarchical organization to include thalamocortical projections. Fast acting excitatory synapses that carry the main perceptual message are described as cortical drivers while all others are loosely classified as signal modulators. Although these categories are based on function, the driver/modulator framework has many anatomical correlates that can hint at a projection's role in cortex. Chapter 4 examines the role intrinsic to galago visual pulvinar within this framework with these anatomical correlates in mind. Anterograde tracer injections observed using both confocal and electron microscopy suggest that the visual pulvinar acts to differentially drive and modulate visual information depending on the cortical target.

Association pulvinar remains even less well characterized than its visual counterpart. This functional group of nuclei reciprocally projects with a wide variety of areas including auditory belt/parabelt, parietal, and frontal cortices (Cappe et al., 2009; Gutierrez et al., 2000; Yeterian and Pandya, 1985; Trojanowski and Jacobson, 1974). Chapter 5 presents galago data collected from a series of retrograde tracer injections made within these cortical areas and reflects a level of homology with the macaque literature.

A brief summary of the work presented in previous chapters is finally presented before placing these collective results in the greater context of both the galago and macaque literature. Following this summary is a proposal for an updated pulvinar subdivision scheme and a discussion on how this proposed organization hints at the pulvinar's role in processing sensory information in parallel with cortex. This dissertation

concludes with an appendix containing an electrophysiological atlas informed by previously described neural activity (Moore et al., 2018; Li et al., 2013; Marion et al., 2013) in LGN and visual pulvinar.

References

Arend, I., Rafal, R., and Ward, R. (2008). Spatial and temporal deficits are regionally dissociable in patients with pulvinar lesions. *Brain*, 131(8):2140–2152.

Baldwin, M. K., Balaram, P., and Kaas, J. H. (2017). The evolution and functions of nuclei of the visual pulvinar in primates. *Journal of Comparative Neurology*, 525(15):3207–3226.

Bender, D. B. and Baizer, J. S. (1990). Saccadic eye movements following kainic acid lesions of the pulvinar in monkeys. *Experimental Brain Research*, 79(3):467–478.

Bender, D. B. and Butter, C. M. (1987). Comparison of the effects of superior colliculus and pulvinar lesions on visual search and tachistoscopic pattern discrimination in monkeys. *Exp Brain Res*, 69:140–154.

Berman, R. A. and Wurtz, R. H. (2011). Signals conveyed in the pulvinar pathway from superior colliculus to cortical area MT. *The Journal of neuroscience : the official journal of the Society for Neuroscience*, 31(2):373–84.

Bickford, M. E. (2016). Thalamic Circuit Diversity: Modulation of the Driver/Modulator Framework. *Frontiers in Neural Circuits*, 9(January):1–8.

Cappe, C., Morel, A., Barone, P., and Rouiller, E. M. (2009). The thalamocortical projection systems in primate: An anatomical support for multisensory and sensorimotor interplay. *Cerebral Cortex*, 19(9):2025–2037.

Clark, L. (1932). The structure and connections of the thalamus. *Brain*, 55(3):406–470.

Felleman, D. J. and Van Essen, D. C. (1991). Distributed hierarchical processing in the primate cerebral cortex. *Cerebral cortex (New York, N.Y. : 1991)*, 1:1–47.

Gutierrez, C., Cola, M. G., Seltzer, B., and Cusick, C. (2000). Neurochemical and connectional organization of the dorsal pulvinar complex in monkeys. *Journal of Comparative Neurology*, 419(1):61–86.

Jameson, N. M., Hou, Z. C., Sterner, K. N., Weckle, A., Goodman, M., Steiper, M. E., and Wildman, D. E. (2011). Genomic data reject the hypothesis of a prosimian primate clade. *Journal of Human Evolution*, 61(3):295–305.

Jones, E. G. (2007). *The Thalamus*. Cambridge University Press, Cambridge, UK, 2 edition.

Kaas, J. H. and Lyon, D. C. (2007). Pulvinar contributions to the dorsal and ventral streams of visual processing in primates. *Brain Research Reviews*, 55(2 SPEC. ISS.):285–296.

Leiby, C. C., Bender, D. B., and Butter, C. M. (1982). Localization and detection of visual stimuli in monkeys with pulvinar lesions. *Experimental brain research*, 48(3):449–54.

Li, K., Patel, J., Purushothaman, G., Marion, R. T., and Casagrande, V. A. (2013). Retinotopic maps in the pulvinar of bush baby (Otolemur garnettii). *Journal of Comparative Neurology*, 521(15):3432–3450.

Lyon, D. C., Nassi, J. J., and Callaway, E. M. (2010). A Disynaptic Relay from Superior Colliculus to Dorsal Stream Visual Cortex in Macaque Monkey. *Neuron*, 65(2):270–279.

Marion, R., Li, K., Purushothaman, G., Jiang, Y., and Casagrande, V. A. (2013). Morphological and neurochemical comparisons between pulvinar and V1 projections to V2. *Journal of Comparative Neurology*, 521(4):813–832.

Moore, B., Li, K., Kaas, J. H., Liao, C.-C., Boal, A. M., Mavity-Hudson, J., and Casagrande, V. (2018). Cortical projections to the two retinotopic maps of primate pulvinar are distinct. *Journal of Comparative Neurology*.

Petersen, S. E., Robinson, D. L., and Morris, J. D. (1987). Contributions of the pulvinar to visual spatial attention. *Neuropsychologia*, 25(1 PART 1):97–105.

Preuss, T. M., Beck, P. D., and Kaas, J. H. (1993). Areal, modular, and connectional organization of visual cortex in a prosimian primate, the slow loris (Nycticebus coucang). *Brain, behavior and evolution*, 42(6):321–335.

Preuss, T. M. and Goldman-Rakic, P. S. (1991). Architectonics of the parietal and temporal association cortex in the strepsirhine primate Galago compared to the anthropoid primate Macaca. *The Journal of comparative neurology*, 310(4):475–506.

Purushothaman, G., Marion, R., Li, K., and Casagrande, V. a. (2012). Gating and control of primary visual cortex by pulvinar. *Nature Neuroscience*, 15(6):905–912.

Radinsky, L. (1975). Primate brain evolution. *American scientist*, 63(6):656–63.

Robinson, D. L. and Petersen, S. E. (1985). Responses of pulvinar neurons to real and self-induced stimulus movement. *Brain Research*, 338(2):392–394.

Robinson, D. L., Petersen, S. E., and Keys, W. (1986). Saccade-related and visual activities in the pulvinar nuclei of the behaving rhesus monkey. *Experimental Brain Research*, 62(3):625–634.

Sherman, S. M. (2001). A wake-up call from the thalamus. *Nature neuroscience*, 4(4):344–6.

Sherman, S. M. (2007). The thalamus is more than just a relay. *Current Opinion in Neurobiology*, 17(4):417–422.

Sherman, S. M. and Guillery, R. W. (1996). Functional organization of thalamocortical relays. *Journal of neurophysiology*, 76(3):1367–95.

Sherman, S. M. and Guillery, R. W. (1998). On the actions that one nerve cell can have on another: distinguishing "drivers" from "modulators". *Proceedings of the National Academy of Sciences of the United States of America*, 95(12):7121–7126.

Sherman, S. M. and Guillery, R. W. (2006). *Exploring the thalamus and its role in cortical function*. MIT Press, Cambridge, MA, 2 edition.

Snow, J. C., Allen, H. A., Rafal, R. D., and Humphreys, G. W. (2009). Impaired attentional selection following lesions to human pulvinar: evidence for homology between human and monkey. *Proceedings of the National Academy of Sciences of the United States of America*, 106(10):4054–9.

Trojanowski, J. Q. and Jacobson, S. (1974). Medial pulvinar afferents to frontal eye fields in rhesus monkey demonstrated by horseradish peroxidase. *Brain Research*, 80(3):395–411.

Ungerleider, L., Galkin, T., and Mishkin, M. (1983). Visuotopic organization of projections from striate cortex to inferior and lateral pulvinar in rhesus monkey. *Journal of Comparative Neurology*, 217(2):137–157.

Ungerleider, L. G., Desimone, R., Galkin, T. W., and Mishkin, M. (1984). Subcortical projections of area MT in the macaque. *The Journal of comparative neurology*, 223(3):368–386.

Van Essen, D. C. (2005). Corticocortical and thalamocortical information flow in the primate visual system. *Progress in Brain Research*, 149(4):173–185.

Van Horn, S. C. and Sherman, S. M. (2004). Differences in projection patterns between large and small corticothalamic terminals. *Journal of Comparative Neurology*, 475(3):406–415.

West, G. L., Al-Aidroos, N., Susskind, J., and Pratt, J. (2011). Emotion and action: The effect of fear on saccadic performance. *Experimental Brain Research*, 209(1):153–158.

Wilke, M., Turchi, J., Smith, K., Mishkin, M., and Leopold, D. A. (2010). Pulvinar Inactivation Disrupts Selection of Movement Plans. *Journal of Neuroscience*, 30(25):8650–8659.

Yeterian, E. H. and Pandya, D. N. (1985). Corticothalamic connections of the posterior parietal cortex in the rhesus monkey. *J. Comp. Neurol.*, 237(3):408–426.

CHAPTER 2
THE PULVINAR IS A HIERARCHICAL COMPLEX OF HIGHER ORDER THALAMIC NUCLEI

The pulvinar is traditionally considered the largest nucleus of the primate thalamus, however, relatively little is known about it compared to other thalamic structures. Lending to the complexity of studying this area is a lack of consensus on nomenclature and architectonic boundaries. This review describes the structure and connections of the primate pulvinar in the context of function to propose a modern model of pulvinar organization by which this area is to be considered a complex of several distinct but related hierarchical nuclei rather than monolithic.

Introduction

While the pulvinar complex is a rather large proportion of the thalamus, a general consensus on it's subdivisions and functionality remains elusive. The nature of this thalamic complex has even recently been described as "mysterious" and "enigmatic" (see Bridge et al., 2016; Vanni et al., 2015; Fischer and Whitney, 2012, for similar sentiments). This confusion is only compounded by decades of inconsistent nomenclature resulting from the misconceptualization of the pulvinar as a unified nucleus exhibiting a single function. Contrary to the idea of a monolithic pulvinar is a body of work implicating this thalamic complex in a wide range of functionality including (but not limited to) attention (Smith et al., 2009; Bender and Youakim, 2001; Desimone et al., 1990), saccadic eye movements (Bender and Butter, 1987; Ungerleider and Christensen, 1979), spatial vision (Fischer and Whitney, 2009; Petersen et al., 1987; Rafal and Posner, 1987), and the gating of sensory cortex (Purushothaman et al., 2012). It is extremely unlikely that such a range of function would emerge from a single nucleus.

Here we propose that the pulvinar complex is comprised of separate higher order thalamic nuclei each falling within the rough hierarchy of their respective cortical circuits. Given that the vast majority of relevant experiments have been performed using macaque monkeys as a model organism, we focus on this species unless otherwise specified. This proposal begins with a review of the architectonic literature using the pulvinar's traditional subdivisions as a rough organizational guide. After this review, we discuss the response properties and perceptual correlates of major functional modules within the pulvinar complex. A detailed outline of both input and output connectivity is then explored before

briefly before being compared to the connections found in primates of the well studied Strepsirrhine suborder.

The overarching question of "What does the pulvinar do?" continues to remain unanswered. Attempts at answering this question often make the presupposition that the pulvinar complex is a single nucleus with either one or a series of related functions, however, current research demonstrates that this is unlikely. With this in mind, we find it necessary to compile a comprehensive review on the structure and function of the pulvinar if only to bring more awareness to this understudied thalamic complex.

Structural organization

Early attempts at a coherent pulvinar subdivision arrangement were based on cell composition and fiber pattern properties visualized by Nissl and myelin staining (Walker, 1938; Olszewski, 1952). A more nuanced understanding of pulvinar architectonic boundaries has been formed in the time since these studies were first conducted. The following discussion begins with an overview of the traditional histologically based subdivisions of the pulvinar complex before examining more contemporary organizational schemes.

Traditional subdivisions

Nissl stained sections of the pulvinar exhibit clear architectonic borders (Figure 2.1). This complex was originally subdivided into three nuclei: lateral (PL), inferior (PI), and medial (PM) (Walker, 1938). The pulvinar was originally described as populated by cells that are "lightly-stained, medium sized, multipolar, and plump" (Olszewski, 1952). This is generally true, however, some architectonic properties specific to each of the three traditional pulvinar subdivisions should be noted.

PM is located dorso-medially and forms a large proportion of the pulvinar's posterior surface; overlying and fusing with the anterior portion of the midbrain at its rostral end (Walker, 1938). This region's small, pale staining cells are fairly evenly dispersed resulting in a somewhat homogenous distribution that is sparsely penetrated by passing fiber bundles (Jones, 2007).

PL is dorso-laterally situated, lying posterior to the ventral posterior (VP) and lateral posterior (LP) thalamic nuclei. This subdivision features cells that are comparable in size to those in PM without the high level of homogeneity. Instead, the cell population is broken up by dense fiber bundles of the corticotectal tract that run horizontally as they traverse the pulvinar (Jones, 2007). At its most rostral point, this region extends below the

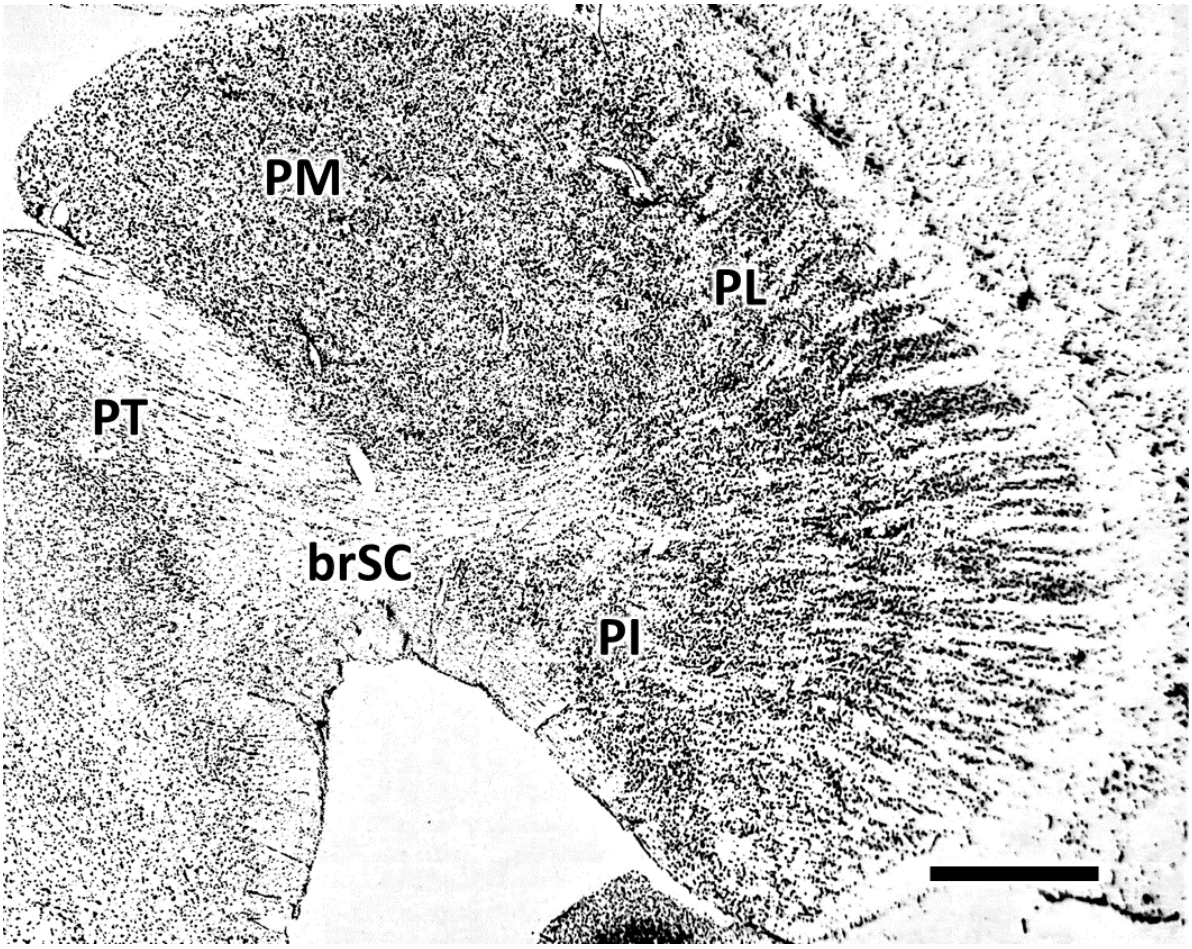

Figure 2.1: Nissl staining shows macaque pulvinar subdivisions. Nissl staining in the coronal plane uncovers the macaque pulvinar's three traditional subdivisions: PI, PL, and PM. PT= pretectal area, brSC = brachium of the superior colliculus, PI = inferior pulvinar, PL = lateral pulvinar, PM = medial pulvinar. Scale bar = 1mm. Adapted from (Jones, 2007).

brachium of the superior colliculus (brSC) enveloping PI at its lateral, ventral, and caudal ends (Walker, 1938).

PI is dorso-medially bounded by PM and is infiltrated by the brSC which medio-laterally traverses almost the entirety of the region's dorsal tip. The mostly small, dark staining, and tightly packed cells of this subdivision fall anteriorly between the medial (MGN) and lateral geniculate nuclei (LGN) (Olszewski, 1952).

Nissl staining is a valuable tool for dividing the pulvinar complex into its component nuclei, however, these traditional boundaries fail to account for other cytoarchitectural properties or functional correlates. More contemporary methods of subdivision attempt to mitigate these issues through a combination of immunohistochemisty and electrophysiological recordings (Figure 2.2).

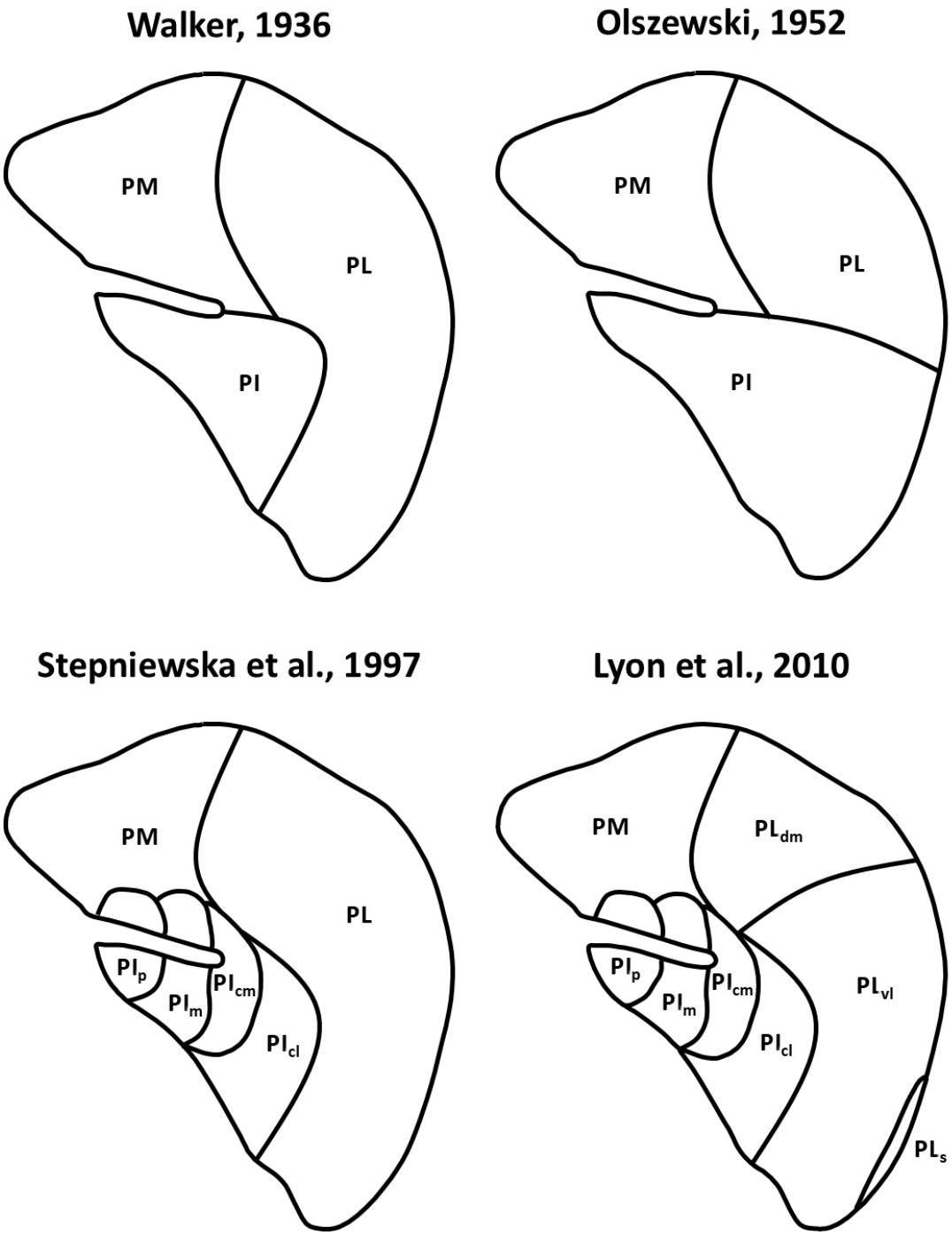

Figure 2.2: Visual comparison of pulvinar subdivision models. The placement of anatomical borders within the pulvinar complex has been historically contentious. Although the earliest attempts at subdividing this thalamic complex have large discrepancies, more modern models have begun to converge on a consistent layout. PI = inferior pulvinar, PL = lateral pulvinar, PM = medial pulvinar, PI = inferior pulvinar, PL = lateral pulvinar, PM_m = medial PM, PM_d = dorsal PM, PM_v = ventral PM, PL_{dm} = dorso-medial PL, PL_{vl} = ventro-lateral PL, PL_s = "shell" of PL, PI_p = posterior PI, PI_m = medial PI, PI_{cm} = centro-medial PI, PI_{cl} = centro-lateral PI. Adapted from (Baldwin et al., 2017).

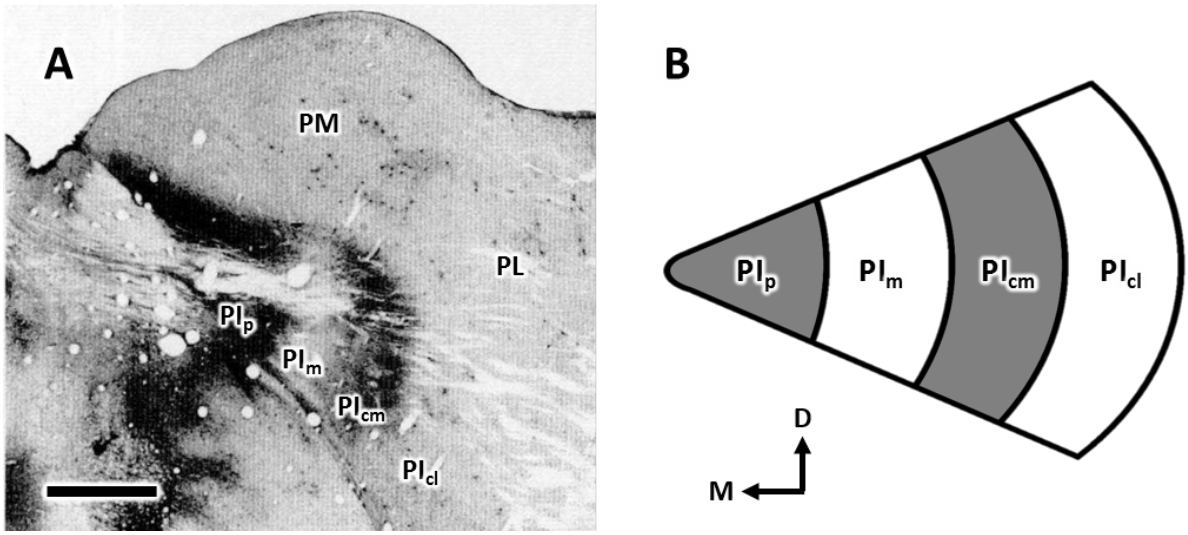

Figure 2.3: Immunostaining reveals PI subdivisions. A) The distribution of calbindin (CB) in coronally cut macaque pulvinar. PI is clearly differentiable into four different subdivisions: PI_p, PI_m, PI_{cm}, and PI_{cl}. Note that PI extends across brSC and has a clear border on the ventral edge of PM. Scale bar = 1mm. B) Diagram representation of PI. Shaded bands indicate CB-dense regions: PI_p and PI_{cm}. PI = inferior pulvinar, PL = lateral pulvinar, PM = medial pulvinar, PI_p = posterior PI, PI_m = medial PI, PI_{cm} = central medial PI, PI_{cl} = central lateral PI. Adapted from (Stepniewska and Kaas, 1997).

PI and ventro-lateral PL

The small tightly packed cells within PI can be further differentiated by staining for CB (Figure 2.3). This staining reveals four clear subdivisions: a CB-poor core on the medial side, two darkly stained areas flanking this core on the medial and lateral sides, and an additional lightly stained region on the lateral side. From medial to lateral, these subdivisions are: posterior (PI_p), medial (PI_m), central medial (PI_{cm}), and central lateral (PI_{cl}). Parvalbumin (PV) staining reveals a complimentary pattern to that revealed by CB immunostaining (Stepniewska and Kaas, 1997).

Three retinotopic maps have been observed that includes most of PI and the ventro-lateral portion of PL (PL_{vl}): P1, P2, and P3 (Figure 2.4). Pulvinar retinotopy was first observed during single and multiunit mapping(Bender, 1981), refined based on the anterograde tracing of reciprocal connections with middle temporal cortex (MT) (Ungerleider et al., 1984), and confirmed via electrophysiology (Petersen et al., 1985). P1 spans PI_{cl}, possesses central visual representation along the medial edge of PL_{vl}, and an upper to lower visual field retinotopy running from ventro-lateral to dorso-medial PI_{cl}. P2 falls within PL_{vl} just laterally to P1 and surrounds it at its ventral and dorsal borders. This map falls within a fiber-rich portion of PL and is differentiable with CB staining (Gray et al., 1999). Although these maps occur within two different traditional pulvinar subdivisions, both P1 and P2 share a vertical meridian representation while connecting to

similar cortical and subcortical targets (Ungerleider et al., 2014; Kaas and Lyon, 2007). Much like P1 and P2, P3 has a retinotopic connection pattern with MT albeit one that is sparser (Ungerleider et al., 1984). This map coincides chemoarchitectonically with PI_m (Adams et al., 2000) as it stains heavily for PV and cytochrome oxidase (CO) but lightly for CB (Cusick et al., 1993).

A converging body of evidence suggests the existence of a ventro-laterally situated "shell" region (PL_s) identified by its thick fiber bundles and dark CB staining (Lyon et al., 2010; Adams et al., 2000; Gutierrez et al., 1995). The properties of this region are generally disagreed upon as CO and CB staining have not been consistent between studies (Adams et al., 2000; Gray et al., 1999; Stepniewska and Kaas, 1997; Gutierrez et al., 1995; Lysakowski et al., 1986), however, electrophysiology and tracer injection studies provide strong evidence for PL_s. This pulvinar "shell" densely projects to both MT and the third visual area (V3) (Lyon et al., 2010; Shipp, 2001) while receiving input from the superior colliculus (SC) (Lysakowski et al., 1986; Benevento and Standage, 1983). PL_s's role as an SC relay to MT has been confirmed electrophysiologically (Berman and Wurtz, 2011, 2010).

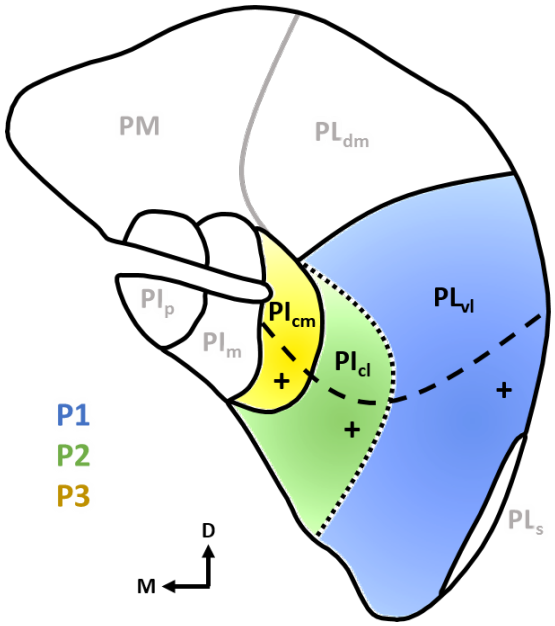

Figure 2.4: PL/PI retinotopy. Dashed line represents the horizontal meridian while dotted line is both the lateral boundary of PI and the vertical meridian. Upper visual field representation indicated by "+". Retinotopic maps P1, P2, and P3 respectively shaded blue, green, and yellow. PI_p = posterior PI, PI_m = medial PI, PI_{cm} = central medial PI, PI_{cl} = central lateral PI, PL_{vl} = ventro-lateral PL.

PM and dorso-medial PL

Boundary demarcation within PM as well as between this subdivision and dorso-medial PL (PL_{dm}) remains poorly characterized as PM's cytoarchitecture is fairly homogeneous (Ma et al., 1998). Despite this apparent homogeneity, tissue staining reveals some subtle characterizations (Figure 2.5). The lateral PM (PM_l) stains moderately for AChE and lightly for CB while medial PM (PM_m) exhibits the inverse of this pattern; staining moderately for CB and only lightly for AChE. Within PM_m there is additionally an AChE-dense, CB-poor patch that we refer to here as PM_c (Gutierrez et al., 2000).

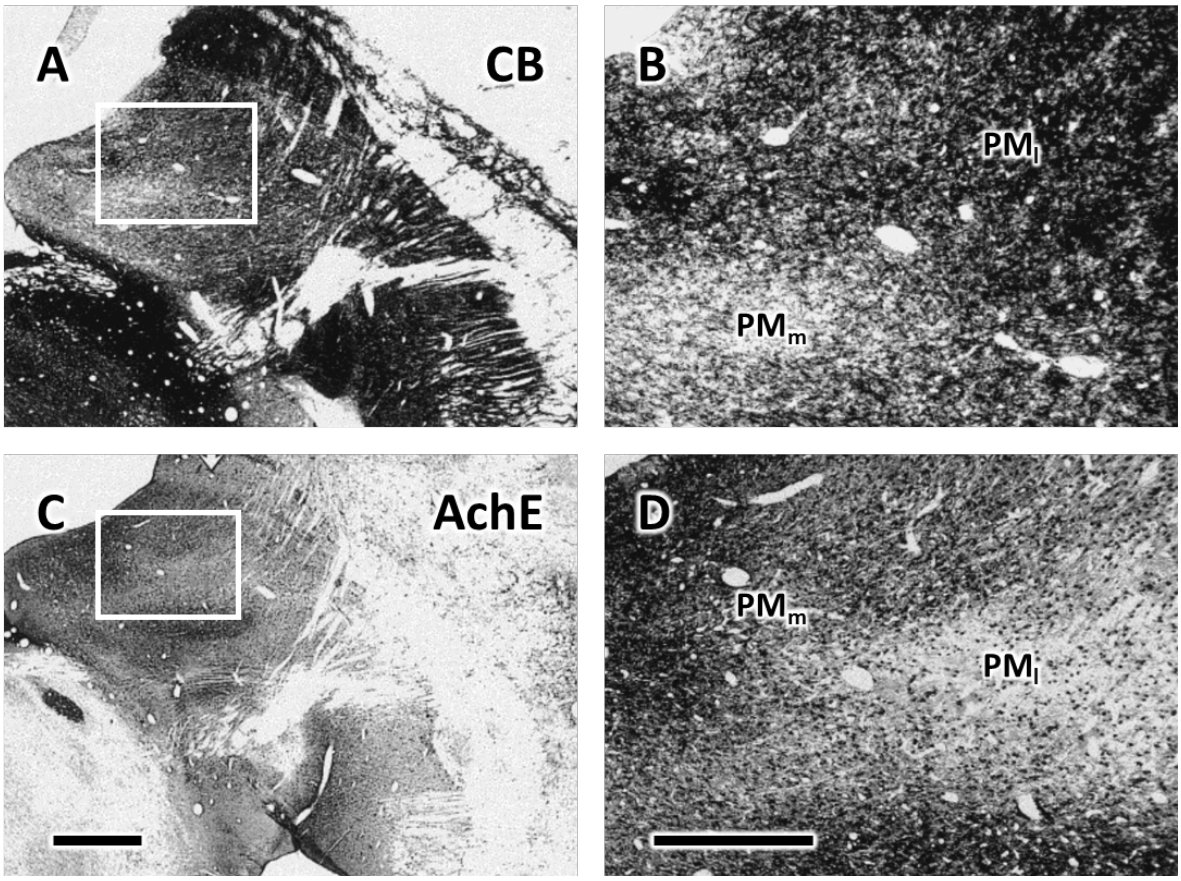

Figure 2.5: PM's chemoarchitecture reveals a medio-lateral division. White boxes indicate location where high magnification images were taken. All images taken along a coronal plane. A) PM's CB immunoreactivity. B) Higher magnification image of A's white bounded area. The darkly stained PM_l stands in contrast to PM_m. C) PM's AchE immunoreactivity. D) Higher magnification image of B's white bounded area. The darkly stained PM_m exhibits a subtle differentiation from PM_l. CB = calbindin, AchE = acetylcholinesterase, PM_m = medial PM, PM_l = lateral PM. Adapted from Gutierrez et al. (2000).

Although clear architectonic borders do not exist in PM (barring PM_c), PM's lateral and medial subdivisions have differentiable cortical connections. The central superior temporal gyrus (STG) and posterior parietal cortex (PPC) receive projections from patches of cells in both PM_m and PM_l, however, cells targeting STG predominately fall within PM_m while those projecting to PCC occur largely within the PM_l region (Gutierrez et al., 2000). A combination of retrograde label injections and GABA staining reveal a population of large, long range (up to 2mm) inhibitory interneurons. When combined with the patchy nature of the cortical projection zones in PM_l and PM_m, this suggests a functionally modular organization of PM interconnected and modulated by these interneurons. (Imura and Rockland, 2006).

PL_{dm} and its vague medial border with PM are distinct from the primarily visually driven PL_{vl} and PI subdivisions. This region lacks a clear retinotopy and exhibits unique

response properties (Bender, 1981). It can be differentiated from the neighboring ventro-lateral partition of PL by its large receptive fields and relatively long response latencies. Additionally, PL_{dm} distinguishes itself by exhibiting covert attentional modulation (Petersen et al., 1985), color opponency, and responses to complex geometric shapes (Benevento and Port, 1995).

Summary

Traditionally, the pulvinar has been treated as a single nucleus made up of three partitions that are differentiable via a combination of Nissl and myelin staining (Walker, 1938; Olszewski, 1952). More modern interpretations of anatomical evidence suggest that the pulvinar is a complex made up of distinct but related nuclei. Although this is the prevailing hypothesis, the number and organization of the pulvinar's subdivisions remain disputed (see Baldwin et al., 2017, for overview of past models). The three divisions of medial PI (PI_p, PI_m, PI_{cm}) have clear chemoarchitectonic features and are generally accepted. The structures of PM and PL_{dm} remain poorly classified both because these regions lack strong histological segmentation and because the neurons found in these subdivisions have complex electrophysiological properties. Small areas like PI_{cm} and PL_s pose the additional challenge that they are difficult to access surgically. With these limitations in mind, we present an updated model for the pulvinar's organization based on the structural, electrophysiological, and connectivity studies gathered in this review (Figure 2.6). Our organization scheme is based primarily on the divisions presented by Lyon et al. (2010) informed by histology and tracer studies (Gutierrez et al., 2000; Adams et al., 2000; Stepniewska and Kaas, 1997) in the context of the traditionally accepted macaque pulvinar areas: PL, PI, and PM (Olszewski, 1952).

We accept that PI is composed of four parts (from medial to lateral): PI_p, PI_m, PI_{cm}, PI_{cl} as per Stepniewska and Kaas (1997). This collection of pulvinar regions extends just dorsal of the brSC and falls medial to PL. The boundary between PI and PL is delineated by dark CB staining in PI_{cl} (Gray et al., 1999). Our representation of PL includes three parts (from dorso-medial to ventro-lateral): PL_{dm}, PL_{vl}, and PL_s. The retinotopic map of PL_{vl} mirrors that of PI_{cl} with a vertical meridian situated along their shared border (Adams et al., 2000). This region is flanked laterally by the chemoarchitectonically distinct PL_s (Lyon et al., 2010) and dorso-medially by PL_{dm}. The dorso-medial and ventro-lateral subdivisions of PL are differentiated from each other via electrophysiological recordings. PL_{vl} has clear retinotopic organization in contrast to the more complex response properties observed in PL_{dm} (Bender, 1981).

The apparent homogeneity of PM typically precludes it from attempts at classifying

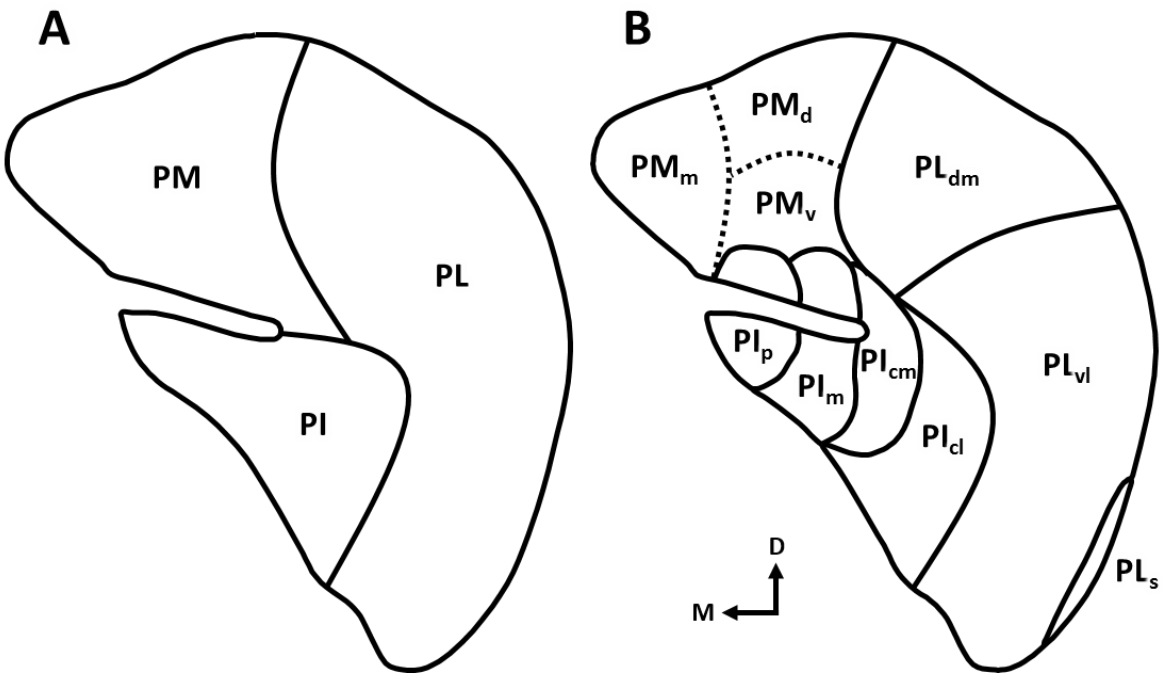

Figure 2.6: Comparison between traditional and proposed model. A) The three traditional subdivisions revealed by Nissl staining. B) Our proposed subdivisions. Dotted lines indicate suspected PM organization. PM = medial pulvinar, PI = inferior pulvinar, PL = lateral pulvinar, PM_m = medial PM, PM_d = dorsal PM, PM_v = ventral PM, PL_{dm} = dorso-medial PL, PL_{vl} = ventro-lateral PL, PL_s = "shell" of PL, PI_p = posterior PI, PI_m = medial PI, PI_{cm} = centro-medial PI, PI_{cl} = centro-lateral PI.

the pulvinar's component nuclei, however, retrograde tracers reveal a population of inhibitory interneurons that suggest a level of modularity that has yet to be well characterized (Imura and Rockland, 2006). Although connectivity studies have helped with classification, consensus on these subdivisions has yet to be reached. Our representation of PM includes four parts (from dorsal to ventral): PM_d, PM_m, PM_v, PM_c. These speculative divisions are based on electrophysiology and tracer studies but are not yet well characterized.

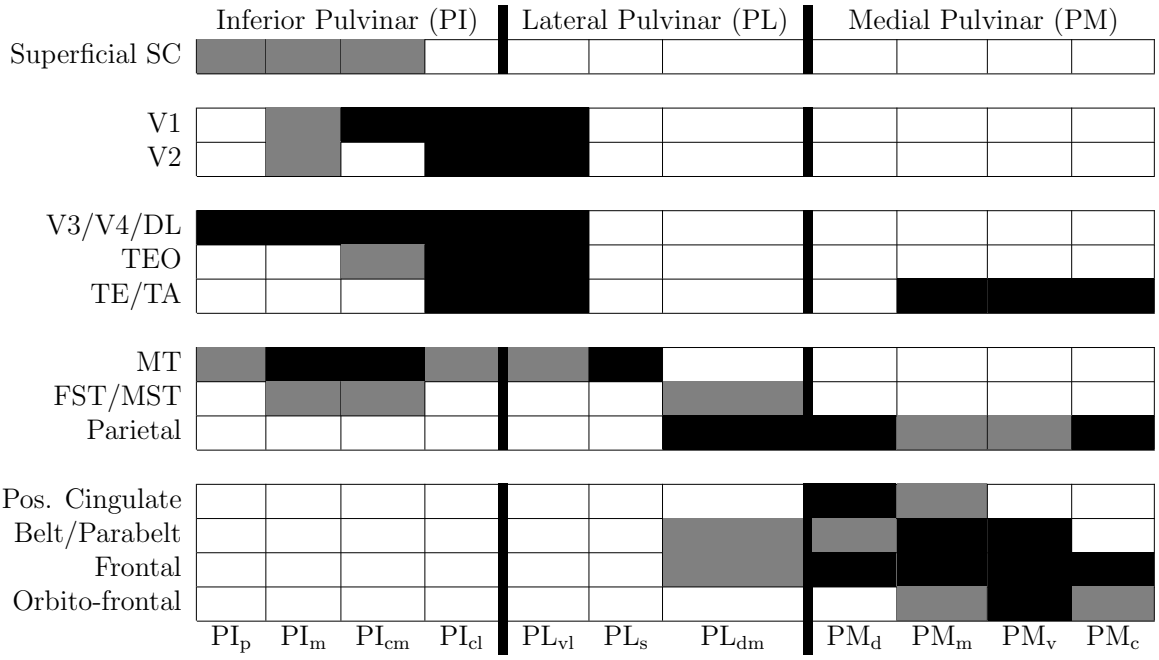

Table 2.1: Macaque pulvinar output. Dark shading indicates projections that are confirmed in two or more studies while light shading represents projections demonstrated only once. Here, SC is divided into deep and superficial compartments by the stratum opticum (SO). V3, V4, and the dorso-lateral cortical area (DL) have been grouped together since the studies reviewed here either do not differentiate between these areas or had large injections that crossed are boundaries. The "frontal" entry in this table refers collectively to the premotor Broadmann areas 8a, 45, and 46. PI = inferior pulvinar, PI_p = posterior PI, PI_m = medial PI, PI_{cm} = central medial PI, PI_{cl} = cental lateral, PL = lateral pulvinar, PL_{vl} = ventro-lateral PL, PL_s = "shell" of PL, PL_{dm} = dorso-medial PL, PM = medial pulvinar, PM_d = dorsal PM, PM_m = medial PM, PM_v = ventral PM, PM_c = central PM, TEO = posterior inferior temporal cortex, TE = anterior inferior temporal cortex, TA = anterior suprior temporal cortex, MT = middle temporal cortex, FST = fundus of the superior temporal area, MST = medial superior temporal area.

Pulvinar connectivity

We summarize the connections between our proposed subdivisions and brain areas of interest in Table 2.1 and Table 2.2. These connectivity tables are based on macaque anatomical studies and are organized in such a way to emphasize grouping into two functional regions: the visual and association pulvinar. The confidence of each intersection in these tables is indicated via shading. Darkly shaded table entries indicate high confidence of connectivity; being supported by two or more different studies. Those entries that are lightly shaded, however, indicate lower confidence as they were reported in only one study.

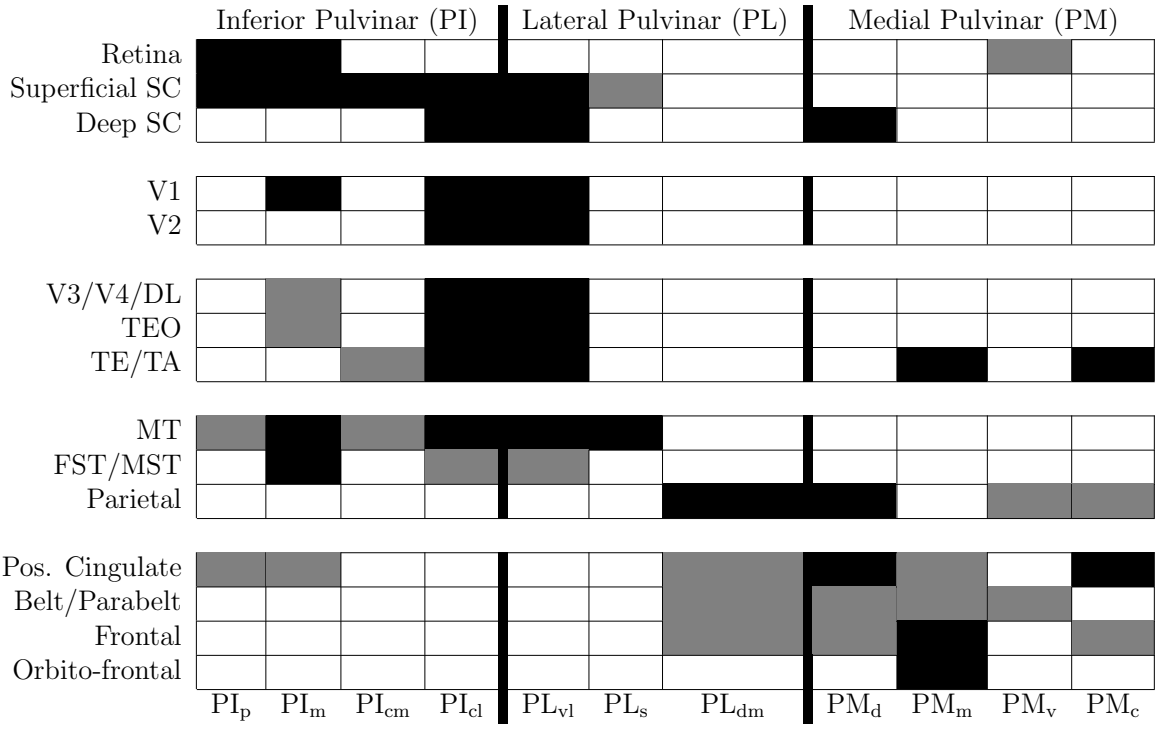

Table 2.2: Macaque pulvinar input. Dark shading indicates projections that are confirmed in two or more studies while light shading represents projections demonstrated only once. Conventions are the same as in Table 2.1. PI = inferior pulvinar, PI_p = posterior PI, PI_m = medial PI, PI_{cm} = central medial PI, PI_{cl} = cental lateral, PL = lateral pulvinar, PL_{vl} = ventro-lateral PL, PL_s = "shell" of PL, PL_{dm} = dorso-medial PL, PM = medial pulvinar, PM_d = dorsal PM, PM_m = medial PM, PM_v = ventral PM, PM_c = central PM, TEO = posterior inferior temporal cortex, TE = anterior inferior temporal cortex, TA = anterior suprior temporal cortex, MT = middle temporal cortex, FST = fundus of the superior temporal area, MST = medial superior temporal area.

Visual pulvinar

The pulvinar's two lateral anatomically defined retinotopic maps are well organized; corresponding with PL_{vl} and PI_{cl} (Ungerleider et al., 1984). This organization is confirmed by electrophysiological data gathered during the presentation of simple light stimuli (Bender, 1981) with a higher proportion of visually responsive cells falling in PI_{cl} (90%) than in PL_{vl} (75%) (Petersen et al., 1985). Receptive field sizes in these two pulvinar subdivisions are comparable and increase with eccentricity (Berman and Wurtz, 2010; Petersen et al., 1985; Bender, 1982). The visually responsive cells in PL_{vl} and PI_{cl} appear to be binocular (Bender, 1982), have larger receptive fields than their corresponding V1 analogs (DeBruyn et al., 1993; Bender, 1982), and are sometimes orientation selective (Robinson and Petersen, 1985; Petersen et al., 1985; Bender, 1982). These maps have known reciprocal projections with not only early visual areas (Lyon et al., 2010; Kaas and Lyon, 2007; Adams et al., 2000; Livingstone and Hubel, 1982; Ogren and Hendrickson,

1976) but also cortical areas falling within both ventral and dorsal visual processing streams (Gutierrez et al., 2000; Adams et al., 2000; Rockland et al., 1999; Baleydier and Morel, 1992). Superficial SC also provides a non-cortical source for visual input to the pulvinar (Berman and Wurtz, 2011; Stepniewska et al., 2000; Benevento and Rezak, 1976).

A wide array of connections made with PL_{vl} and PI_{cl} are consistent with the role of a subcortical facilitator between cortical areas. Saalmann et al. (2012) explore this suspected functionality in their study of electrophysiological dynamics between V4, TEO, and PL_{vl}. These animals were trained to perform a simple task requiring the subject to attend to a visual target after presentation of a cue. Cross correlograms between the recordings made within all three areas have a predominant alpha band (8-15Hz) when attending to targets. Additionally, Granger causality analysis shows that pulvinar activity causes increased synchrony between TEO and V4. The same causality has not been observed in the corticothalamic direction suggesting that PL_{vl} (and by extension, other pulvinar regions) has a role in the high level facilitation of cortical synchrony (Saalmann et al., 2012).

The cortical input that PL_{vl} and PI_{cl} receive comes from infragranular layers 5a and 6b (Conley and Raczkowski, 1990; Lund et al., 1975). Projections from the pulvinar to visual areas other than V1 end densely in layers 3/4 with collaterals in layer 1 (Benevento and Rezak, 1976). This granular termination pattern (Figure 2.7) often marks feed-forward driving projections (Felleman and Van Essen, 1991). In contrast, axons from PL_{vl} and PI_{cl} end in V1's layer 1 (Carey et al., 1979; Ogren and Hendrickson, 1976) which suggests a modulatory role. Net inhibition occurs in V1 layer 2/3 pyramidal cells following pulvinar inactivation such that the magnitude of this inhibition is greatest at the cell's preferred orientation (Purushothaman et al., 2012). These combined findings suggest that the lateral maps within PL_{vl} and PI_{cl} modulate and are driven by V1, in turn, driving a large number of downstream visual areas.

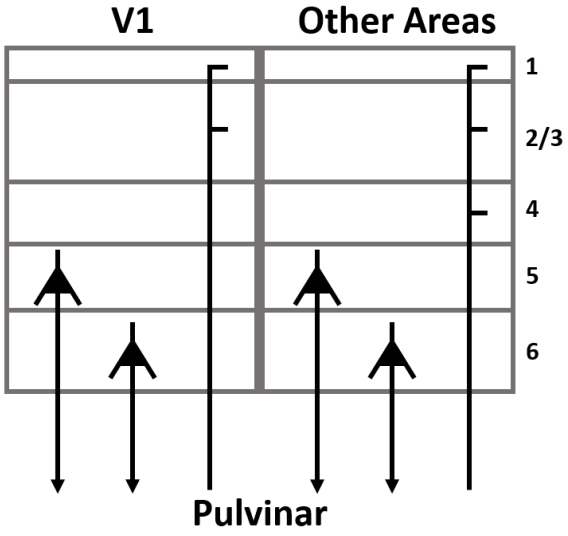

Figure 2.7: Laminar distribution of projections. Cortical projections to the pulvinar originate from pyramidal neurons within layers 5a and 6b of cortex. The pulvinar, when not targeting V1, project primarily to layers 3/4 with collaterals in layer 1. In V1, however, the pulvinar projects mainly to layer 1.

Medial to the lateral retinotopic maps falling within PL_{vl} and PI_{cl} are the three

remaining regions of PI: PI_p, PI_m, PI_{cm}. These PI subdivisions differentially provide input to V1, V4, and MT. PI_p connection patterns are poorly classified due to its small size. V1 and FST/MST send denser projections to PI_m than to PI_{cm} which may relate to PI_m's large projections to MT (Stepniewska et al., 2000). PI_{cm} serves as both a structural (Stepniewska, 1999) and functional (Berman and Wurtz, 2010) relay between SC and MT but does not supply directional preference (Berman and Wurtz, 2011).

Association pulvinar

Posterior PL_{dm} is heavily involved with the ventral visual processing stream as it reciprocally projects to V4 (Lyon et al., 2010; Weller et al., 2002), TEO, and TE (Webster et al., 1993; Baizer et al., 1993; Yeterian and Pandya, 1991). This region has exhibited the capacity for high-level visual processing and has even been implicated in the perceptual differentiation of faces, face-like cartoons, eyes, and non-face images (Nguyen et al., 2013). Additionally, the posterior portion of PL_{dm} is known to have a role in decision making. Komura et al. (2013) identified neurons within this region whose activity correlated with a subject's confidence in identifying the direction of random dot motion. These cells showed similar responses regardless of the direction of motion but decreased firing rate when the stimulus had low coherence resulting in response hesitation. Artificially silencing PL_{dm} triggers an increase in response hesitation and drop-out suggesting a causal relationship.

Anterior PL_{dm} is heavily involved with the dorsal visual processing stream as it reciprocally projects to parietal cortex, FEF, and the auditory parabelt (Gutierrez et al., 2000; Yeterian and Pandya, 1985). This region contains neurons with both covert attentional modulation and presaccadic activation. This implicates the anterior portion of PL_{dm} in spatial attention and saccade control (Robinson et al., 1986; Robinson and Petersen, 1985). Blockading this subdivision with a GABA agonist results in attention biased to the ipsilesional side (Wilke et al., 2010; Petersen et al., 1987). Similar deficits have been demonstrated in humans (Ward and Arend, 2007). To determine the exact structure of PL_{dm}, more detailed connectivity studies need to be conducted.

PM shares a poorly defined border with PL_{dm} and lacks discrete architectonic subdivisions. Despite classification difficulties, some organization can be inferred. Tracer injections made in premotor, auditory belt/parabelt, and parietal cortices reveal connectivity differences between PM subdivisions. Tracer studies have identified that PM_m projects within the auditory belt/parabelt, PM_d reciprocally with parietal cortex, and PM_v to frontal cortical areas (Cappe et al., 2009; Gutierrez et al., 2000; Trojanowski and Jacobson, 1974). PM_m also receives input from orbito-frontal cortex (Cavada et al., 1995) and shares a reciprocal connection with TE/TEA(Romanski et al., 1997; Yeterian and

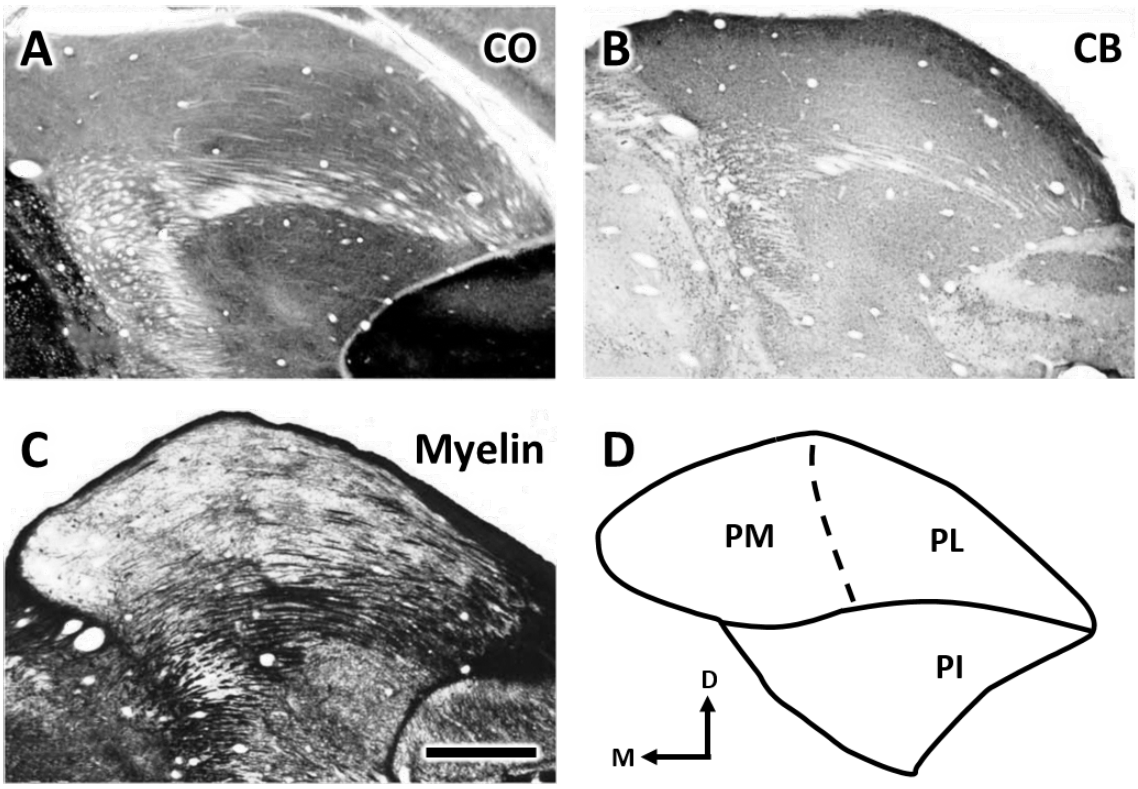

Figure 2.8: Histology reveals galago pulvinar subdivisions. Stereotaxically comparable coronal galago pulvinar sections stained for: A) cytochrome oxidase (CO), B) calbindin (CB), and C) myelin. D) Line drawing of pulvinar with major subdivisions labeled. The vague border between PM and PL is indicated by a dashed line. Note that PI is separated from the rest of the pulvinar by the brSC. PM = medial pulvinar, PI = inferior pulvinar, PL = lateral pulvinar, brSC = brachium of the superior colliculus, CO = cytochrome oxidase, CB = calbindin. Scale bar = 1mm. Adapted from Li et al. (2013).

Pandya, 1991). PM_c is quite difficult to classify due to its small size, however, it has well documented projections to parietal and frontal cortices (Contini et al., 2010; Schmahmann and Pandya, 1990; Trojanowski and Jacobson, 1977).

Comparison to strepsirrhine primates

Members of the Strepsirrhine suborder more closely resemble the common ancestors of primates and have been a popular model organism for investigators interested in evolution (Jerison, 1979). Galago pulvinar, much like its macaque analog, sits on the dorso-lateral surface of the thalamus. This thalamic complex falls medial to LGN, dorso-lateral to the posterior nuclear group, and is separated from both of these regions by white matter tracts (Glendenning et al., 1975). The pulvinar complex in this species is divided into superior (PS) and inferior(PI) divisions which are separated as brSC runs horizontally between them. Horizontally running fibers on the lateral side of PS divide it further into a lateral

(PL) and medial (PM) regions (Figure 2.8). This border is even less clearly defined than in macaques and further differentiation based on chemoarchitecture has not been particularly successful (Li et al., 2013; Glendenning et al., 1975).

The galago pulvinar has a large area reciprocally connected with V1 that straddles the brSC (Campos-Ortega, 1968). This area contains two dorso-ventral retinotopic maps that correspond to PL and PI much like the macaque visual pulvinar (Figure 5.2). Both the dorsal and ventral maps have medial lower field and a lateral upper field representations that join at a central field along their border (Moore et al., 2018; Li et al., 2013; Raczkowski and Diamond, 1980; Carey et al., 1979; Symonds and Kaas, 1978). These two maps also have V1, V2, and MT connectivity that is similar to that observed in the macaque's PI_{cl} and PL_{dm} (Raczkowski and Diamond, 1981; Wall et al., 1982). PI contains two regions that project to MT: a medial area and a lateral area containing sparser connections (Wong et al., 2009; Wall et al., 1982; Raczkowski and Diamond, 1980). The medial subdivision of PI is also suspected to project to V1 without precise retinotopy (Raczkowski and Diamond, 1981). These properties taken together respectively suggest that medial and lateral galago PI is homologous to macaque PI_m and PI_{cl}. The vague border region between PM and PL receives projections from posterior temporal cortical areas in a similar manner to macaque PL_{dm} (Raczkowski and Diamond, 1981; Rezak and Benevento, 1979), however, this region does not receive SC input (Raczkowski and Diamond, 1981; Benevento and Standage, 1983). The overall structure of galago pulvinar is an apparent caudo-ventral rotational shift of macaque pulvinar (Baldwin et al., 2013). It should be noted that although galago and macaque pulvinar appear to be homologous, similarity should not be assumed without strong architectonic, connectivity, or electrophysiological evidence.

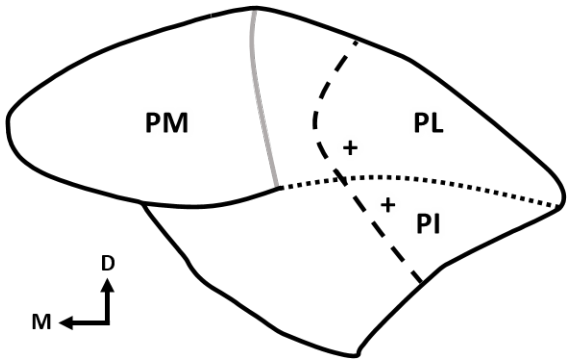

Figure 2.9: Galago pulvinar retinotopy. Dashed line represents the horizontal meridian while dotted line is both the dorsal boundary of PI (brSC) and the vertical meridian. Grey line indicates the medial bound of the retinotopic maps. Upper visual field representation indicated by "+".

Conclusions

The pulvinar complex contains subdivisions with distinct connection patterns and functionality, however, it remains poorly understood. We propose that the pulvinar

contains a sensory hierarchy similar to that of the visual hierarchy found in cortex. This proposal is based on the chemoarchitecture, connectivity, and function studies presented here. The pulvinar's visual information flow begins in PI_{cl}/PL_{vl} running roughly from its ventro-lateral to dorso-medial end. This is not unlike the cortical visual hierarchy that flows in a caudo-rostral manner as information progresses beyond early cortical areas to the dorsal and ventral processing streams (Felleman and Van Essen, 1991). The visual pulvinar also exhibits a suspected dual processing stream with PI_m sharing reciprocal connections with the ventral stream (primarily MT, V3/V4/DL) while PL_{dm} is associated with posterior parietal areas. This subcortical hierarchy eventually ends within PM functioning as a multisensory integration area.

The suggestion that the pulvinar functions in a hierarchical manner has been proposed before, however, this idea was limited to being informed by only connection patterns between PL, PI, and early visual cortices (Benevento and Davis, 1977). Our model shares many of the early segments of the one proposed by Kaas and Lyon (2007), however, we've expanded this understanding to include PM subdivisions into our theoretical framework.

References for connectivity tables

Pulvinar output

Superficial SC

PI_p : Berman and Wurtz (2011, 2010)
PI_m : Berman and Wurtz (2011, 2010)
PI_{cm} : Berman and Wurtz (2011, 2010)

V1

PI_m : Lysakowski et al. (1988)
PI_{cm} : Kaas and Lyon (2007); Lysakowski et al. (1988)
PI_{cl} : Kaas and Lyon (2007); Adams et al. (2000); Lysakowski et al. (1988); Livingstone and Hubel (1982); Benevento and Rezak (1976); Rezak and Benevento (1979); Ogren and Hendrickson (1976)
PL_{vl} : Kaas and Lyon (2007); Adams et al. (2000); Lysakowski et al. (1988); Livingstone and Hubel (1982); Benevento and Rezak (1976); Rezak and Benevento (1979); Ogren and Hendrickson (1976)

V2

PI_m : Mizuno et al. (1983)
PI_{cl} : Lyon et al. (2010); Adams et al. (2000); Rockland et al. (1999); Levitt et al. (1995); Mizuno et al. (1983); Livingstone and Hubel (1982); Lund et al. (1981); Rezak and Benevento (1979); Benevento and Rezak (1976); Ogren and Hendrickson (1976)
PL_{vl} : Lyon et al. (2010); Adams et al. (2000); Rockland et al. (1999); Levitt et al. (1995); Mizuno et al. (1983); Livingstone and Hubel (1982); Lund et al. (1981); Rezak and Benevento (1979); Benevento and Rezak (1976); Ogren and Hendrickson (1976)

V3/V4/DL

PI_p : Adams et al. (2000); Gray et al. (1999); Baleydier and Morel (1992) PI_m : Lyon et al. (2010); Shipp (2001); Lysakowski et al. (1988) PI_{cm} : Shipp (2001); Adams et al. (2000); Gray et al. (1999); Baleydier and Morel (1992); Lysakowski et al. (1988)
PI_{cl} : Lyon et al. (2010); Adams et al. (2000); Rockland et al. (1999); Baleydier and Morel (1992); Benevento and Rezak (1976)
PL_{vl} : Lyon et al. (2010); Adams et al. (2000); Rockland et al. (1999); Baleydier and Morel (1992); Benevento and Rezak (1976)
PL_{dm} : Lyon et al. (2010); Gray et al. (1999); Lysakowski et al. (1988) PM_c : Lysakowski et al. (1988)

TEO

PI_{cm} : Webster et al. (1993)
PI_{cl} : Webster et al. (1993); Baleydier and Morel (1992); Benevento and Rezak (1976)
PL_{vl} : Webster et al. (1993); Baleydier and Morel (1992); Benevento and Rezak (1976)
PL_{dm} : Webster et al. (1993)

TE/TA

PI_{cl} : Webster et al. (1993)
PL_{vl} : Webster et al. (1993)
PL_{dm} : Baizer et al. (1993); Webster et al. (1993); Baleydier and Morel (1992); Yeterian and Pandya (1989)
PM_m : Yeterian and Pandya (1989); Markowitsch et al. (1985)
PM_v : Yeterian and Pandya (1989); Markowitsch et al. (1985)
PM_c : Webster et al. (1993); Trojanowski and Jacobson (1977)

MT

PI_p : Berman and Wurtz (2011, 2010)
PI_m : Berman and Wurtz (2011, 2010); Lyon et al. (2010); Shipp (2001); Stepniewska et al. (2000); Adams et al. (2000); Gray et al. (1999); Maunsell and van Essen (1983)
PI_{cm} : Berman and Wurtz (2011, 2010); Lyon et al. (2010)
PI_{cl} : Adams et al. (2000)
PL_{vl} : Adams et al. (2000)
PL_s : Berman and Wurtz (2010); Lyon et al. (2010); Shipp (2001)

FST/MST

PI_m : Boussaoud et al. (1992)
PI_{cm} : Adams et al. (2000)
PL_{dm} : Rezak and Benevento (1979)

Parietal

PL_{dm} : Cappe et al. (2009); Matsuzaki et al. (2004); Patrick Hardy and Lynch (1992); Acuña et al. (1990); Rezak and Benevento (1979)
PM_d : Matsuzaki et al. (2004); Cavada et al. (1995); Morecraft et al. (1993); Patrick Hardy and Lynch (1992); Baleydier and Mauguière (1987)
PM_m : Baleydier and Mauguiere (1985)
PM_v : Morecraft et al. (1993)
PM_c : Schmahmann and Pandya (1990); Trojanowski and Jacobson (1977)

Posterior Cingulate

PM_d : Baleydier and Mauguière (1987); Baleydier and Mauguiere (1985)
PM_m : Baleydier and Mauguiere (1985)

Belt/Parabelt

PL_{dm} : Hackett et al. (1998)
PM_d : Hackett et al. (1998)
PM_m : Cappe et al. (2009); Hackett et al. (1998); Baleydier and Mauguiere (1985)
PM_v : Cappe et al. (2009); Hackett et al. (2007, 1998)

Frontal

PL_{dm} : Huerta et al. (1986)
PM_d : Cappe et al. (2009); Asanuma et al. (1985); Baleydier and Mauguiere (1985); Trojanowski and Jacobson (1974)
PM_m : Morecraft et al. (1993); Trojanowski and Jacobson (1976)
PM_v : Cappe et al. (2009); Asanuma et al. (1985); Huerta et al. (1986); Trojanowski and Jacobson (1974)
PM_c : Contini et al. (2010); Romanski et al. (1997); Trojanowski and Jacobson (1977, 1974)

Orbito-frontal

PM_d : Cavada et al. (1995)
PM_m : Itaya and Van Hoesen (1983); O'Brien et al. (2001); Cowey et al. (1994); Mizuno et al. (1982)
PM_v : Trojanowski and Jacobson (1976)
PL_c : Trojanowski and Jacobson (1977)

Pulvinar input

Retina

PI_p : O'Brien et al. (2001); Mizuno et al. (1982)
PI_m : O'Brien et al. (2001); Cowey et al. (1994); Itaya and Van Hoesen (1983); Mizuno et al. (1982)
PM_v : Itaya and Van Hoesen (1983)

Superficial SC

PI_p : Berman and Wurtz (2011, 2010); Stepniewska et al. (2000); Lysakowski et al. (1986); Harting et al. (1980); Benevento and Rezak (1976)
PI_m : Berman and Wurtz (2011, 2010); Lysakowski et al. (1986)
PI_{cm} : Berman and Wurtz (2011, 2010); Stepniewska et al. (2000); Lysakowski et al. (1986); Harting et al. (1980); Partlow et al. (1977); Benevento and Rezak (1976)
PI_{cl} : Lyon et al. (2010); Lysakowski et al. (1986); Benevento and Standage (1983); Benevento and Rezak (1976)
PL_{vl} : Lyon et al. (2010); Lysakowski et al. (1986); Benevento and Standage (1983); Benevento and Rezak (1976)
PL_s : Berman and Wurtz (2011, 2010)

Deep SC

PM_d : Lysakowski et al. (1986); Benevento and Standage (1983); Benevento and Fallon (1975)
PL_{dm} : Benevento and Standage (1983); Harting et al. (1980)

V1

PI_{cl} : Rockland (1998); Gutierrez and Cusick (1997); Kennedy and Bullier (1985); Ungerleider et al. (1983); Ogren and Hendrickson (1977, 1976); Lund et al. (1975)
PL_{vl} : Rockland (1998); Gutierrez and Cusick (1997); Kennedy and Bullier (1985); Ungerleider et al. (1983); Ogren and Hendrickson (1977, 1976); Lund et al. (1975)
PI_{m} : Rockland (1998); Ogren and Hendrickson (1976)

V2

PI_{cl} : Kennedy and Bullier (1985); Ogren and Hendrickson (1977)
PL_{vl} : Kennedy and Bullier (1985); Ogren and Hendrickson (1977)
PL_{dm} : Ungerleider et al. (2014)

V3/V4/DL

PI_{m} : Benevento and Davis (1977)
PI_{cl} : Shipp (2001); Yeterian and Pandya (1997); Benevento and Davis (1977)
PL_{vl} : Shipp (2001); Yeterian and Pandya (1997); Benevento and Davis (1977)
PL_{dm} : Weller et al. (2002); Benevento and Davis (1977)

TEO

PI_{m} : Rockland (1996)
PI_{cl} : Webster et al. (1993); Rockland (1996)
PL_{vl} : Webster et al. (1993); Rockland (1996)
PL_{dm} : Romanski et al. (1997); Rockland (1996); Webster et al. (1993); Yeterian and Pandya (1991); Benevento and Davis (1977)

TE/TA

PI_{cm} : Webster et al. (1993)
PI_{cl} : Webster et al. (1993); Rockland (1996)
PL_{vl} : Webster et al. (1993); Rockland (1996)
PL_{dm} : Webster et al. (1993); Yeterian and Pandya (1991)
PM_{m} : Romanski et al. (1997); Yeterian and Pandya (1988, 1991)
PM_{c} : Rockland (1996); Webster et al. (1993); Yeterian and Pandya (1991)

MT

PI_{p} : Berman and Wurtz (2011, 2010)
PI_{m} : Shipp (2001); Stepniewska et al. (2000); Gray et al. (1999); Rockland (1998); Ungerleider et al. (1984); Lund et al. (1981)
PI_{cm} : Berman and Wurtz (2011, 2010)
PI_{cl} : Gray et al. (1999); Rockland (1998); Ungerleider et al. (1984)
PL_{vl} : Gray et al. (1999); Rockland (1998); Ungerleider et al. (1984)
PL_{s} : Maunsell and van Essen (1983); Berman and Wurtz (2010); Shipp (2001)

FST/MST

PI_{m} : Gutierrez et al. (2000); Boussaoud et al. (1992)
PI_{cl} : Gutierrez et al. (2000)
PL_{vl} : Gutierrez et al. (2000)

Parietal

PL_{dm} : Benevento and Davis (1977); Gutierrez et al. (2000); Yeterian and Pandya (1985)
PM_{d} : Gutierrez et al. (2000); Cavada et al. (1995); Asanuma et al. (1985); Yeterian and Pandya (1985)
PM_{v} : Asanuma et al. (1985)
PM_{c} : Asanuma et al. (1985)

Posterior Cingulate

PI_{p} : Rockland (1996)
PI_{m} : Rockland (1996)
PM_{d} : Rockland (1996); Yeterian and Pandya (1988); Baleydier and Mauguiere (1985)
PM_{m} : Rockland (1996)
PM_{c} : Rockland (1996); Yeterian and Pandya (1988)

Belt/Parabelt

PL_{dm} : Gutierrez et al. (2000)
PM_{d} : Gutierrez et al. (2000)
PM_{m} : Gutierrez et al. (2000)
PM_{v} : Gutierrez et al. (2000)

Frontal

PL_{dm} : Stanton et al. (1988)
PM_{d} : Gutierrez et al. (2000)
PM_{m} : Gutierrez et al. (2000); Stanton et al. (1988)
PM_{c} : Contini et al. (2010)

Orbito-frontal

PM_{d} : Cavada et al. (1995); Yeterian and Pandya (1988)
PM_{m} : Cavada et al. (1995); Yeterian and Pandya (1988)

References

Acuña, C., Cudeiro, J., Gonzalez, F., Alonso, J. M., and Perez, R. (1990). Lateral-posterior and pulvinar reaching cells-comparison with parietal area 5a: a study in behaving Macaca nemestrina monkeys. *Experimental Brain Research*, 82(1):158–166.

Adams, M. M., Hof, P. R., Gattass, R., Webster, M. J., and Ungerleider, L. G. (2000). Visual cortical projections and chemoarchitecture of macaque monkey pulvinar. *Journal of Comparative Neurology*, 419(3):377–393.

Asanuma, C., Andersen, R. A., and Cowan, W. M. (1985). The thalamic relations of the caudal inferior parietal lobule and the lateral prefrontal cortex in monkeys: divergent cortical projections from cell clusters in the medial pulvinar nucleus. *The Journal of Comparative Neurology*, 241:357–81.

Baizer, J. S., Desimone, R., and Ungerleider, L. G. (1993). Comparison of subcortical connections of inferior temporal and posterior parietal cortex in monkeys. *Visual neuroscience*, 10(1):59–72.

Baldwin, M. K., Balaram, P., and Kaas, J. H. (2017). The evolution and functions of nuclei of the visual pulvinar in primates. *Journal of Comparative Neurology*, 525(15):3207–3226.

Baldwin, M. K. L., Balaram, P., and Kaas, J. H. (2013). Projections of the superior colliculus to the pulvinar in prosimian galagos (Otolemur garnettii) and VGLUT2 staining of the visual pulvinar. *Journal of Comparative Neurology*, 521(7):1664–1682.

Baleydier, C. and Mauguiere, F. (1985). Anatomical evidence for medial pulvinar connections with the posterior cingulate cortex, the retrosplenial area, and the posterior parahippocampal gyrus in monkeys. *The Journal of comparative neurology*, 232(2):219–28.

Baleydier, C. and Mauguière, F. (1987). Network organization of the connectivity between parietal area 7, posterior cingulate cortex and medial pulvinar nucleus: a double fluorescent tracer study in monkey. *Experimental brain research*, 66(2):385–93.

Baleydier, C. and Morel, A. (1992). Segregated thalamocortical pathways to inferior parietal and inferotemporal cortex in macaque monkey. *Visual neuroscience*, 8(5):391–405.

Bender, D. B. (1981). Retinotopic organization of macaque pulvinar. *Journal of neurophysiology*, 46(3):672–693.

Bender, D. B. (1982). Receptive field properties of neurons in the macaque inferior pulvinar. *J Neurophysiol*, 48(I):1–17.

Bender, D. B. and Butter, C. M. (1987). Comparison of the effects of superior colliculus and pulvinar lesions on visual search and tachistoscopic pattern discrimination in monkeys. *Exp Brain Res*, 69:140–154.

Bender, D. B. and Youakim, M. (2001). Effect of attentive fixation in macaque thalamus and cortex. *Journal of neurophysiology*, 85(1):219–34.

Benevento, L. A. and Davis, B. (1977). Topographical projections of the prestriate cortex to the pulvinar nuclei in the macaque monkey: An autoradiographic study. *Experimental Brain Research*, 30(2-3):405–424.

Benevento, L. A. and Fallon, J. H. (1975). The ascending projections of the superior colliculus in the rhesus monkey (Macaca mulatta). *Journal of Comparative Neurology*, 160(3):339–361.

Benevento, L. A. and Port, J. D. (1995). Single neurons with both form/color differential responses and saccade-related responses in the nonretinotopic pulvinar of the behaving macaque monkey. *Visual neuroscience*, 12(3):523–44.

Benevento, L. A. and Rezak, M. (1976). The cortical projections of the inferior pulvinar and adjacent lateral pulvinar in the rhesus monkey (macaca mulatta): An autoradiographic study. *Brain Research*, 108(1):1–24.

Benevento, L. a. and Standage, G. P. (1983). The organization of projections of the retinorecipient and nonretinorecipient nuclei of the pretectal complex and layers of the superior colliculus to the lateral pulvinar and medial pulvinar in the macaque monkey. *The Journal of comparative neurology*, 217:307–336.

Berman, R. A. and Wurtz, R. (2010). Functional identification of a pulvinar path from superior colliculus to cortical area MT. *Journal of Neuroscience*, 30(18):6342–6354.

Berman, R. A. and Wurtz, R. H. (2011). Signals conveyed in the pulvinar pathway from superior colliculus to cortical area MT. *The Journal of neuroscience : the official journal of the Society for Neuroscience*, 31(2):373–84.

Boussaoud, D., Desimone, R., and Ungerleider, L. G. (1992). Subcortical connections of visual areas MST and FST in macaques. *Visual neuroscience*, 9(3-4):291–302.

Bridge, H., Leopold, D. A., and Bourne, J. A. (2016). Adaptive Pulvinar Circuitry Supports Visual Cognition. *Trends in Cognitive Sciences*, 20(2):146–157.

Campos-Ortega, J. A. (1968). Descending subcortical projections from the occipital lobe of Galago crassicaudatus. *Experimental neurology*, 21(4):440–454.

Cappe, C., Morel, A., Barone, P., and Rouiller, E. M. (2009). The thalamocortical projection systems in primate: An anatomical support for multisensory and sensorimotor interplay. *Cerebral Cortex*, 19(9):2025–2037.

Carey, R. G., Fitzpatrick, D., and Diamond, I. T. (1979). Layer I of striate cortex of Tupaia glis and Galago senegalensis: Projections from thalamus and claustrum revealed by retrograde transport of horseradish peroxidase. *Journal of Comparative Neurology*, 186(3):393–437.

Cavada, C., Compañy, T., Hernández-González, A., and Reinoso-Suárez, F. (1995). Acetylcholinesterase histochemistry in the macaque thalamus reveals territories selectively connected to frontal, parietal and temporal association cortices. *Journal of Chemical Neuroanatomy*, 8(4):245–257.

Conley, M. and Raczkowski, D. (1990). Sublaminar organization within layer VI of the striate cortex in Galago. *Journal of Comparative Neurology*, 302(2):425–436.

Contini, M., Baccarini, M., Borra, E., Gerbella, M., Rozzi, S., and Luppino, G. (2010). Thalamic projections to the macaque caudal ventrolateral prefrontal areas 45A and 45B. *European Journal of Neuroscience*, 32(8):1337–1353.

Cowey, A., Stoerig, P., and Bannister, M. (1994). Retinal ganglion cells labelled from the pulvinar nucleus in macaque monkeys. *Neuroscience*, 61(3):691–705.

Cusick, C. G., Scripter, J. L., Darensbourg, J. G., and Weber, J. T. (1993). Chemoarchitectonic subdivisions of the visual pulvinar in monkeys and their connectional relations with the middle temporal and rostral dorsolateral visual areas, MT and DLr. *The Journal of comparative neurology*, 336:1–30.

DeBruyn, E. J., Casagrande, V. A., Beck, P. D., and Bonds, A. B. (1993). Visual resolution and sensitivity of single cells in the primary visual cortex (V1) of a nocturnal primate (bush baby): correlations with cortical layers and cytochrome oxidase patterns. *Journal of neurophysiology*, 69(1):3–18.

Desimone, R., Wessinger, M., Thomas, L., and Schneider, W. (1990). Attentional control of visual perception: cortical and subcortical mechanisms. *Cold Spring Harbor symposia on quantitative biology*, 55(23):963–71.

Felleman, D. J. and Van Essen, D. C. (1991). Distributed hierarchical processing in the primate cerebral cortex. *Cerebral cortex (New York, N.Y. : 1991)*, 1:1–47.

Fischer, J. and Whitney, D. (2009). Precise discrimination of object position in the human pulvinar. *Human brain mapping*, 30(1):101–11.

Fischer, J. and Whitney, D. (2012). Attention gates visual coding in the human pulvinar. *Nature Communications*, 3:1051–1059.

Glendenning, K. K., Hall, J. A., Diamond, I. T., and Hall, W. C. (1975). The pulvinar nucleus of Galago senegalensis. *J Comp Neurol*, 161(3):419–458.

Gray, D., Gutierrez, C., and Cusick, C. G. (1999). Neurochemical organization of inferior pulvinar complex in squirrel monkeys and macaques revealed by acetylcholinesterase histochemistry, calbindin and Cat-301 immunostaining, and Wisteria floribunda agglutinin binding. *Journal of Comparative Neurology*, 409(3):452–468.

Gutierrez, C., Cola, M. G., Seltzer, B., and Cusick, C. (2000). Neurochemical and connectional organization of the dorsal pulvinar complex in monkeys. *Journal of Comparative Neurology*, 419(1):61–86.

Gutierrez, C. and Cusick, C. G. (1997). Area V1 in macaque monkeys projects to multiple histochemically defined subdivisions of the inferior pulvinar complex. *Brain Research*, 765(2):349–356.

Gutierrez, C., Yaun, A., and Cusick, C. G. (1995). Neurochemical subdivisions of the inferior pulvinar in macaque monkeys. *Journal of Comparative Neurology*, 363(4):545–562.

Hackett, T. A., De La Mothe, L. A., Ulbert, I., Karmos, G., Smiley, J., and Schroeder, C. E. (2007). Multisensory convergence in auditory cortex, II. Thalamocortical connections of the caudal superior temporal plane. *The Journal of comparative neurology*, 502(6):924–52.

Hackett, T. a., Stepniewska, I., and Kaas, J. H. (1998). Thalamocortical connections of the parabelt auditory cortex in macaque monkeys. *Journal of Comparative Neurology*, 400(January):271–286.

Harting, J. K., Huerta, M. F., Frankfurter, a. J., Strominger, N. L., and Royce, G. J. (1980). Ascending pathways from the monkey superior colliculus: an autoradiographic analysis. *The Journal of comparative neurology*, 192(4):853–82.

Huerta, M. F., Krubitzer, L. A., and Kaas, J. H. (1986). Frontal eye field as defined by intracortical microstimulation in squirrel monkeys, owl monkeys, and macaque monkeys: I. Subcortical connections. *The Journal of comparative neurology*, 253(4):415–39.

Imura, K. and Rockland, K. S. (2006). Long-range interneurons within the medial pulvinar nucleus of macaque monkeys. *The Journal of comparative neurology*, 498(5):649–66.

Itaya, S. K. and Van Hoesen, G. W. (1983). Retinal projections to the inferior and medial pulvinar nuclei in the old-world monkey. *Brain Research*, 269(2):223–230.

Jerison, H. J. (1979). Brain, body and encephalization in early primates. *Journal of Human Evolution*, 8(6):615–635.

Jones, E. G. (2007). *The Thalamus*. Cambridge University Press, Cambridge, UK, 2 edition.

Kaas, J. H. and Lyon, D. C. (2007). Pulvinar contributions to the dorsal and ventral streams of visual processing in primates. *Brain Research Reviews*, 55(2 SPEC. ISS.):285–296.

Kennedy, H. and Bullier, J. (1985). A double-labeling investigation of the afferent connectivity to cortical areas V1 and V2 of the macaque monkey. *The Journal of neuroscience : the official journal of the Society for Neuroscience*, 5(10):2815–2830.

Komura, Y., Nikkuni, A., Hirashima, N., Uetake, T., and Miyamoto, A. (2013). Responses of pulvinar neurons reflect a subject's confidence in visual categorization. *Nature Neuroscience*, 16(6):749–55.

Levitt, J. B., Yoshioka, T., and Lund, J. S. (1995). Connections between the pulvinar complex and cytochrome oxidase-defined compartments in visual area V2 of macaque monkey. *Experimental brain research*, 104:419–430.

Li, K., Patel, J., Purushothaman, G., Marion, R. T., and Casagrande, V. A. (2013). Retinotopic maps in the pulvinar of bush baby (Otolemur garnettii). *Journal of Comparative Neurology*, 521(15):3432–3450.

Livingstone, M. S. and Hubel, D. H. (1982). Thalamic inputs to cytochrome oxidase-rich regions in monkey visual cortex. *Proceedings of the National Academy of Sciences of the United States of America*, 79(19):6098–101.

Lund, J. S., Hendrickson, a. E., Ogren, M. P., and Tobin, E. a. (1981). Anatomical organization of primate visual cortex area VII. *The Journal of comparative neurology*, 202(1):19–45.

Lund, J. S., Lund, R. D., Hendrickson, A. E., Bunt, A. H., and Fuchs, A. F. (1975). The origin of efferent pathways from the primary visual cortex, area 17, of the macaque monkey as shown by retrograde transport of horseradish peroxidase. *The Journal of comparative neurology*, 164(3):287–303.

Lyon, D. C., Nassi, J. J., and Callaway, E. M. (2010). A Disynaptic Relay from Superior Colliculus to Dorsal Stream Visual Cortex in Macaque Monkey. *Neuron*, 65(2):270–279.

Lysakowski, A., Standage, G. P., and Benevento, L. A. (1986). Histochemical and architectonic differentiation of zones of pretectal and collicular inputs to the pulvinar and dorsal lateral geniculate nuclei in the macaque. *Journal of Comparative Neurology*, 250(4):431–448.

Lysakowski, A., Standage, G. P., and Benevento, L. A. (1988). An investigation of collateral projections of the dorsal lateral geniculate nucleus and other subcortical structures to cortical areas V1 and V4 in the macaque monkey: a double label retrograde tracer study. *Experimental brain research*, 69(3):651–61.

Ma, T. P., Lynch, J. C., Donahoe, D. K., Attallah, H., and Rafols, J. A. (1998). Organization of the medial pulvinar nucleus in the Macaque. *Anatomical Record*, 250(2):220–237.

Markowitsch, H. J., Emmans, D., Irle, E., Streicher, M., and Preilowski, B. (1985). Cortical and subcortical afferent connections of the primate's temporal pole: A study of rhesus monkeys, squirrel monkeys, and marmosets. *Journal of Comparative Neurology*, 242(3):425–458.

Matsuzaki, R., Kyuhou, S. I., Matsuura-Nakao, K., and Gemba, H. (2004). Thalamo-cortical projections to the posterior parietal cortex in the monkey. *Neuroscience Letters*, 355(1-2):113–116.

Maunsell, J. H. R. and van Essen, D. C. (1983). The connections of the middle temporal visual area (MT) and their relationship to a cortical hierarchy in the macaque monkey. *The Journal of Neuroscience*, 3(12):2563–2586.

Mizuno, N., Itoh, K., Uchida, K., Uemura-Sumi, M., and Matsushima, R. (1982). A retino-pulvinar projection in the macaque monkey as visualized by the use of anterograde transport of horseradish peroxidase. *Neuroscience letters*, 30(3):199–203.

Mizuno, N., Takahashi, O., Itoh, K., and Matsushima, R. (1983). Direct projections to the prestriate cortex from the retino-recipient zone of the inferior pulvinar nucleus in the macaque monkey. *Neuroscience letters*, 43(2-3):155–60.

Moore, B., Li, K., Kaas, J. H., Liao, C.-C., Boal, A. M., Mavity-Hudson, J., and Casagrande, V. (2018). Cortical projections to the two retinotopic maps of primate pulvinar are distinct. *Journal of Comparative Neurology*.

Morecraft, R. J., Geula, C., and Mesulam, M. M. (1993). Architecture of Connectivity Within a Cingulo-Fronto-Parietal Neurocognitive Network for Directed Attention. *Archives of Neurology*, 50(3):279–284.

Nguyen, M. N., Hori, E., Matsumoto, J., Tran, A. H., Ono, T., and Nishijo, H. (2013). Neuronal responses to face-like stimuli in the monkey pulvinar. *European Journal of Neuroscience*, 37(1):35–51.

O'Brien, B. J., Abel, P. L., and Olavarria, J. F. (2001). The retinal input to calbindin-D28k-defined subdivisions in macaque inferior pulvinar. *Neuroscience Letters*, 312(3):145–148.

Ogren, M. and Hendrickson, A. (1976). Pathways between striate cortex and subcortical regions in Macaca mulatta and Saimiri sciureus: Evidence for a reciprocal pulvinar connection. *Experimental Neurology*, 53(3):780–800.

Ogren, M. P. and Hendrickson, a. E. (1977). The distribution of pulvinar terminals in visual areas 17 and 18 of the monkey. *Brain Research*, 137(2):343–350.

Olszewski, J. (1952). *The Thalamus of the Macaca Mulatta: an atlas for use with the stereotaxic instrument*. Basle Switzerland, New York, USA.

Partlow, G. D., Colonnier, M., and Szabo, J. (1977). Thalamic projections of the superior colliculus in the rhesus monkey, Macaca mulatta. A light and electron microscopic study. *The Journal of comparative neurology*, 72(3):285–318.

Patrick Hardy, S. G. and Lynch, J. C. (1992). The spatial distribution of pulvinar neurons that project to two subregions of the inferior parietal lobule in the macaque. *Cerebral Cortex*, 2(3):217–230.

Petersen, S. E., Robinson, D. L., and Keys, W. (1985). Pulvinar nuclei of the behaving rhesus monkey: visual responses and their modulation. *Journal of neurophysiology*, 54(4):867–86.

Petersen, S. E., Robinson, D. L., and Morris, J. D. (1987). Contributions of the pulvinar to visual spatial attention. *Neuropsychologia*, 25(1 PART 1):97–105.

Purushothaman, G., Marion, R., Li, K., and Casagrande, V. a. (2012). Gating and control of primary visual cortex by pulvinar. *Nature Neuroscience*, 15(6):905–912.

Raczkowski, D. and Diamond, I. (1980). Cortical Connections of the Pulvinar Nucleus in Galago. *Journal of Comparative Neurology*, 193(1):1–40.

Raczkowski, D. and Diamond, I. T. (1981). Projections from the superior colliculus and the neocortex to the pulvinar nucleus in Galago. *The Journal of comparative neurology*, 200(2):231–254.

Rafal, R. D. and Posner, M. I. (1987). Deficits in human visual spatial attention following thalamic lesions. *Proceedings of the National Academy of Sciences of the United States of America*, 84(20):7349–53.

Rezak, M. and Benevento, L. A. (1979). A comparison of the organization of the projections of the dorsal lateral geniculate nucleus, the inferior pulvinar and adjacent lateral pulvinar to primary visual cortex (area 17) in the macaque monkey. *Brain Research*, 167(1):19–40.

Robinson, D. L. and Petersen, S. E. (1985). Responses of pulvinar neurons to real and self-induced stimulus movement. *Brain Research*, 338(2):392–394.

Robinson, D. L., Petersen, S. E., and Keys, W. (1986). Saccade-related and visual activities in the pulvinar nuclei of the behaving rhesus monkey. *Experimental Brain Research*, 62(3):625–634.

Rockland, K. S. (1996). Two types of corticopulvinar terminations: Round (type 2) and elongate (type 1). *Journal of Comparative Neurology*, 368(1):57–87.

Rockland, K. S. (1998). Convergence and branching patterns of round, type 2 corticopulvinar axons. *Journal of Comparative Neurology*, 390(4):515–536.

Rockland, K. S., Andresen, J., Cowie, R. J., and Robinson, D. L. (1999). Single axon analysis of pulvinocortical connections to several visual areas in the macaque. *Journal of Comparative Neurology*, 406(2):221–250.

Romanski, L. M., Giguere, M., Bates, J. F., and Goldman-Rakic, P. S. (1997). Topographic organization of medial pulvinar connections with the prefrontal cortex in the rhesus monkey. *Journal of Comparative Neurology*, 379(June 1996):313–332.

Saalmann, Y. B., Pinsk, M. A., Wang, L., Li, X., and Kastner, S. (2012). The pulvinar regulates information transmission between cortical areas based on attention demands. *Science (New York, N.Y.)*, 337(6095):753–6.

Schmahmann, J. D. and Pandya, D. N. (1990). Anatomical investigation of projections from thalamus to posterior parietal cortex in the rhesus monkey: A WGA-HRP and fluorescent tracer study. *Journal of Comparative Neurology*, 295(2):299–326.

Shipp, S. (2001). Corticopulvinar connections of areas V5, V4, and V3 in the macaque monkey: A dual model of retinal and cortical topographies. *Journal of Comparative Neurology*, 439(4):469–490.

Smith, S. M., Fox, P. T., Miller, K. L., Glahn, D. C., Fox, P. M., Mackay, C. E., Filippini, N., Watkins, K. E., Toro, R., Laird, A. R., and Beckmann, C. F. (2009). Correspondence of the brain's functional architecture during activation and rest. *Proceedings of the National Academy of Sciences of the United States of America*, 106(31):13040–5.

Stanton, G. B., Goldberg, M. E., and Bruce, C. J. (1988). Frontal eye field efferent in the macaque monkey. *The Journal of Comparative Neurology*, 271:473–506.

Stepniewska, I. (1999). Do superior colliculus projection zones in the inferior pulvinar project to MT in primates? *European Journal of Neuroscience*, 11(2):469–480.

Stepniewska, I. and Kaas, J. H. (1997). Architectonic subdivisions of the inferior pulvinar in New World and Old World monkeys. *Vis Neurosci*, 14(6):1043–1060.

Stepniewska, I., Ql, H. X., and Kaas, J. H. (2000). Projections of the superior colliculus to subdivisions of the inferior pulvinar in New World and Old World monkeys. *Visual neuroscience*, 17(4):529–49.

Symonds, L. L. and Kaas, J. H. (1978). Connections of striate cortex in the prosimian, Galago senegalensis. *The Journal of comparative neurology*, 181(3):477–512.

Trojanowski, J. Q. and Jacobson, S. (1974). Medial pulvinar afferents to frontal eye fields in rhesus monkey demonstrated by horseradish peroxidase. *Brain Research*, 80(3):395–411.

Trojanowski, J. Q. and Jacobson, S. (1976). Areal and laminar distribution of some pulvinar cortical efferents in rhesus monkey. *The Journal of comparative neurology*, 169:371–392.

Trojanowski, J. Q. and Jacobson, S. (1977). Brain The Morphology and Laminar Distribution of Cortico-Pulvinar Neurons in the Rhesus Monkey. *Experimental Brain Research*, 62(1-2):51–62.

Ungerleider, L., Galkin, T., and Mishkin, M. (1983). Visuotopic organization of projections from striate cortex to inferior and lateral pulvinar in rhesus monkey. *Journal of Comparative Neurology*, 217(2):137–157.

Ungerleider, L. G. and Christensen, C. A. (1979). Pulvinar lesions in monkeys produce abnormal scanning of a complex visual array. *Neuropsychologia*, 17(5):493–501.

Ungerleider, L. G., Desimone, R., Galkin, T. W., and Mishkin, M. (1984). Subcortical projections of area MT in the macaque. *The Journal of comparative neurology*, 223(3):368–386.

Ungerleider, L. G., Galkin, T. W., Desimone, R., and Gattass, R. (2014). Subcortical projections of area V2 in the macaque. *Journal of cognitive neuroscience*, 26(6):1220–33.

Vanni, M. P., Thomas, S., Petry, H. M., Bickford, M. E., and Casanova, C. (2015). Spatiotemporal Profile of Voltage-Sensitive Dye Responses in the Visual Cortex of Tree Shrews Evoked by Electric Microstimulation of the Dorsal Lateral Geniculate and Pulvinar Nuclei. *Journal of Neuroscience*, 35(34):11891–11896.

Walker, A. E. (1938). *The Primate Thalamus*. University of Chicago Press, Chicago, USA.

Wall, J. T., Symonds, L. L., and Kaas, J. H. (1982). Cortical and subcortical projections of the middle temporal area (MT) and adjacent cortex in galagos. *The Journal of comparative neurology*, 211(2):193–214.

Ward, R. and Arend, I. (2007). An object-based frame of reference within the human pulvinar. *Brain*, 130(9):2462–2469.

Webster, M. J., Bachevalier, J., and Ungerleider, L. G. (1993). Subcortical connections of inferior temporal areas TE and TEO in macaque monkeys. *The Journal of comparative neurology*, 335(1):73–91.

Weller, R. E., Steele, G. E., and Kaas, J. H. (2002). Pulvinar and other subcortical connections of dorsolateral visual cortex in monkeys. *Journal of Comparative Neurology*, 450(3):215–240.

Wilke, M., Turchi, J., Smith, K., Mishkin, M., and Leopold, D. A. (2010). Pulvinar Inactivation Disrupts Selection of Movement Plans. *Journal of Neuroscience*, 30(25):8650–8659.

Wong, P., Collins, C. E., Baldwin, M. K. L., and Kaas, J. H. (2009). Cortical connections of the visual pulvinar complex in prosimian galagos (Otolemur garnetti). *Journal of Comparative Neurology*, 517(4):493–511.

Yeterian, E. H. and Pandya, D. N. (1985). Corticothalamic connections of the posterior parietal cortex in the rhesus monkey. *J. Comp. Neurol.*, 237(3):408–426.

Yeterian, E. H. and Pandya, D. N. (1988). Corticothalamic connections of paralimbic regions in the rhesus monkey. *J Comp Neurol*, 269(1):130–146.

Yeterian, E. H. and Pandya, D. N. (1989). Thalamic connections of the cortex of the superior temporal sulcus in the rhesus monkey. *The Journal of comparative neurology*, 282(November 1986):80–97.

Yeterian, E. H. and Pandya, D. N. (1991). Corticothalamic connections of the superior temporal sulcus in rhesus monkeys. *Experimental brain research*, 83(2):268–84.

Yeterian, E. H. and Pandya, D. N. (1997). Corticothalamic connections of extrastriate visual areas in rhesus monkeys. *The Journal of comparative neurology*, 378(4):562–85.

CHAPTER 3
CORTICAL PROJECTIONS TO THE RETINOTOPIC MAPS OF GALAGO PULVINAR ARE DISTINCT

The study described in this chapter was published as Moore et al. (2018).

Comprised of at least five distinct nuclei, the pulvinar complex of primates includes two large visually driven nuclei; one in the dorsal (lateral) pulvinar and one in the ventral (inferior) pulvinar, that contain similar retinotopic representations of the contralateral visual hemifield. Both nuclei also appear to have similar connections with areas of visual cortex. Here we determined the cortical connections of these two nuclei in galagos, members of the strepsirrhine primate radiation, to see if the nuclei differed in ways that could support differences in function. Injections of different retrograde tracers in each nucleus produced similar patterns of labeled neurons, predominately in layer 6 of V1, V2, V3, MT, regions of temporal cortex, and other visual areas. More complete labeling of neurons with a modified rabies virus identified these neurons as pyramidal cells with apical dendrites extending into superficial cortical layers. Importantly, the distributions of cortical neurons projecting to each of the two nuclei were highly overlapping, but formed separate populations. Double labeled neurons were not found. Finally, the labeled cortical neurons were predominately in layer 6 and layer 5 neurons were labeled only in extrastriate areas. Terminations of pulvinar projections to area 17 was largely in superficial cortical layers, especially layer 1.

Introduction

After many years of study on the visual pulvinar of monkeys, there is general agreement that the visual pulvinar is a complex of five, or possibly more, nuclei with different architecture, connections, and functionality (Baldwin et al., 2017; Kaas and Lyon, 2007; Cola et al., 2005; O'Brien et al., 2001; Adams et al., 2000; Stepniewska and Kaas, 1997). While major features of this organization may apply to all anthropoid primates, including humans, how these features correspond with the visual pulvinar of stepsirrhine primates remain less certain. Importantly, early anatomical studies (Symonds and Kaas, 1978) and more recent electrophysiological mapping (Li et al., 2013) provide evidence for two large nuclei in stepsirrhine galagos that correspond to maps of the contralateral visual hemifield, and have connections with visual areas 17 and 18. In addition, the larger and more dorsal of these two nuclei appears to have a major role in gating the visual activity evoked in area

17 (Purushothaman et al., 2012). This more dorsal nucleus appears to be homologous to the lateral pulvinar nucleus, PL, of monkeys, while the more ventral nucleus likely corresponds to the central lateral nucleus, PI_{cl}, of monkeys (Baldwin et al., 2017). In galagos, these two nuclei were called the central nucleus of the superior pulvinar, SP_c, and the central nucleus of the inferior pulvinar, PI_c, in early studies (Symonds and Kaas, 1978) and the PL and PI_c more recently (Li et al., 2013). Here we refer to the two nuclei as the dorsal and ventral representations, corresponding to PL and PI_c, respectively.

A prominent feature of the visually responsive pulvinar in primates is the existence of two distinct retinotopic maps. Originally described in macaques (Ungerleider et al., 1983; Bender, 1981), these maps have also been observed in other primate species including capuchins and galagos (Li et al., 2013; Gattass et al., 1978) as well as functional imaging of retinotopy in humans (Arcaro et al., 2015). The earliest microelectrode map made being of what we now recognize as the PI_{cl} in owl monkeys (Allman et al., 1972). The retinotopic patterns of connections of parts of the visual pulvinar with cortical areas V1 and V2 across primate species are largely consistent with the existence of two maps (Baldwin et al., 2017). The two maps in the galagos are known to have reciprocal connections with early visual areas (Marion et al., 2013; Wong et al., 2009; Raczkowski and Diamond, 1981, 1980) that are involved in both ventral and dorsal streams of visual processing (Goodale and Milner, 1992; Mishkin and Ungerleider, 1982). The pulvinar maps have been reported to have major connections with cortical areas V1, V2, V3, V4, and MT (Raczkowski and Diamond, 1981). The galago's two maps in the visual pulvinar have been mapped and demonstrated to form almost mirrored representations from the dorsal to ventral nucleus (Li et al., 2013). Why does such an apparent redundancy exist? The answer may lie in the differences in circuitry that exists between these two visual pulvinar maps and the visual cortex. We used injections of tracer guided by concurrent electrophysiological recordings in the anesthetized galagos to show that cortical projections to the two maps are from distinct populations of cells spanning much of visual cortex. Additionally, we demonstrate that almost all of the labeled projecting neurons are layer 6 pyramidal neurons.

Materials and methods

Subjects

Four adult galagos (*Otolemur garnettii*) were used this study. These animals were cared for according to the National Institutes of Health Guide for the Care and Use of Laboratory Animals and according to a protocol approved by the Vanderbilt University Institutional Animal Care and Use Committee (IACUC). To reduce the number of these valuable primates used in experiments, some of the tissue from these animals was used in separate studies.

Surgery

Each of the following experiments shared a common surgical preparation (Li et al., 2013; Marion et al., 2013). Ketamine was used as an initial anesthetic sedative (10.3 mg/kg), in order to allow for surgical preparation and intubations. Anesthesia was then maintained via inhaled isoflurane (1-2% mixed in O_2). While fully anesthetized, the galagos were placed in a stereotaxic frame. The surgery was performed under aseptic conditions, and vital signs including heart rate, respiration rate, blood pressure, and body temperature were regularly monitored throughout the procedure. A unilateral craniotomy was made over occipital-parietal cortex, and the dura covering the exposed brain area was removed to allow the microelectrode mapping and tracer injection in the pulvinar. The anesthesia was then switched to intravenous propofol (2 mg/kg/hr) and respiration with nitrous oxide (67%). Intravenous paralytic (vecuronium bromide, 0.6 mg/kg/hr) was used to reduce eye movements and subtle modifications in the animal's lens so that our visual power correction with contact lenses remained correct for the animal.

Pulvinar injections

Parts of the dorsal and ventral retinotopic maps were carefully mapped with single tungsten electrodes (FHC, Inc., ME) at stereotaxic coordinates A-P: 3 mm, M-L: 5.5 mm, using visually evoked potentials in response to a simple stimulus consisting of a spot of light containing a crosshair pattern. The size of the spot was varied with eccentricity from the center of the visual field, becoming larger as it was moved farther from center, as the receptive fields of the visually-responsive pulvinar neurons get larger with eccentricity. These maps were compared to the data from previous experiments in order to corroborate locations (Li et al., 2013). In-house manufactured injectrodes, glass tubes pulled out to a fine (30μm) tip and attached to an electrode, were used to record and confirm locations,

and make subsequent injections. Injection locations were chosen as corresponding peripherally located (5-10° eccentricity from the center of the visual field) areas in the visual field within both maps to assure that: 1) the same area of the visual cortex was labeled from injections in each map and 2) there was no overlap between the injections. Injections were made via manual pressure, over the course of a few minutes. After each injection, the injectrode was left in the same position for 30 minutes to ensure that all the liquid had been evacuated before the injectrode was retracted.

The organization of corticopulvinar connections was revealed by injection of neuroanatomical tracers into the electrophysiology-identified representations in pulvinar. Two cholera toxin subunit B (CTB), two rabies, and one biotinylated dextran amine (BDA) tracers were used. The tracers were stored frozen at -80°C and kept frozen on dry ice until just before injection to prevent degradation. In 2 galagos, a total of 4μL of 1% CTB conjugated to Alexa-fluor 488 (green, Thermo Fisher) was injected at 2 different locations spaced 50μm apart within the ventral map, and a total of 4μL of 1% CTB conjugated to Alexa-fluor 594 (red, Thermo Fisher) was injected at 2 different locations spaced 50μm apart within the dorsal map in the same hemisphere. In addition, two different fluorescently-labeled modified rabies virus variants were injected into the other hemisphere in the same galagos. The tracers were designed to infect neurons at the injection site, but not infect other neurons by crossing synapses (Wickersham et al., 2007). A total of 4 μL of SADΔG–dsRed (red, 2 X 109 infectious units / ml) and a total of 4 μL of SADΔG–GFP (green, 2 X 109 infectious units / ml) were each injected at 2 different locations spaced 50μm apart within the dorsal and ventral maps, respectively, in one animal. CTB injections were made in one hemisphere of each animal's brain and, one week later, rabies injections were made in the other hemisphere. In another 2 galagos, a total of 300-450nL of 20kDA BDA conjugated to Alexafluor 488 (green, Thermo Fisher Scientific, Waltham, MA) was injected into the dorsal retinotopic map to label the thalamocortical projections to visual cortex.

After each surgery, the galagos were treated with prophylactic antibiotic and analgesics after recovery from anesthesia. After a one-week survival time following the CTB/rabies injection series or 2-4 weeks following BDA injections, the galagos were euthanized via sodium pentobarbital overdose (>120 mg/kg), their blood was cleared with 0.1M PBS, and then they were perfused transcardially with 1.5 L of a fixative consisting of 3% paraformaldehyde and 0.1% glutaraldehyde with 0.2% picric acid.

Tissue preparation

For all experiments, the brain was stereotaxically blocked in the coronal plane, with cuts immediately anterior and posterior to the pulvinar. After blocking, the brain was removed from the skull. The brain was then cryoprotected in 30% sucrose in 0.1M phosphate buffer solution, frozen, and cut into 50μm slices using a freezing microtome. Sections were stored at -80°C in a 20% glycerol in Tris buffer solution. Every third section was mounted on glass slides and coverslipped with Vectashield (Vector Labs). The sections were not dehydrated. These sections were used to visualize labeled cell bodies, axons, and dendrites. Adjacent sections were stained for cytochrome oxidase (CO) (Boyd and Matsubara, 1996) or parvalbumin (PV) (Wong and Kaas, 2010) and then mounted glass slides, dried overnight, and then dehydrated and coverslipped with DPX (Fisher). These CO and PV sections were used to reveal the architectural boundaries in the thalamus (Baldwin et al., 2012) and cortex (Wong and Kaas, 2010).

Antibody characterization

Anti-PV primary antibody: The mouse monoclonal antibody PV (mouse anti PV, Cat#P3088, Sigma-Aldrich, St. Louis, MO; Immunogen is frog parvalbumin) recognizes parvalubumin in a Ca^{2+} ion-dependent manner without reacting to other members of the EF-hand family. This primary antibody was used at the concentration of 1:2000.

Tissue imaging and analysis

Sections of pulvinar and visual cortex were observed using fluorescent microscopy (Zeiss M2 with an Axiocam MRC camera) to confirm that: 1) injections were made successfully into the general locations of the two maps and 2) there was labeling of neurons or axons in cortex. Locations of the labeled neurons within the cortical layers that were identified in adjacent brain sections processed for CO or PV. The boundary of areas 17/18 was determined by alignment with adjacent CO stained sections and the boundary of MT was determined using PV stained sections. The anterior boundary of area 18 was estimated based off of previously reported orientation maps gathered via optical imaging (Fan et al., 2012). Photoshop 6.0 (Adobe, San Jose, CA) was used to count the number of labeled cells of each tracer in selected brain areas that were identified by the adjacent CO or PV-processed sections. This was accomplished by using Photoshop's "count" tool which keeps a running count of cells as they are plotted. These values were then transcribed into a spreadsheet for final analysis.

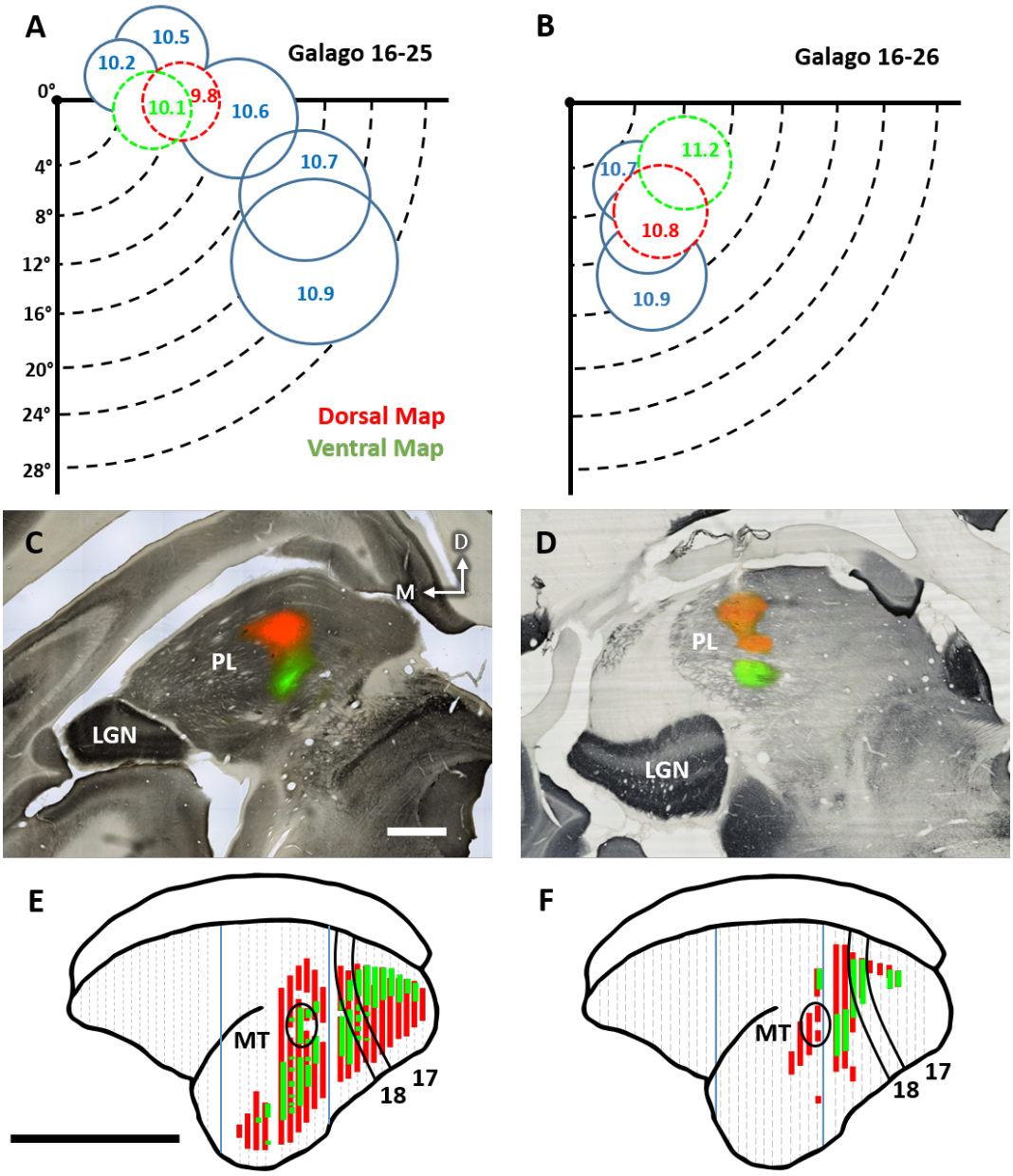

Figure 3.1: Distribution of cortical neurons labeled by CTB. A-B) Receptive fields for multiunit recordings in the dorsal and ventral maps in the pulvinar of galagos 16-25 and 16-26. The receptive fields are drawn on a depiction of the contralateral lower visual quadrant with 0° corresponding to area centralis of the retina. Receptive fields drawn in blue correspond to retinotopic mapping done using a tungsten electrode. Those fields drawn in red and green were obtained at the dorsal and ventral map injection sites, respectively. Indicated values are the cortical depths at which the circumscribed receptive fields were recorded. C-D) Coronal sections stained for CO overlaid on adjacent sections stained fluorescently for the injected CTB. Injection sites for the dorsal (red) and ventral (green) maps are shown. Scale bar is 1mm. E-F) The locations of populations of labeled neurons projecting to the dorsal map (red) and ventral map (green) in the coronal plane projected at a 45° angle onto the reconstructed dorsolateral surface of cortex. Borders of areas 17, 18, and MT indicated in black. Blue lines indicate tissue blocking cuts. Dashed grey lines indicate every ninth section of tissue. Scale bar is 1cm.

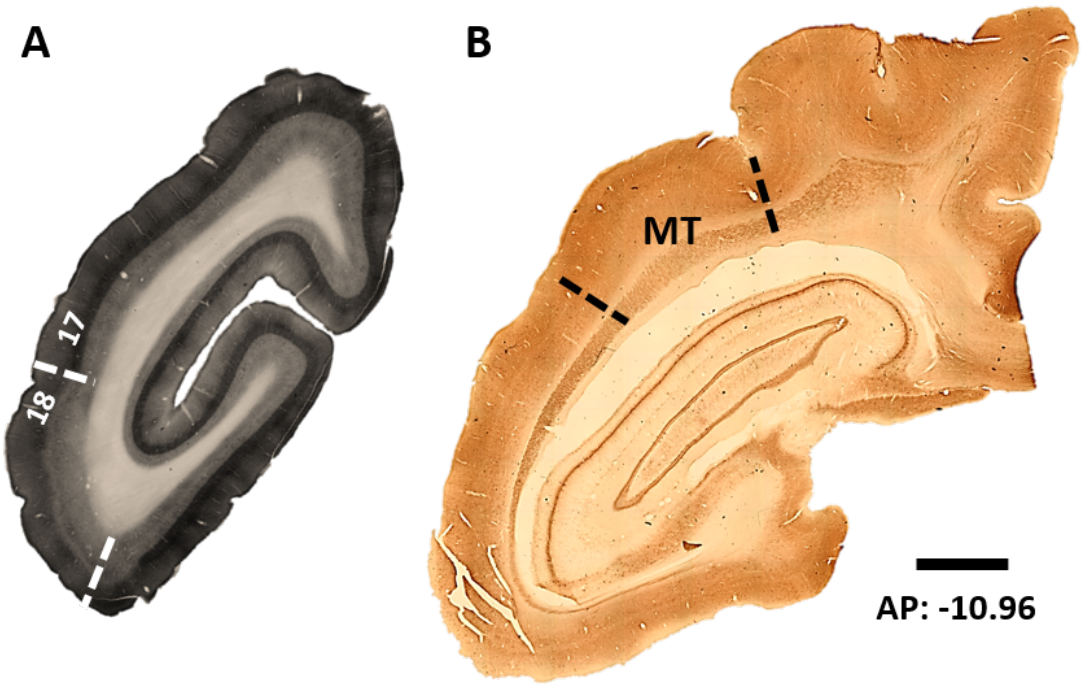

Figure 3.2: Histology shows Area 17/18 border and boundaries of area MT. A) A coronal section stained for CO not only reveals the border between areas 17 and 18 but also allows for the discrimination of different cortical layers. B) A coronal section stained for PV reveals the boundaries of area MT. Scale bar is 1000μm.

Results

The present study focused on two main issues, determining the cortical areas and regions that project to each of the two large, retinotopically organized nuclei of the pulvinar complex, and characterizing the laminar distribution of the projecting neurons. Injections of retrograde tracers into physiologically identified sites in the two nuclei, revealed both the areal and laminar patterns of the projecting neurons. In addition, similar injections of modified rabies as a tracer confirmed the results from the CTB injection, while labeling fewer cortical neurons but more completely. Thus, labeled neurons were clearly revealed as pyramidal neurons with long apical dendrites. Finally, injections of BDA into the dorsal (lateral) nucleus revealed the projections of this nucleus into layer 1 of area 17. Given the limited availability of galagos for these studies, our results are based on relatively few cases.

CTB injections reveal overlapping distributions of layer 6 neurons

Cortical areas and layers with neurons projecting to each of the two pulvinar maps were identified by injecting distinguishable red or green tracers into the two maps into the same cerebral hemisphere. It was important to inject the tracers into retinotopically matched

parts of the two nuclei, as only retinotopically congruent injections would likely double label neurons having projections to both nuclei (Cusick et al., 1985). Thus, recordings were made with tungsten microelectrodes to locate the visual fields in the two nuclei, and favorable recording sites in the two nuclei were targeted with an injection pipette attached to an electrode, CTB-red was injected into the dorsal map and CTB-green in the ventral map. Results from the two more successful cases are shown in (Figure 3.1).

As shown in (Figure 3.1), the injections were placed by the receptive fields of pulvinar neurons into paracentral vision of both maps, near the horizontal meridian in case 16-25 and 10° into the lower visual quadrant in case 16-26. The CTB uptake zone spread in both nuclei for both cases, but did not overlap. In both cases, large regions of visual cortex contained labeled neurons (Figure 3.1E,F). Many more neurons were labeled in case 16-25 and these neurons were distributed in area 17 within the contralateral portion representing the central 10° of visual space near the horizontal meridian (Rosa et al., 1997). The zone of labeled neurons also included parts of V2 and V3 devoted to central vision, much of the territory of visual area DL (V4), visual area MT and other areas of the MT complex, and much of inferior temporal cortex. Only the borders of V1 and MT were histologically evident, so that the appropriate locations of other areas were estimated from previous studies (Wong and Kaas, 2010). Results from case 16-26 were less extensive, but similar. Labeled neurons in V1, V2, and V3 were more medial than in case 16-25, as expected as this part of cortex represents central vision in the lower visual quadrant, matching the physiological location of the injection sites. Often labeled neurons were in DL, the MT complex, and upper parts of the inferior temporal (IT) cortex. Importantly, the distribution of red (dorsal map) and green (ventral map) labeled neurons largely overlapped. Thus, both the nuclei receive inputs from overlapping parts of several visual areas. Note also that many parts of cortex were not labeled. Notably, retinotopically mismatched parts of early visual areas, V1, V2, and V3 were not labeled, nor were regions of cortex with connections to the medial pulvinar (association areas of the temporal, parietal, and frontal lobes).

In both cases, the 17/18 border was clearly apparent in the brain sections processed for CO (Figure 3.2A). The prominent layer 4 of area 17 was apparent, as was a slightly less prominent layer 6. Thus, it was possible to assign labeled neurons to area 17 (V1) and to area 18 region (due to the estimated width of V2), and to area MT in sections processed for PV (Figure 3.2B).

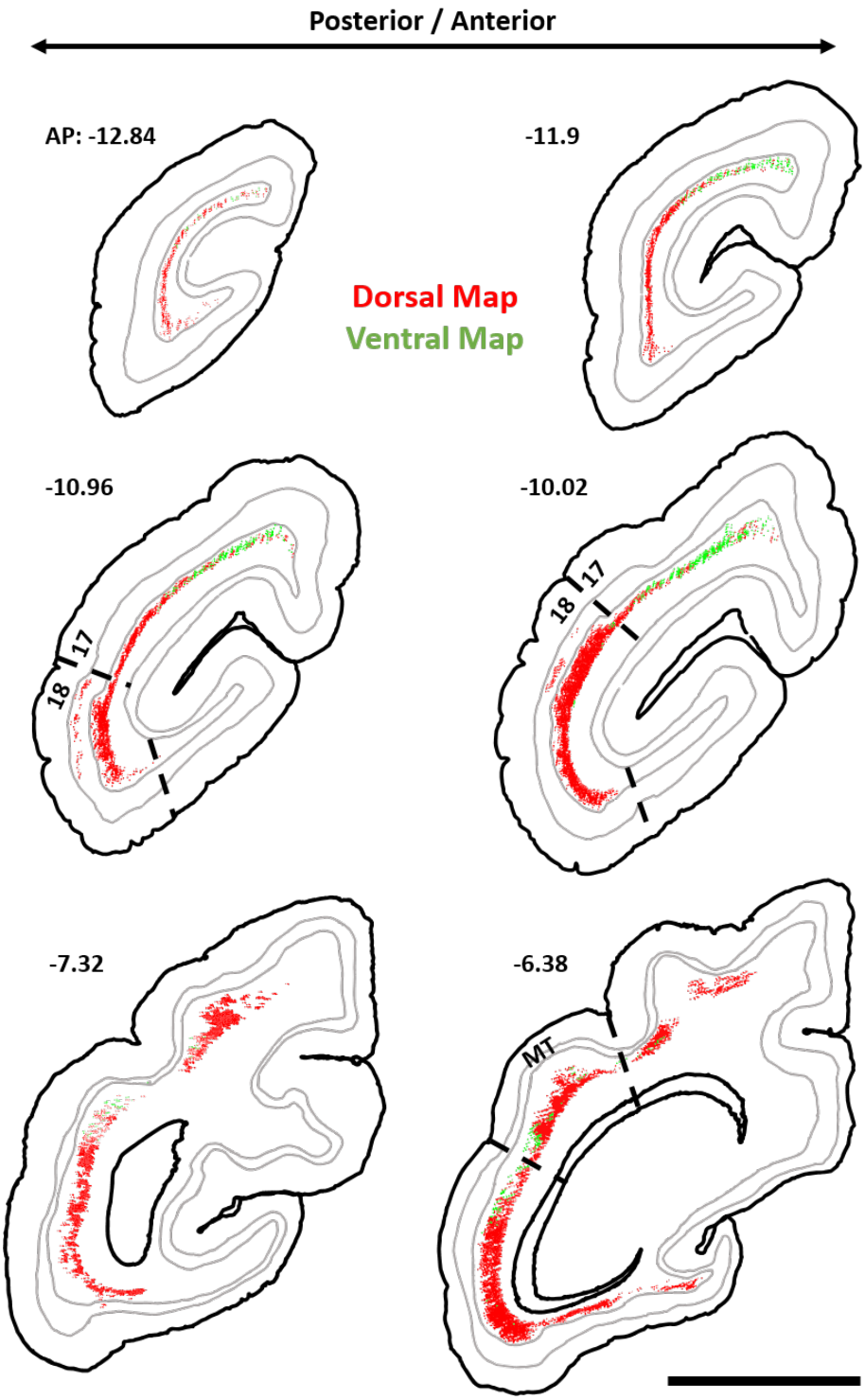

Figure 3.3: Coronal sections of CTB labeled cortex. Subject 16-25's CTB labeled cortex arranged posterior to anterior in a left-to-right descending direction. The location of labeled cells projecting to the dorsal map are shown in red while those projecting to the ventral map are shown in green. The internal borders drawn in grey are the layer 4/5 and 5/6 borders. Areas 17, 18, and MT are delineated on appropriate sections. AP level indicated for each section.

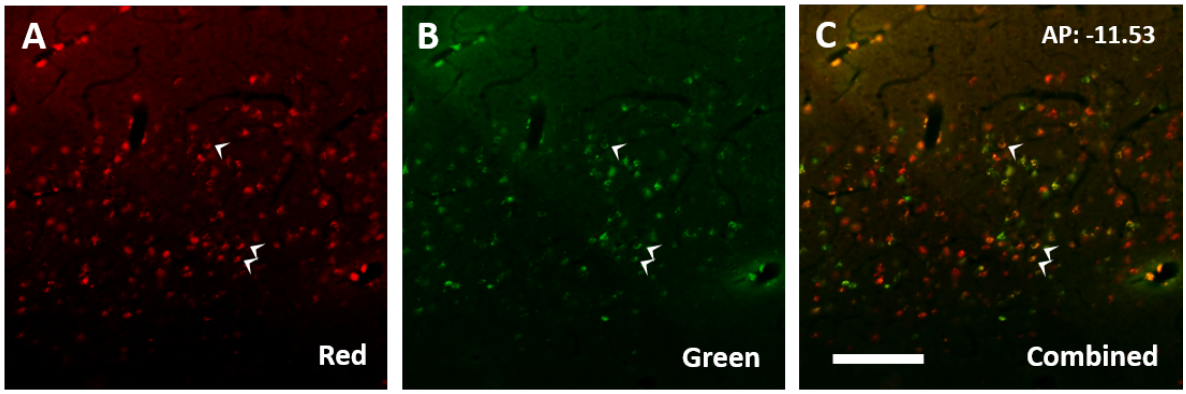

Figure 3.4: Coronal sections of CTB labeled cortex. These images show neurons labeled by CTB within area 17 of subject 16-26. Labeled neurons in layer 6 of area 18 as seen through a red (A), green (B), and combined (C) filters. Double labeled neurons are indicated by white arrowheads. Scale bar is 60μm.

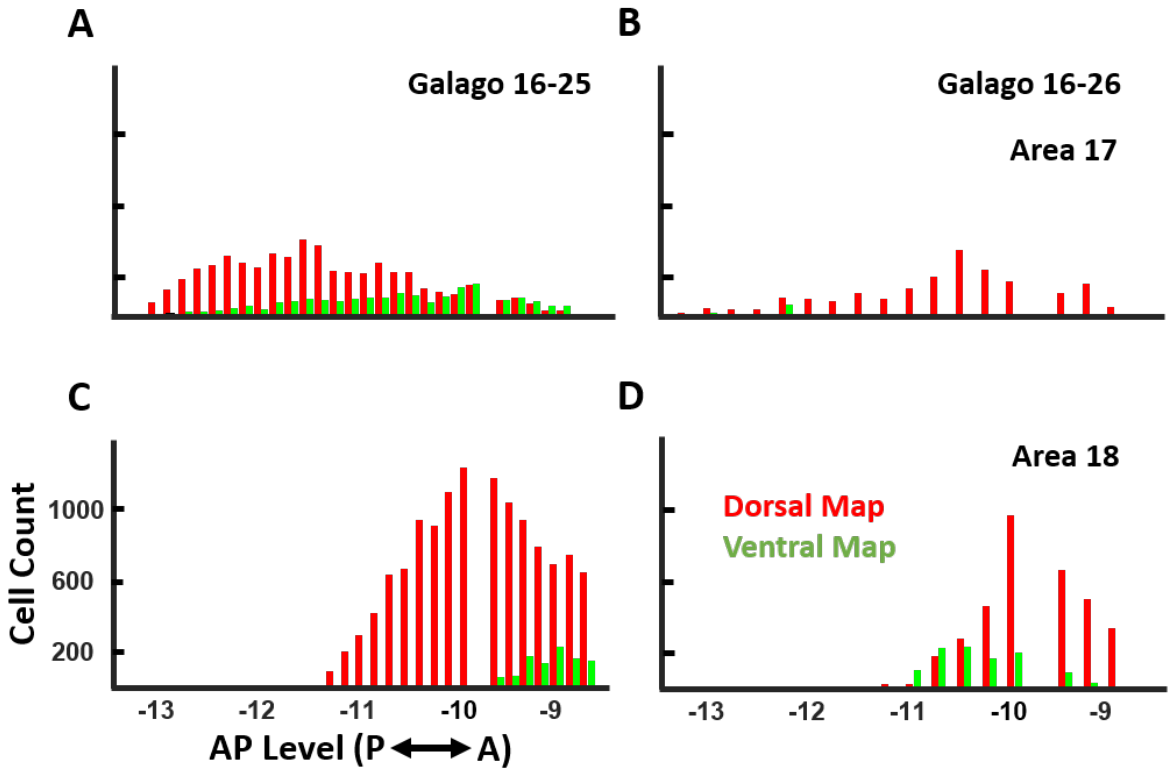

Figure 3.5: Histogram of pulvinar projecting cells in V1 and V2. Cell counts from two subjects for layer 6 neurons projecting to the dorsal (red) and ventral (green) maps from A-B) area 17 and C-D) area 18, arranged from posterior to anterior.

	Galago 16-25			Galago 16-26		
	Area 17	**Area 18**	**Area MT**	**Area 17**	**Area 18**	**Area MT**
Layer 5	0 ; 0	296 ; 0	0 ; 0	0 ; 0	0 ; 0	0 ; 0
Layer 6	5795 ; 2117	13461 ; 1140	547 ; 144	2234 ; 100	3419 ; 1047	171 ; 18

Table 3.1: CTB labeled cell counts by cortical area and layer. A count of all observed cells in areas 17, 18, and MT. Numbers on the left in each couplet correspond to those cells labeled by dorsal map injections while those on the right represent the ventral map injection.

The injections also revealed the laminar locations of the labeled cortical neurons. Examples of these are illustrated for case 16-25 in Figure 3.3. The sections shown are those more densely labeled in caudal visual cortex from area 17 through to the middle of MT. Throughout areas V1, V2, V3, DL, MT, and IT, the labeled neurons were almost exclusively in layer 6, although a few were in layer 5 in area 18 (V2) (see AP -10.96 and -10.02). Of the over 14,000 area 18 neurons labeled in this case, only 296 were in layer 5. Results from case 16-26 were less extensive, but again labeled neurons were almost exclusively found within layer 6 (Figure 3.4). As projections from layer 6 are thought to have a modulating influence on thalamic neurons, while layer 5 projections are thought to have a driving influence (Bickford et al., 2015), these results suggest that cortical inputs to the pulvinar maps are predominately modulating.

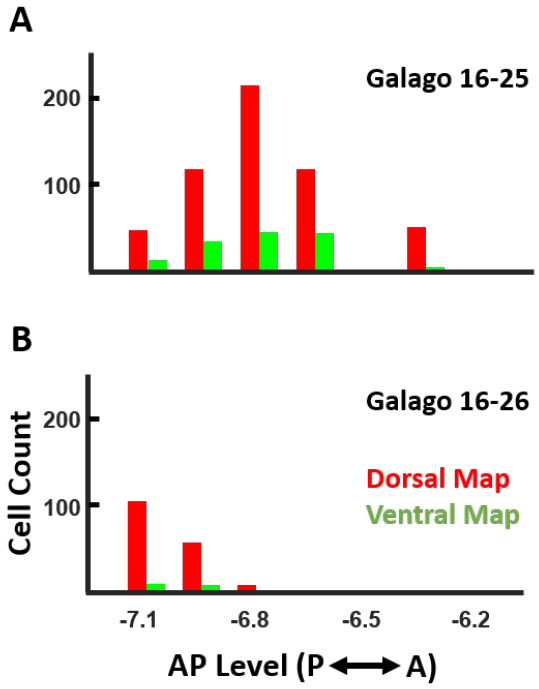

Figure 3.6: Histogram of pulvinar projecting cells in MT. Cell count histograms of layer 6 MT neurons projecting to the dorsal (red) and ventral (green) maps of two subjects, galagos A) 16-25 and B) 16-26 with 0 on the horizontal axis representing the location of our blocking cut.

Quantitative measures of numbers of labeled neurons in V1 and V2 are shown for the two cases in Figure 3.5. Labeled neurons were counted in a series of posterior to anterior coronal brain sections for each cortical region or area. For case 16-25, 5795 neurons were labeled in V1 by the dorsal map injection (red) and 2117 were labeled by the ventral map injection (green). The number of labeled neurons varied across sections, with the ventral map green neurons numbers shifted somewhat toward anterior sections compared to the

dorsal map red neurons, although the populations overlapped extensively. This slight shift toward the V1-V2 border for the population of neurons labeled by the injection in the ventral map likely reflects the slightly more central location of the ventral injection site within the retinotopic maps (Figure 3.1C,D).

In the V2-V3 region, neuron counts for case 16-25 were high with 13461 red dorsal map projecting neurons and 1140 green ventral map projecting neurons, again with a high level of overlap. The peak of the distribution of green labeled neurons was more anterior. Based on previously reported cortical mapping, this peak possibly occurs more within V3. Results from the injection in case 16-26 were similar, but fewer neurons were labeled. The overlap in V1 was limited, as the ventral injection labeled few V1 neurons. More overlap of labeled neurons occurred in the V2-V3 distributions, possibly as a result of the larger receptive fields for V2 and V3 neurons, and the repeating modular organizations of these areas (Fan et al., 2012). Results from case 16-26 also show higher cell counts in the V2-V3 region, but fewer labeled neurons from the ventral pulvinar map injection.

Counts of labeled neurons in area MT were also obtained for the injections in the dorsal and ventral pulvinar maps (Figure 3.6). For case 16-25, a total of 691 neurons were labeled in the MT region within layer 6. The counts were lower for the injection into ventral map than for the dorsal map, but the distributions overlapped extensively with no incidence of double labeled neurons. A smaller number of neurons were labeled in the MT region in case 16-26, but again the population overlapped.

Cortical neurons labeled by modified rabies virus

We injected a modified rabies virus into the pulvinar maps of two galagos. The virus was modified to infect neurons at the injection sites, but not infect other neurons by crossing synapses (Wickersham et al., 2007). As for the CTB injections, the modified rabies virus also presented a red or green fluorescent marker. The advantage of the virus injections was that cortical neurons projecting to the injection sites would be infected, and the replicating virus within the cortical neurons would intensify the signal, revealing more of the cell morphology of the cortical neurons. We made red and green viral injections in the pulvinar in case 16-25 with limited success. Only the injection in the ventral map (GFP tagged virus) labeled cortical neurons and these were scattered in throughout V1-V3 and more rostral visual areas. In case 16-26, the virus injections were more readily taken up from both injection sites, and a large number of cortical neurons were labeled.

The results from the two virus cases fully support the conclusions based on the CTB injections. In case 16-26 where the injections were more effective, large numbers of cortical neurons were labeled across visual areas V1, V2, V3, DM, DL, MT, and IT (Figure 3.7).

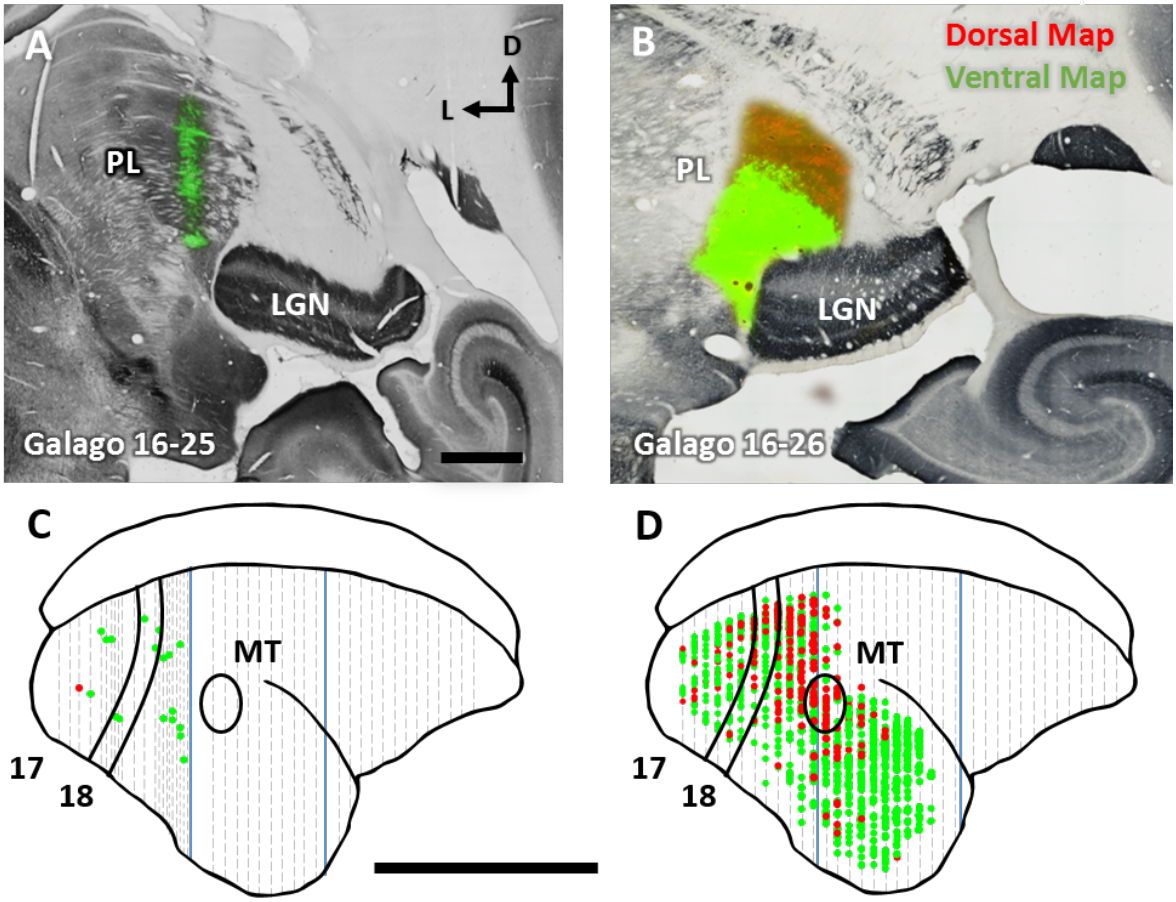

Figure 3.7: Distribution of cortical neurons labeled by rabies. Distributions of labeled neurons in visual cortex after injections of rabies tracers into the retinotopic maps in the lateral and inferior pulvinar in two galagos. A-B) Coronal sections stained for CO overlaid on adjacent sections stained fluorescently for the injected rabies. Injection sites for the dorsal (red) and ventral (green) maps are shown. Scale bar is 1cm. C-D) Labeled neurons descending to the dorsal map (red) and ventral map (green) projected at a 45° angle onto the surface of cortex, as in Figure 3.1. Borders of areas 17, 18, and MT indicated in black. Scale bar is 1cm

Rostral parts of temporal cortex, possibly including higher order auditory or multisensory cortex were also labeled suggesting that especially the ventral injection may have spread to other pulvinar nuclei. Part of posterior parietal cortex was damaged so labeled neurons may have been overlooked in this region. Overall, 15292 neurons in these cortical areas were labeled and all but relatively few were in layer 6 (Figure 3.8). Examples of labeled neurons are shown for areas 17, 18, and MT in Figure 3.9. The virus more fully labeled neurons so that apical dendrites extending toward layer 1 were fluorescent and revealed in detail. All labeled neurons, red or the more numerous green, appeared to be pyramidal neurons with long apical dendrites that extended into superficial cortical layers toward or into layer 1. Finally, we did not find neurons that were double labeled from the two

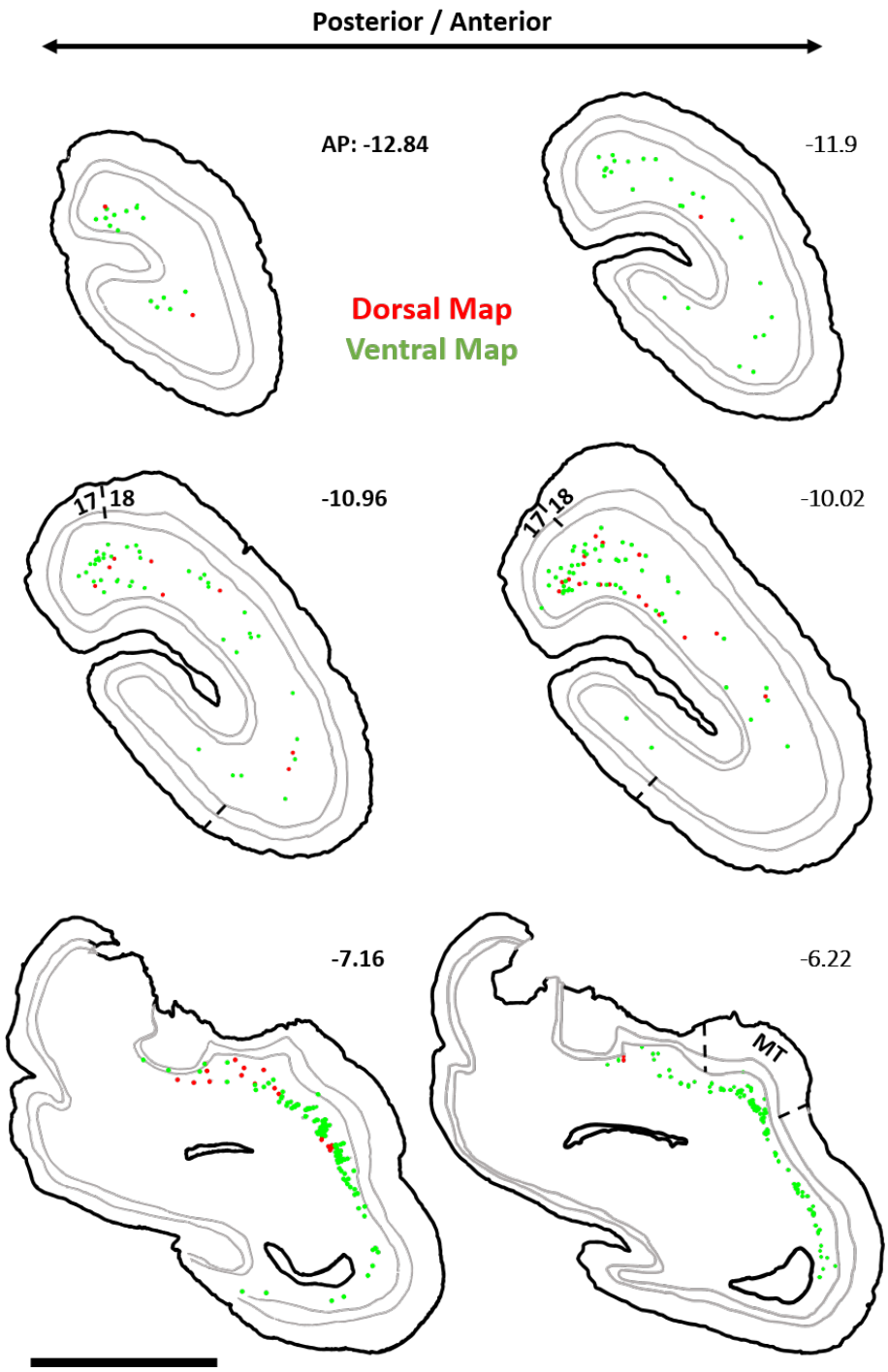

Figure 3.8: Coronal sections of rabies labeled cortex. Neurons labeled in visual cortex after rabies virus injections into the dorsal and ventral pulvinar maps in galago 16-26. The locations of labeled cells projecting to the dorsal map are shown in red while those projecting to the ventral map are shown in green. The coronal sections are arranged in a posterior to anterior sequence. The internal borders drawn in grey are the layer 4/5 and 5/6 borders. Areas 17, 18, and MT are delineated on appropriate sections. AP level indicated for each section.

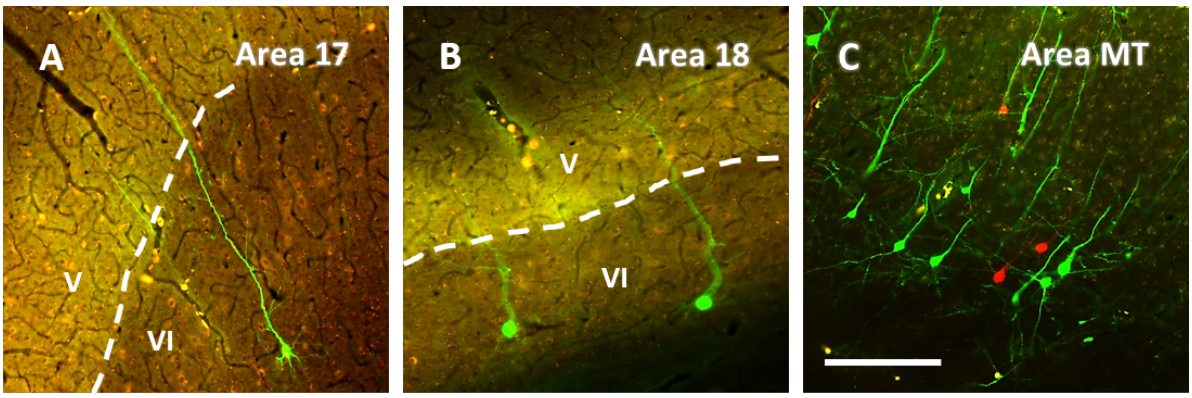

Figure 3.9: Representative rabies labeled cells in areas 17, 18, and MT Representative sections from areas 17 (A), 18 (B), and MT (C) demonstrating rabies labeled cells projecting to the dorsal (red) and ventral (green) maps of visual pulvinar. The border between layers 5 and 6 is indicated with a white dotted line when visible in the image. Scale bar is

pulvinar injections. Thus, projections from cortical areas to the dorsal and ventral maps were from distinct, but overlapping distributions of neurons.

BDA injections in the dorsal map

The pulvinar's thalamocortical projections to V1 were examined using injections of BDA as an anterograde tracer placed in the dorsal map of two galagos. The tracer injection locations were guided by microelectrode recordings and confirmed to be in the region of the dorsal pulvinar maps histologically. Injections spread along the injection tract (dorso-ventral axis) with the largest observed spread spanning about 1mm along this dimension (Figure 3.10A).

Much like the retrogradely labeled cortical neurons described above, labeled axons were observed within several visual areas in cortex. Projections that terminate in area 17 tended to ascend through the layers of cortex in a largely non-branching matter only arborizing once they reach layer 1. In layer 1, the processes branch and send collaterals in opposite directions at the border between the upper and lower halves of layer 1 . A small number of axons were observed to ascend to the top of layer 1 and have only local arborizations. Additionally, a few axons produced boutons as they passed through the inner half of layer 1. However, no extensive arborization was observed. Rarely, axons were observed to form arbors in layers 2/3 that continued to climb into layer 1 where they arborized more broadly. The arbors that were contained in layers 2/3 tended to remain confined locally to an area smaller than a single vertical column.

Projections to area 18 were also examined. These projections primarily terminated in layer 4 with a small minority terminating in lower layer 2 and upper layer 1. Axons

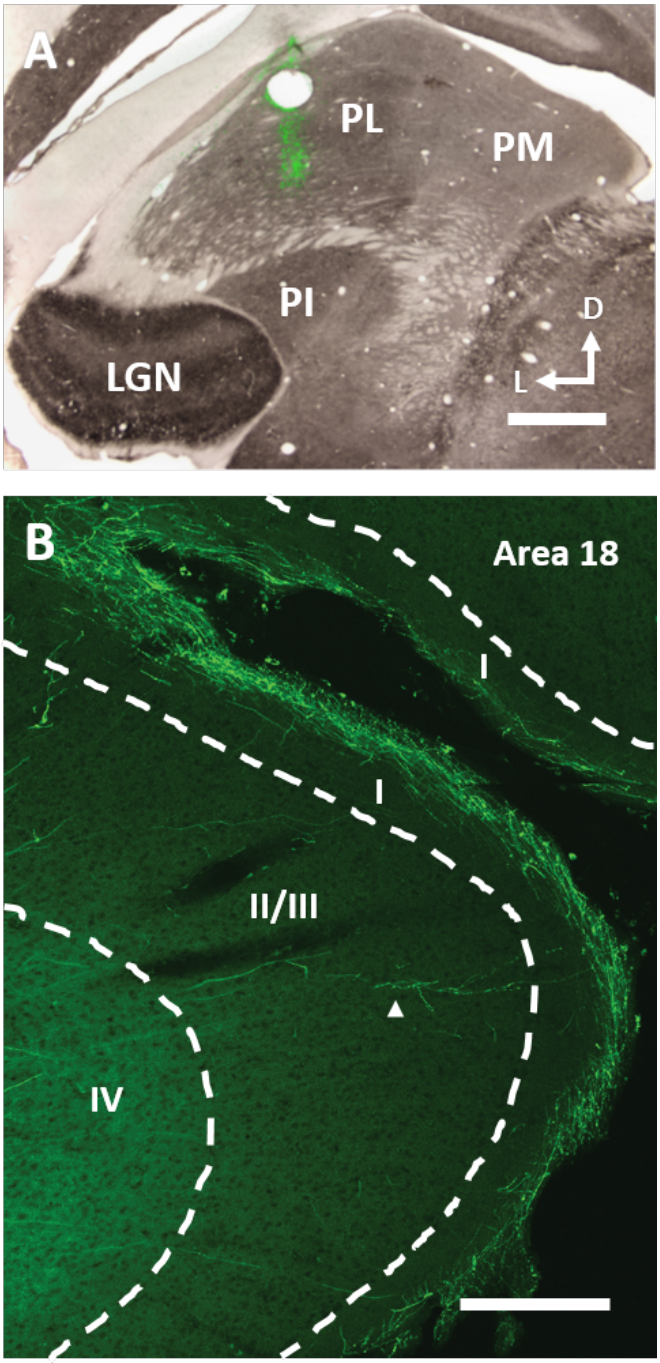

Figure 3.10: BDA reveals the pulvinar's V1 terminations. Distributions of labeled processes in visual cortex after injections of BDA into the dorsal map in the lateral pulvinar of the galago. A) A coronal section stained for CO overlaid on an adjacent section stained fluorescently for the injected BDA. The injections were localized to the dorsal map within PL. Scale bar is 1mm. B) Pulvinar projections to area 17 (green). Axons can be seen to form arbors in a dense band in the most superficial part of layer 1. Sometimes arbors are observed in upper layer 2/3 (indicated by an arrow). CO = cytochrome oxydase, BDA = biotinylated dextran amine, PI = inferior pulvinar, PL = lateral pulvinar, PM = medial pulvinar, LGN = lateral geniculate nucleus. Scale bar is 200μm.

extending into layer 1 branched in a similar pattern as seen in area 17. The spread of these layer 1 processes, however, matched the spread of the axons in layers 3/4 below them. This terminal labeling of area 18 has been previously reported in detail by Marion et al. (2013). Projections to other areas were sparse and were not examined in detail.

Discussion

In the present study, we injected tracers into two nuclei of the pulvinar complex in galagos, a stepsirrhine primate, in order to come to a better understanding of the connections and functions of these two nuclei. Galagos, as for other studied primates, have two large nuclei in the visual pulvinar that contain similar retinotopic maps with similar connections with primary visual cortex and other visual areas (Baldwin et al., 2017). In monkeys, the more ventral map corresponds to the central-lateral nucleus of the inferior pulvinar, PI_{cl}, while the more dorsolateral map occupies most or all of the lateral pulvinar, PL. Other parts of the inferior pulvinar include the posterior nucleus, PI_p, the medial nucleus, PI_m, and the central-medial nucleus, PI_cm. PI_p, CI, and PI_cm all project to the upper part of the temporal lobe where the middle temporal visual area, MT, and functionally associated visual areas (see Kaas and Morel, 1993) are located. PI_p and PI_cm get their activating VGluT2 positive inputs from neurons in the deep superficial grey of the superior colliculus, while PI_{cl} and PL receive only sparse inputs from the superior colliculus (Kwan et al., 2018). Thus, the two large retinotopic maps in PI_{cl} and PL appear to be most clearly related to early visual areas, while the more medial nuclei of the inferior pulvinar, PI_p, PI_m, and PI_cm, appear to be more related to cortex in the upper temporal lobe (Kaas and Lyon, 2007).

The organization of the visual pulvinar in galagos is similar to that of monkeys in that two large retinotopic maps have been defined. One of these maps is in the inferior pulvinar and one is in the superior pulvinar (Li et al., 2013; Symonds and Kaas, 1978) suggesting that part of the pulvinar complex is rotated so that PL is superior and PI_{cl} is inferior but more lateral. Other parts of the inferior pulvinar are medial, but rotated dorsally and caudally so that part of the thalamus occupied by the medial pulvinar in monkeys is occupied by the inferior pulvinar in galagos (Baldwin et al., 2013). As the different nuclei of the visual pulvinar in galagos are more difficult to distinguish architechtonically in galagos than in monkeys, it was important in the present study to locate injection sites in the large dorsal and ventral retinotopic maps with microelectrode recordings. While some slight spread of injected tracers could have included other parts of the pulvinar, such spread appeared to be minimal. And no significant spread occurred into

the dorsal lateral geniculate nucleus, LGN, as judged by the spread of tracer around injection sites in histological brain sections and the lack of anterograde transport of tracer to layer 4 of area 17.

Distribution of cortical neurons projecting to the pulvinar's maps

Injections of either CTB or the modified rabies virus into the dorsal or the ventral retinotopic maps in the visual pulvinar labeled populations of neurons extending over much of visual cortex of galagos, including areas 17 (V1), 18 (V2), and MT as well as the regions of V3, DL (V4), MST, and the caudal temporal lobe (IT). As V1 and V2 are the largest of visual areas, V1 and V2 provided most of the cortical inputs to the dorsal and ventral maps. As expected from the locations of the injection sites in parts of the two maps, the labeled neurons were in dorsolateral parts of V1 and V2 representing central and paracentral vision (Rosa et al, 1997). The distribution of labeled neurons in the cortical map in MT (Allman et al, 1973) was proportionately larger, as expected from the larger receptive fields of neurons in MT and in adjoining cortex.

After all injections into both pulvinar maps, labeled neurons were exclusively in layer 6 of area 17, and largely, but not exclusively, in layer 6 in other visual areas. In the cortical territories of V2 and V3, some neurons were labeled in layer 5. In the CTB cases with retinotopically matched injections in the two maps, neurons in overlapping populations were either labeled by the ventral or the dorsal map injection, and double labeled neurons were not seen in any of the cortical areas. Thus, it seems likely that the vast majority of cortical inputs to the two maps are from separate populations of neurons that spead across several cortical areas. While the information transmitted from each cortical area to the two pulvinar maps may be similar, it could be as least slightly different due to the separate populations of projecting neurons across cortical areas and functional divisions within cortical areas of columns and minicolumns (Kaas, 2012).

Our finding that a number of cortical visual areas, but especially V1 and V2, project to the dorsal (PL) and ventral (PI_{cl}) maps is largely consistent with previous findings. In galagos, precise comparisons can be difficult as previous results were based on injection sites that were not identified by microelectrode recordings, and the injection sites could be larger, and involve more nuclei. For example, in the study of Raczkowski and Diamond (1981), injections of horseradish peroxidase (HRP) were placed in either the superior or inferior pulvinar and neurons in variable locations in visual cortex were labeled, including areas 17, 18, 19, MT, and much of temporal cortex, as in the present study. Overall, the results from injections in the inferior and superior pulvinar were roughly similar. While the injections almost certainly involved the dorsal and ventral maps, other parts of the

pulvinar were likely involved as injections also labeled neurons in the lower superficial layer of the superior colliculus, where the neurons are known to project to the inferior pulvinar homologs of PI_p and PI_cm (Baldwin et al., 2017, 2013).

Unlike the present results, neurons labeled in V1 (area 17) of the Raczkowski and Diamond (1981) were only in layer 5. While the great majority of labeled neurons in other areas were in layer 6, a few in areas 18 and 19 were in layer 5, as in the present study. Thus, the major difference in findings was in the labeling of only layer 5 neurons in area 17 in the Raczkowski and Diamond (1981) study and only layer 6 neurons in the present study. However, the projections of layer 5 neurons in area 17 to the pulvinar was expected from the results of anatomical and physiological experiments in monkeys. In macaque monkeys, projections to the pulvinar have repeatedly been described as coming from layer 5, while projections from other visual areas have been described as coming almost completely from layer 6 (Levitt et al., 1995; Trojanowski and Jacobson, 1977; Lund et al., 1975). This laminar distinction is important as layer 5 is considered the source "driving" inputs to the thalamus, while layer 6 provides modulating inputs (Bickford, 2016; Rovo et al., 2012; Sherman and Guillery, 1998). Thus, layer 5 inputs to the dorsal and ventral maps would activate neurons, provide these neurons with their basic response characteristics, and mediate retinotopy. As expected from this proposed role of the layer 5 projections to the pulvinar, lesions of area 17 in macaque monkeys renders neurons in the retinotopic pulvinar maps to be largely unresponsive to visual stimuli (Bender, 1983, 1981).

The laminar differences in the labeling of only layer 5 or only layer 6 neurons in area 17 of galagos in the study of Raczkowski and Diamond (1981) and the present study in galagos, and that of others in monkeys, are difficult to explain. However, somewhat different results were reported when Conley and Raczkowski (1990) reexamined the pattern of cortical projections to the pulvinar in galagos. After injections of the retrograde tracer, wheat germ agglutinin conjugated to horseradish peroxidase (WGA-HRP) into the pulvinar of three galagos, large regions of area 17 had large populations of labeled neurons in layer 6 (as many as 75%). Smaller numbers of larger neurons were labeled in the upper half of layer 5. By injecting another tracer into the LGN in the same cases, it was apparent that pulvinar and LGN injections labeled separate populations of layer 6 neurons in area 17. In macaque monkeys, Rockland (1996) made injections in area 17 to label terminations in the pulvinar, and described two types: type one had anatomical features of modulator functions, while type 2 had the expected features of driving functions. While Rockland (1996) assumed that all projections to the pulvinar from area 17 were from layer 5 neurons, based on Lund et al. (1981), it now seems more likely that the type 1 modulator projections from area 17 to the pulvinar were from layer 6 neurons, and only type 2 driving projections

were from layer 5 neurons. Both type 1 and type 2 terminations have been reported in the lateral posterior "nucleus", the homolog of the pulvinar, in rats after area 17 injections (Bourassa and Deschenes, 1995; Marion et al., 2013), and they likely exist in all mammals.

It remains uncertain why the injections in the dorsal and ventral pulvinar maps in the present cases did not label layer 5 neurons in area 17, and labeled relatively few in extrastriate cortex. Conley and Raczkowski (1990) argued that pulvinar injections in their cases labeled both layer 6 and layer 5 neurons in area 17 because WGA-HRP is a "much more sensitive method". Layer 5 neurons in area 17 of galagos were clearly labeled after pulvinar injections in earlier studies (Conley and Raczkowski, 1990; Raczkowski and Diamond, 1981), and Conley and Raczkowski (1990) also found that area 17 sends projections from layer 5 neurons to the pulvinar. The differences in results across experiments could reflect the use of different tracers, the placements of injections within the maps, the lack of involvement of injected tracers in other parts of the pulvinar, and the post injection transport times. The large representations in PL and in PI_cm are likely to be involved in many of the injection sites, but other parts of the pulvinar could be variably involved. In addition, the three dimensional retinotopic maps have a dimension of isorepresentation and the cortical inputs along the columns of isorepresentation could differ, as suggested by Shipp (2001). For now, it is uncertain why layer 6 neurons or layer 5 neurons are sometimes labeled with pulvinar injections, and sometimes not. Finally, the inactivation of the retinotopic maps in PL or PI_{cl} by lesions of area 17 could be the result of the loss of area 17 layer 5 inputs to the pulvinar, in combination with the inactivation of V2 and other areas of extrastriate cortex by the lesions (Schiller and Malpeli, 1977), as these areas send some layer 5 projections to the pulvinar maps.

Projections from the dorsal map to cortex

The dorsal retinotopic map (PL) of galagos projects to area 17 (V1), area 18 (V2), and more sparsely to other visual areas. These projections were revealed by BDA injections into the dorsal map in two galagos. The terminations in area 17 were mainly in layer 1, which suggests that they have a modulating role by synapsing on the ends of apical dendrites of pyramidal cells in layers 3, 5, and 6. In our galago cases, the labeling of layer 6 neurons in area 17 by the rabies virus injected in the dorsal map was dense enough to reveal long apical dendrites that extended well into layer 3 and likely into layer 1. Thus, dorsal map projections to layer 1 of area 17 could modulate the layer 6 feedback to the dorsal map. Other terminations in layers 2 and superficial third of layer 3 could also synapse on the dendrites of layer 6 neurons. The projections of the dorsal map (PL) neurons to area 18 (V2) terminate near the layer 4 junction with layer 3. These inputs

could be a source of driving input to V2. Projections to more rostral visual areas could be detected but were sparse. These results are similar to those reported previously in galagos (Marion et al., 2013) where dense projections were described from the dorsal map to layer 1 of area 17, and inputs to area 18 (V2) were mainly to layer 4 and inner layer 3. Marion et al. (2013) concluded from these results that PL could be a driver of neural activity in V2, while inputs to V1 would gate information outflow from V1 to V2 (Purushothaman et al., 2012). In squirrel monkeys, large injections involving the lateral and inferior pulvinar labeled axon terminations in much of the temporal lobe and into the temporal lobe that were more dense in lower layer 3 in area 18 but also in layers 5 and 6 (Curcio and Harting, 1978). Similar findings have been reported in macaque monkeys where injections including PI and PL labeled terminals in layers 1 and 2 of area 17 and layers 4 and lower 3 in area 18 (Ogren and Hendrickson, 1977; Benevento and Rezak, 1976). In monkey studies, the area 18 (V2) terminations from pulvinar injections were patchy (Curcio and Harting, 1978; Levitt et al., 1995; Livingstone and Hubel, 1982), reflecting the modular organization of V2 (Kaskan et al., 2009; Lim et al., 2009). Finally, at the single axon level, injections into PL in macaques labeled terminations in V2 and other visual areas (V3, V4/DL and MT) that were concentrated in layer 3, but also involved layers 4, 5, 6, and sometimes layer 1 (Rockland et al., 1999). Overall, the dorsal map (PL) projections to early visual areas appear to be similar between galagos and those observed in monkeys.

References

Adams, M. M., Hof, P. R., Gattass, R., Webster, M. J., and Ungerleider, L. G. (2000). Visual cortical projections and chemoarchitecture of macaque monkey pulvinar. *Journal of Comparative Neurology*, 419(3):377–393.

Allman, J. M., Kaas, J. H., Lane, R. H., and Miezin, F. M. (1972). A representation of the visual field in the inferior nucleus of the pulvinar in the owl monkey (Aotus trivirgatus). *Brain research*, 40(2):291–302.

Arcaro, M. J., Pinsk, M. A., and Kastner, S. (2015). The Anatomical and Functional Organization of the Human Visual Pulvinar. *Journal of Neuroscience*, 35(27):9848–9871.

Baldwin, M. K., Balaram, P., and Kaas, J. H. (2017). The evolution and functions of nuclei of the visual pulvinar in primates. *Journal of Comparative Neurology*, 525(15):3207–3226.

Baldwin, M. K. L., Balaram, P., and Kaas, J. H. (2013). Projections of the superior colliculus to the pulvinar in prosimian galagos (Otolemur garnettii) and VGLUT2 staining of the visual pulvinar. *Journal of Comparative Neurology*, 521(7):1664–1682.

Baldwin, M. K. L., Kaskan, P. M., Zhang, B., Chino, Y. M., and Kaas, J. H. (2012). Cortical and subcortical connections of V1 and V2 in early postnatal macaque monkeys. *The Journal of comparative neurology*, 520(3):544–69.

Bender, D. B. (1981). Retinotopic organization of macaque pulvinar. *Journal of neurophysiology*, 46(3):672–693.

Bender, D. B. (1983). Visual activation of neurons in the primate pulvinar depends on cortex but not colliculus. *Brain research*, 279(1-2):258–261.

Benevento, L. A. and Rezak, M. (1976). The cortical projections of the inferior pulvinar and adjacent lateral pulvinar in the rhesus monkey (macaca mulatta): An autoradiographic study. *Brain Research*, 108(1):1–24.

Bickford, M. E. (2016). Thalamic Circuit Diversity: Modulation of the Driver/Modulator Framework. *Frontiers in Neural Circuits*, 9(January):1–8.

Bickford, M. E., Zhou, N., Krahe, T. E., Govindaiah, G., and Guido, W. (2015). Retinal and Tectal "Driver-Like" Inputs Converge in the Shell of the Mouse Dorsal Lateral Geniculate Nucleus. *Journal of Neuroscience*, 35(29):10523–10534.

Bourassa, J. and Deschenes, M. (1995). Corticothalamic projections from the primary visual cortex in rats: a single fiber study using biocytin as an anterograde tracer. *Neuroscience*, 66(2):253–263.

Boyd, J. D. and Matsubara, J. A. (1996). Laminar and columnar patterns of geniculocortical projections in the cat: Relationship to cytochrome oxidase. *Journal of Comparative Neurology*, 365(4):659–682.

Cola, M. G., Seltzer, B., Preuss, T. M., and Cusick, C. G. (2005). Neurochemical organization of chimpanzee inferior pulvinar complex. *Journal of Comparative Neurology*, 484(3):299–312.

Conley, M. and Raczkowski, D. (1990). Sublaminar organization within layer VI of the striate cortex in Galago. *Journal of Comparative Neurology*, 302(2):425–436.

Curcio, C. A. and Harting, J. K. (1978). Organization of pulvinar afferents to area 18 in the squirrel monkey: evidence for stripes. *Brain Research*, 143(1):155–161.

Cusick, C. G., Steindler, D. A., and Kaas, J. H. (1985). Corticocortical and collateral thalamocortical connections of postcentral somatosensory cortical areas in squirrel monkeys: A double-labeling study with radiolabeled wheatgerm agglutinin and wheatgerm agglutinin conjugated to horseradish peroxidase. *Somatosensory & Motor Research*, 3(1):1–31.

Fan, R. H., Baldwin, M. K. L., Jermakowicz, W. J., Casagrande, V. A., Kaas, J. H., and Roe, A. W. (2012). Intrinsic signal optical imaging evidence for dorsal V3 in the prosimian galago (Otolemur garnettii). *Journal of Comparative Neurology*, 520(18):4254–4274.

Gattass, R., Oswaldo-Cruz, E., and Sousa, A. P. B. (1978). Visuotopic organization of the Cebus pulvinar: A double representation of the contralateral hemifield. *Brain Research*, 152(1):1–16.

Goodale, M. a. and Milner, a. D. (1992). Separate visual pathways for perception and action. *Trends in Neurosciences*, 15(1):20–25.

Kaas, J. H. (2012). Evolution of columns, modules, and domains in the neocortex of primates. *Proceedings of the National Academy of Sciences*, 109(Supplement_1):10655–10660.

Kaas, J. H. and Lyon, D. C. (2007). Pulvinar contributions to the dorsal and ventral streams of visual processing in primates. *Brain Research Reviews*, 55(2 SPEC. ISS.):285–296.

Kaas, J. H. and Morel, A. (1993). Connections of visual areas of the upper temporal lobe of owl monkeys: the MT crescent and dorsal and ventral subdivisions of FST. *The Journal of neuroscience : the official journal of the Society for Neuroscience*, 13(2):534–46.

Kaskan, P. M., Lu, H. D., Dillenburger, B. C., Kaas, J. H., and Roe, A. W. (2009). The organization of orientation-selective, luminance-change and binocular- preference domains in the second (V2) and third (V3) visual areas of new world owl monkeys as revealed by intrinsic signal optical imaging. *Cerebral Cortex*, 19(6):1394–1407.

Kwan, W. C., Mundinano, I. C., de Souza, M. J., Lee, S. C., Martin, P. R., Grünert, U., and Bourne, J. A. (2018). Unravelling the subcortical and retinal circuitry of the primate inferior pulvinar. *Journal of Comparative Neurology*, (December 2017).

Levitt, J. B., Yoshioka, T., and Lund, J. S. (1995). Connections between the pulvinar complex and cytochrome oxidase-defined compartments in visual area V2 of macaque monkey. *Experimental brain research*, 104:419–430.

Li, K., Patel, J., Purushothaman, G., Marion, R. T., and Casagrande, V. A. (2013). Retinotopic maps in the pulvinar of bush baby (Otolemur garnettii). *Journal of Comparative Neurology*, 521(15):3432–3450.

Lim, H., Wang, Y., Xiao, Y., Hu, M., and Felleman, D. J. (2009). Organization of Hue Selectivity in Macaque V2 Thin Stripes. *Journal of Neurophysiology*, 102(5):2603–2615.

Livingstone, M. S. and Hubel, D. H. (1982). Thalamic inputs to cytochrome oxidase-rich regions in monkey visual cortex. *Proceedings of the National Academy of Sciences of the United States of America*, 79(19):6098–101.

Lund, J. S., Hendrickson, a. E., Ogren, M. P., and Tobin, E. a. (1981). Anatomical organization of primate visual cortex area VII. *The Journal of comparative neurology*, 202(1):19–45.

Lund, J. S., Lund, R. D., Hendrickson, A. E., Bunt, A. H., and Fuchs, A. F. (1975). The origin of efferent pathways from the primary visual cortex, area 17, of the macaque monkey as shown by retrograde transport of horseradish peroxidase. *The Journal of comparative neurology*, 164(3):287–303.

Marion, R., Li, K., Purushothaman, G., Jiang, Y., and Casagrande, V. A. (2013). Morphological and neurochemical comparisons between pulvinar and V1 projections to V2. *Journal of Comparative Neurology*, 521(4):813–832.

Mishkin, M. and Ungerleider, L. G. (1982). Contribution of striate inputs to the visuospatial functions of parieto-preoccipital cortex in monkeys. *Behavioural Brain Research*, 6(1):57–77.

Moore, B., Li, K., Kaas, J. H., Liao, C.-C., Boal, A. M., Mavity-Hudson, J., and Casagrande, V. (2018). Cortical projections to the two retinotopic maps of primate pulvinar are distinct. *Journal of Comparative Neurology*.

O'Brien, B. J., Abel, P. L., and Olavarria, J. F. (2001). The retinal input to calbindin-D28k-defined subdivisions in macaque inferior pulvinar. *Neuroscience Letters*, 312(3):145–148.

Ogren, M. P. and Hendrickson, a. E. (1977). The distribution of pulvinar terminals in visual areas 17 and 18 of the monkey. *Brain Research*, 137(2):343–350.

Purushothaman, G., Marion, R., Li, K., and Casagrande, V. a. (2012). Gating and control of primary visual cortex by pulvinar. *Nature Neuroscience*, 15(6):905–912.

Raczkowski, D. and Diamond, I. (1980). Cortical Connections of the Pulvinar Nucleus in Galago. *Journal of Comparative Neurology*, 193(1):1–40.

Raczkowski, D. and Diamond, I. T. (1981). Projections from the superior colliculus and the neocortex to the pulvinar nucleus in Galago. *The Journal of comparative neurology*, 200(2):231–254.

Rockland, K. S. (1996). Two types of corticopulvinar terminations: Round (type 2) and elongate (type 1). *Journal of Comparative Neurology*, 368(1):57–87.

Rockland, K. S., Andresen, J., Cowie, R. J., and Robinson, D. L. (1999). Single axon analysis of pulvinocortical connections to several visual areas in the macaque. *Journal of Comparative Neurology*, 406(2):221–250.

Rosa, M. G., Casagrande, V. A., Preuss, T., and Kaas, J. H. (1997). Visual field representation in striate and prestriate cortices of a prosimian primate (Galago garnetti). *Journal of Neurophysiology*, 77(6):3193–217.

Rovo, Z., Ulbert, I., and Acsady, L. (2012). Drivers of the Primate Thalamus. *Journal of Neuroscience*, 32(49):17894–17908.

Schiller, P. H. and Malpeli, J. G. (1977). The effect of striate cortex cooling on area 18 cells in the monkey. *Brain Research*, 126(2):366–369.

Sherman, S. M. and Guillery, R. W. (1998). On the actions that one nerve cell can have on another: distinguishing "drivers" from "modulators". *Proceedings of the National Academy of Sciences of the United States of America*, 95(12):7121–7126.

Shipp, S. (2001). Corticopulvinar connections of areas V5, V4, and V3 in the macaque monkey: A dual model of retinal and cortical topographies. *Journal of Comparative Neurology*, 439(4):469–490.

Stepniewska, I. and Kaas, J. H. (1997). Architectonic subdivisions of the inferior pulvinar in New World and Old World monkeys. *Vis Neurosci*, 14(6):1043–1060.

Symonds, L. L. and Kaas, J. H. (1978). Connections of striate cortex in the prosimian, Galago senegalensis. *The Journal of comparative neurology*, 181(3):477–512.

Trojanowski, J. Q. and Jacobson, S. (1977). Brain The Morphology and Laminar Distribution of Cortico-Pulvinar Neurons in the Rhesus Monkey. *Experimental Brain Research*, 62(1-2):51–62.

Ungerleider, L., Galkin, T., and Mishkin, M. (1983). Visuotopic organization of projections from striate cortex to inferior and lateral pulvinar in rhesus monkey. *Journal of Comparative Neurology*, 217(2):137–157.

Wickersham, I. R., Finke, S., Conzelmann, K.-K., and Callaway, E. M. (2007). Retrograde neuronal tracing with a deletion-mutant rabies virus. *Nature methods*, 4(1):47–49.

Wong, P., Collins, C. E., Baldwin, M. K. L., and Kaas, J. H. (2009). Cortical connections of the visual pulvinar complex in prosimian galagos (Otolemur garnetti). *Journal of Comparative Neurology*, 517(4):493–511.

Wong, P. and Kaas, J. H. (2010). Architectonic subdivisions of neocortex in the galago (Otolemur garnetti). *Anatomical Record*, 293(6):1033–1069.

CHAPTER 4
ULTRASTRUCTURE OF GALAGO VISUAL PULVINAR PROJECTIONS

The study described in this chapter includes data published in Moore et al. (2018) and Marion et al. (2013) as well as unpublished data gathered in collaboration with Keji Li and Julie Mavity-Hudson.

The pulvinar complex is the largest thalamic subdivision and is comprised of several higher order nuclei. This complex receives its main input from cortical areas unlike primary thalamic nuclei like the lateral geniculate nucleus which receives its input directly from the sensory periphery. Projections from the thalamus either drive or modulate the flow of information to cortex but where pulvinocortical projections fall within this driver/modulator framework remains unknown. To better understand these projections, anterograde tracers were placed in the visual pulvinar of thirteen galagos. After being properly processed, the tissue from these subjects was then examined with both confocal and electron microscopy. These results demonstrate that the pulvinar may act differentially as either a driver or modulator depending on the cortical target.

Introduction

The lateral (PL) and inferior (PI) pulvinar nuclei, known collectively as the visual pulvinar, are higher order thalamic nuclei that reciprocally connect with both primary (V1) and secondary (V2) visual cortices (Sherman, 2007). Although primary sensory nuclei like the lateral geniculate nucleus (LGN) push an essential sensory signal or "drive" their cortical targets, the projections of higher order thalamic nuclei are not as well understood. These nuclei can either drive cortex or "modulate" these driving signals (Sherman and Guillery, 1998). Proper placement of a neural population within the driver/modulator framework requires causal electrophysiological recordings which can be difficult or impossible to obtain. This classification, however, has been correlated with bouton size, location, and synaptic protein content.

LGN serves as the main driver of V1 activity (Jones, 2007) and sends its projections primarily to granular cortex. Thalamocortical driving projections from primary sensory nuclei usually terminate in cortical layer 4 (Sherman and Guillery, 1998; Rockland and Pandya, 1979) while modulating projections from secondary thalamic nuclei typically end more superficially (Felleman and Van Essen, 1991). The visual pulvinar's projections to early visual cortical areas reveal a complex pattern. Specifically, PL greatly gates V1's

output signals to V2 (Purushothaman et al., 2012) while also terminating in granular V2 with boutons of comparable size to coming from V1 (Moore et al., 2018; Marion et al., 2013). This seems paradoxical as the latter is a property of driving projections while the former is indicative of the pulvinar functioning as a cortical modulator. Does the visual pulvinar function as a thalamocortical "driver" or "modulator"? To understand how the pulvinar interacts with the local networks of V1 and V2, we examined and compared the synaptic targets of PL in both of these cortical areas. With this goal in mind, anterograde anatomical tracers placed in PL were used to examine the laminar distribution and size of pulvinocortical boutons. Electron microscopy was also employed to examine the synaptic ultrastructure of these projections.

Materials and methods

Subjects

Thirteen adult galagos (*Otolemur garnettii*) were used this study. These animals were cared for according to the National Institutes of Health Guide for the Care and Use of Laboratory Animals and according to a protocol approved by the Vanderbilt University Institutional Animal Care and Use Committee (IACUC). To reduce the number of these valuable primates used in experiments, some of the tissue from these animals was used in separate studies.

Surgery

Each of the following experiments shared a common surgical preparation (Li et al., 2013; Marion et al., 2013). Ketamine was used as an initial anesthetic sedative (10.3 mg/kg), in order to allow for surgical preparation and intubations. Anesthesia was then maintained via inhaled isoflurane (1-2% mixed in O_2). While fully anesthetized, the galagos were placed in a stereotaxic frame. The surgery was performed under aseptic conditions, and vital signs including heart rate, respiration rate, blood pressure, and body temperature were regularly monitored throughout the procedure. A unilateral craniotomy was made over occipital-parietal cortex, and the dura covering the exposed brain area was removed to allow the microelectrode mapping and tracer injection in the pulvinar. The anesthesia was then switched to intravenous propofol (2 mg/kg/hr) and respiration with nitrous oxide (67%). Intravenous paralytic (vecuronium bromide, 0.6 mg/kg/hr) was used to reduce eye movements and subtle modifications in the animal's lens so that our visual power correction with contact lenses remained correct for the animal.

Tracer placement

Parts of the visual pulvinar were carefully mapped with a tungsten electrode (FHC, Inc., ME) at various stereotaxic coordinates using visually evoked responses to simple light stimuli consisting of a crosshair pattern. The size of this pattern varied with eccentricity from the center of the visual field, becoming larger as it is moved farther from center, as the receptive fields of the visually-responsive pulvinar neurons get larger with eccentricity. These maps were compared to data from previous experiments in order to corroborate injection locations (Moore et al., 2018; Marion et al., 2013). In-house manufactured injectrodes, glass tubes pulled out to a fine (30μm) tip and attached to an electrode, were used to confirm placement locations and make subsequent injections. Tracer injections were made within the retinotopic map of PL via manual pressure, over the course of a few minutes. After each injection, the injectrode was left in the same position for 30 minutes to ensure complete liquid evacuation before the injectrode was retracted.

High molecular weight dextran amines (all 20kDa) were used to yield detailed labeling of axons and terminals within early visual cortex. Four of the cases were used for electron microscopy and had 1500nL of 10% biotinylated dextran amine (BDA) placed within PL. All other cases received 300-450nL injections of either 10% BDA or 10% dextran conjugated to Alexa-fluor 488 (green, Thermo Fisher Scientific, Waltham, MA) in PL.

After each surgery, the galagos were treated with prophylactic antibiotic and analgesics after recovery from anesthesia. After a 2-4 week survival time following tracer injections, the galagos were euthanized via sodium pentobarbital overdose (>120 mg/kg), their blood was cleared with 0.1M PBS, and then they were perfused transcardially with 1.5 L of a fixative consisting of 3% paraformaldehyde and 0.1% glutaraldehyde with 0.2% picric acid.

Tissue preparation

For confocal microscopy, the brain was stereotaxically blocked in the coronal plane, with cuts immediately anterior and posterior to the pulvinar. After blocking, the brain was removed from the skull. The brain was then cryoprotected in 30% sucrose in 0.1M phosphate buffer solution, frozen, and cut into 50μm slices using a freezing microtome. Sections were stored at -80°C in a 20% glycerol in Tris buffer solution. BDA was visualized by incubating sections free floating in 1:400 streptavidin Alexa-fluor 488 for two hours. Every third section was mounted on glass slides and coverslipped with Vectashield (Vector Labs). The sections were not dehydrated. These sections were used to visualize labeled cell bodies, axons, and dendrites. Adjacent sections were stained for cytochrome oxidase (CO)

(Boyd and Matsubara, 1996) mounted glass slides, dried overnight, then dehydrated and coverslipped with DPX (Fisher). These CO sections were used to reveal the architectural boundaries in the thalamus (Baldwin et al., 2012) and cortex (Wong and Kaas, 2010).

The five cases used for electron microscopy were blocked in the coronal plane, with a cut just anterior to the pulvinar. After blocking, the brain was removed from the skull and cut coronally at 100μm using a vibratome. The BDA labeled pulvinar axons were visualized by using a standard ABC kit (Vector Labs, UK) followed by a diaminobenzidine (DAB) reaction (Ichida et al., 2014). Sections showing BDA labeled axons in V1 were postfixed in 1% osmium tetroxide, dehydrated in an ethanol series, and flat embedded in Durcapan resin between two sheets of Aclar plastic. Layer 1 of selected V1 sections were punched out, mounted on EPON resin blocks, and cut into ultrathin sections of 70nm which were collected on carbon backed Formvar (Electron Microscopy Science, Hatfield, PA) coated nickel slot grids. Ultrathin sections near the most superficial edge of the tissue block were immunostained for the presence of GABA. The GABA stained sections were then counterstained with 2% uranyl acetate and 8% lead citrate to increase contrast.

Antibody characterization

Anti-GABA primary antibody: The rabbit polyclonal antibody GABA (rabbit anti GABA, Cat#A2052, Sigma-Aldrich, St. Louis, MO) used at the concentration of 1:300.

Anti-rabbit secondary antibody: The goat polyclonal anti-rabbit (goat anti rabbit, Cat#G7402, Sigma-Aldrich, St. Louis, MO) conjugated to 10nm gold particles and used at the concentration of 1:20.

Bouton size quantification

Measurement of bouton size was accomplished via confocal microscopy. Sections were selected from near the center of the pulvinocortical target location within early visual cortex where multiple layer 2/3 arbors were visible. A dense population of axons extending radially from the white matter to infragranular cortex can approximate the location of sections that contain the center of labeled pulvinar targets.

High power confocal stacks were taken using a confocal microscope (Zeiss LSM 510, Zeiss Int., DE). After each stack had been acquired an observer naive to the origin of the stack was recruited to identify boutons. For each bouton, the areas at 50% maximum intensity on the image flattened across the Z axis was taken as its area. Rare cases where saturated pixels existed were not included in analysis. In instances where stacks contain a great number of boutons, only those that occupied the densest central 50% of the stack

area were analyzed (Marion et al., 2013). Photoshop 6.0 (Adobe, San Jose, CA) was used for area size measurements. This was accomplished using Photoshop's "selection statistics" tool.

Ultrastructural analysis

An electron microscope (Tecnai 12, Thermo Fisher Scientific, Waltham, MA) was used to examine the ultrastructure of pulvinar projections terminating in early visual cortex. All labeled axons with a visible synapse and an equal number of random positive and negative controls were photographed. Pre- and post-synaptic profiles for nonlabeled axons were determined on the basis presynaptic vesicle existence. Photoshop was used for pre- and post-synaptic area size measurements using the "selection statistics" tool. Gold particles were counted using Photoshop's "count" tool. Presynaptic gold particle density of asymmetric and symmetric synapses were respectively used as negative and positive controls of GABA staining.

Statistical inference

Bouton sizes residing in the same cortical area and layer did not differ significantly between subjects and data was pooled for all cases. Bouton sizes greatly deviate from the normal distribution for pulvinar projections terminating in superficial V1 (Shapiro-Wilk, $p = 6.44 \times 10^{-7}$) and, as a result, non-parametric methods were used for statistical comparisons. Bouton sizes were compared using Kruskal Wallis tests followed by post-hoc Wilcoxon rank-sum tests. Post-hoc tests were Bonferroni corrected to conservatively adjust the alpha value thus accounting for the number of comparisons being performed. The distribution of gold particle densities in presynaptic profiles of positive (presumed GABAergic) and negative (presumed non-GABAergic) controls were compared to those densities in postsynaptic profiles of labeled pulvinar axons with the Kolmogorov-Smirnov test.

Results

Tracer placement

Reconstructed injection sites were widest along the dorsoventral dimension with the largest observed site being 1.1mm long. Despite these large sites, injections were primarily confined to PL with several cases featuring minor infiltration into PI (Figure 4.1). Electrophysiological recordings prior to tracer placement combined with the reconstructed injection site confirm known visuotopic maps within pulvinar (Li et al., 2013). Tracer

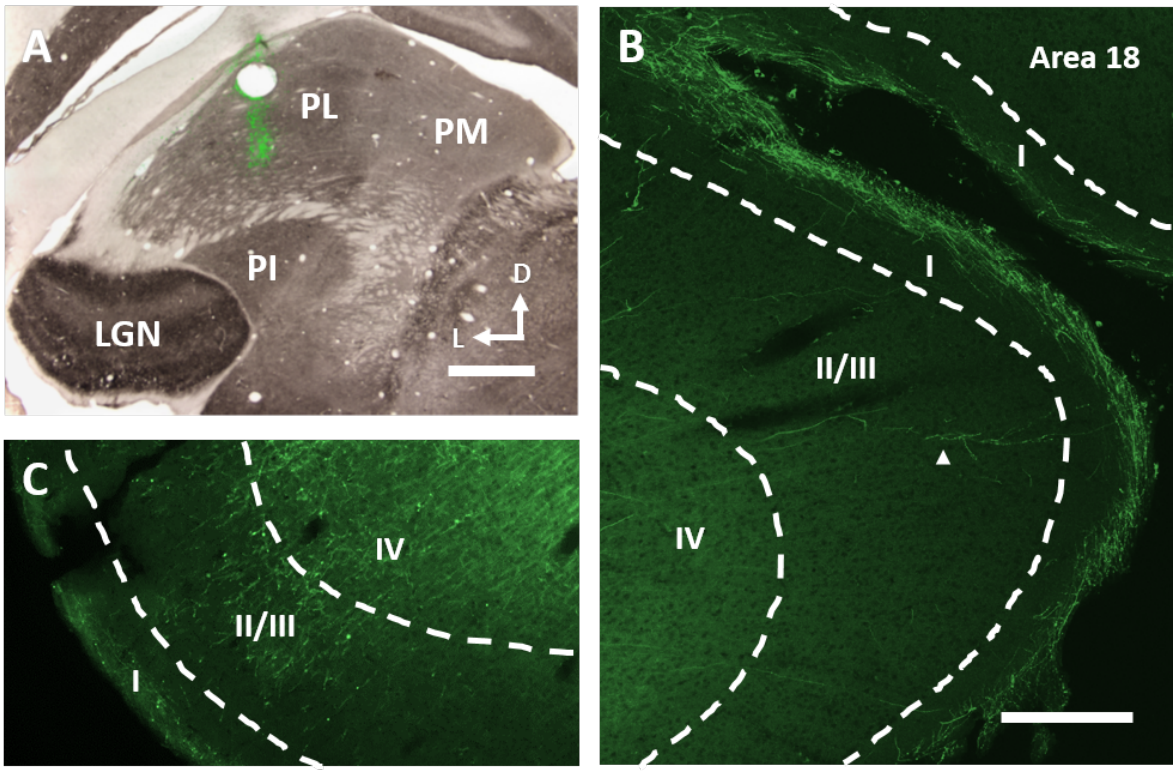

Figure 4.1: BDA reveals the pulvinar's projections to early visual cortex. Distributions of labeled processes in visual cortex after injections of BDA into galago PL. A) Coronal section stained for CO overlaid on an adjacent section stained fluorescently for the injected BDA. The injections were localized to PL. Scale bar is 1mm. B) Pulvinar projections to area 17 (green). Axons can be seen to form arbors in a dense band in the most superficial part of layer 1. Sometimes arbors are observed in upper layer 2/3 (indicated by arrow). Scale bar is 200μm. C) Pulvinar projections to area 18 (green). Axons form arbors both in superficial and granular cortex. CO = cytochrome oxydase, BDA = biotinylated dextran amine, PI = inferior pulvinar, PL = lateral pulvinar, PM = medial pulvinar, LGN = lateral geniculate nucleus.

injections labeled projections ending in early visual areas (V1, V2, V3, and MT) as well as revealing targets in both parietal and temporal cortices.

Striate and extrastriate projections

Labeled projections ending in V1 ascended radially in a columnar matter. These axons rarely branched in all but the most superficial layer of cortex where they split in the center of layer 1 and send collaterals in opposite directions (Figure 4.2). This arborization typically covered long distances greater than a single cortical column ($> 800\mu$m) occasionally forming boutons en passant. Some of these superficially projecting axons were unique in that they terminated without extensive arbors. Sparse terminations were also observed occasionally terminating within layers 2/3 with moderate sized arbors confined within a single cortical column ($< 400\mu$m). In contrast to V1's primarily superficial

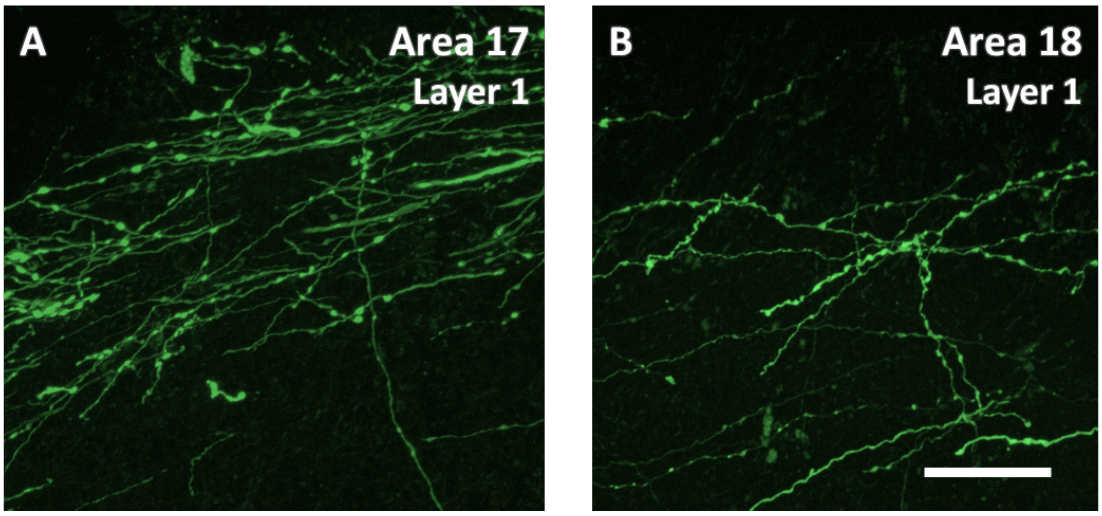

Figure 4.2: Pulvinar axons in superficial V1/V2. High power confocal photomicrographs of pulvinar projections (green) to layer 1 of A) area 17 and B) area 18. Scale bar is 20μm.

termination sites, those in extrastriate cortex occur heavily within layers 3/4 with a minority of projections ending their radial climb within upper layer 2 or layer 1 (Figure 4.3). Axons extending into extrastriate layer 1 arborize in a similar manner to those in superficial V1. All of these arbors extend parallel to each other along the radial dimension and are confined within a single column. Branches that occur within granular and supragranular layers are likely from the same axonal population as all axons observed within layers 3/4 contained branches and boutons en passant.

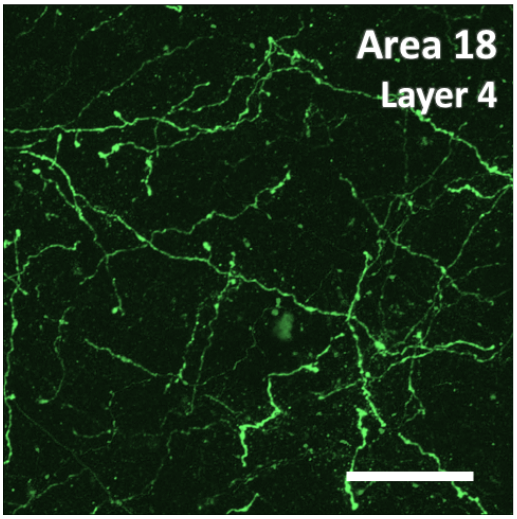

Figure 4.3: Pulvinar axons in granular V2. High power confocal photomicrographs of pulvinar projections (green) to layer 4 of area 18. Scale bar is 20μm.

The area of boutons within superficial V1 had a median of 0.33 μm^2 and a mean 0.38μm^2 (SEM = 0.001μm^2, n = 97). This is comparable the relatively sparser layer 1 of V2 that has a median area of 0.34μm^2 with a mean of 0.33μm^2 (SEM = 0.004μm^2, n = 38). Granular V2 boutons were large with a median area of 0.48μm^2 and a mean of 0.47μm^2 (SEM = 0.002μm^2, n = 87). The bouton sizes in each of these projection target zones differ significantly from each other (Figure 4.4) (Kruskal-Wallis, H = 22.96, p = 1.03$\times$10^{-5}). Posthoc pair-wise comparisons

reveal the source of this difference as arising from the size of V2's granular boutons which are significantly larger than those found in layer 1 of both V2 (T = -4.00, p = 6.47×10^{-5}) and V1 (T = -4.14, p = 3.48×10^{-5}).

Ultrastructure of pulvinar output

The majority of the 83 projections observed formed multiple synapses with adjacent profiles. Some of these labeled pulvinar axons had neighboring profiles that were identified as presynaptic due to high vessicle density which included both GABA and non-GABA staining profiles (Figure 4.5). Unfortunately, any potential synapses formed on pulvinar axons were obscured during histological processing. Gold particle densities of symmetric and asymmetric synapses in these presynaptic profiles were respectively used as positive and negative controls. The distribution of gold particle densities observed in positive and negative controls show no overlap and are significantly different from each other (Wilcoxon rank-sum, T = 8.9, p = 1.15×10^{-16}). Profiles that were postsynaptic to pulvinar axons were not significantly different from the negative controls (Kolmogorov-Smirnov, D = 0.13, p = 0.66), however, the distribution of gold particle densities in these profiles were found to be significantly sparser than in positive controls (Figure 4.6) (Kolmogorov-Smirnov, D = 1.0, p = 1.07×10^{-21}).

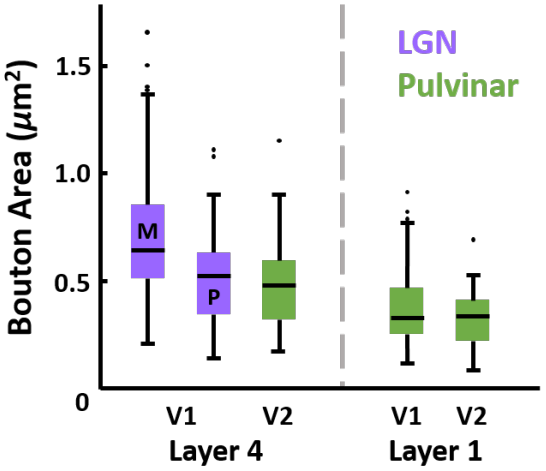

Figure 4.4: Thalamocortical bouton sizes in the early visual system. Distribution of bouton sizes for LGN (purple) and pulvinar (green) within granular and superficial V1 and V2. LGN bouton sizes taken for comparison from the dataset published in Marion et al. (2013).

Discussion

Thalamocortical projections can be classified as either driving a sensory signal or providing input that modifies such a signal (Sherman and Guillery, 1998). Projections from higher order thalamic nuclei, like those found within the pulvinar complex, are not as well understood as those from primary sensory nuclei like LGN. Although the driver/modulator paradigm requires functional evidence to properly classify these thalamocortical projections, the difficult logistics of such experiments has lead to an incomplete

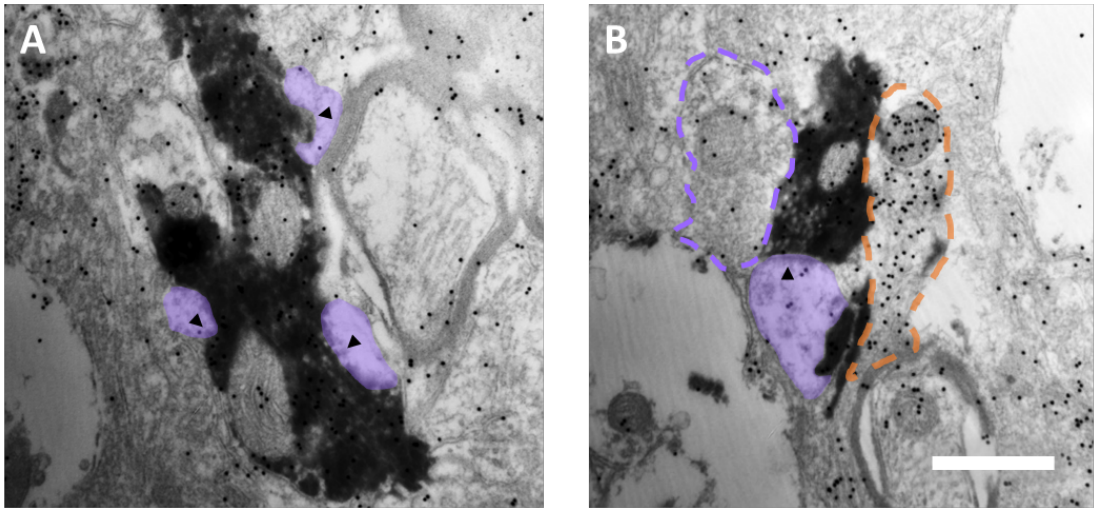

Figure 4.5: Example labeled pulvinar axons in superficial V1. Two example of labeled pulvinar axons in layer 1 of V1. A) Labeled pulvinar axon (black) forming synapses (black arrows) with three post-synaptic profiles (purple). All of these profiles reflect negative GABA immunostaining. B) Labeled pulvinar axon (black) forming a synapse (black arrow) with one post-synaptic profile (purple) reflecting negative GABA immunostaining. Dashed outlines indicate pre-synaptic GABAergic (orange) and non-GABAergic (purple) profiles adjacent to the pulvinar axon terminal. Scale bar is 1μm.

understanding of secondary thalamic nuclei for which the study of anatomical correlates can be a convenient foundation. These correlates include bouton size as well as synapse location and protein content. Driving projections typically terminate in cortical layer 4 (Rockland and Pandya, 1979) while modulating projections synapse supragranularly (Felleman and Van Essen, 1991). The nuclei of the visual pulvinar provide a classification challenge as they have some functional correlates suggesting a modulatory role in cortex (Purushothaman et al., 2012) while also being implicated as drivers projecting to layer 4 in extrastriate cortices (Moore et al., 2018; Marion et al., 2013). To better understand how the pulvinar interacts with the early visual system, we used anterograde tracer injections to examine and compare the fine structure of PL's synaptic targets in both V1 and V2 of the galago.

Tracer injections placed in PL revealed projections terminating primarily in layer 1 of area 17. This finding is consistent with data reported for the macaque (Rezak and Benevento, 1979; Ogren and Hendrickson, 1977) and fits the expectations for layer 1 thalamocortical projections as observed arborizations span more than one cortical column, have boutons en passant, and sometimes form collaterals in layers 2/3 (Rubio-Garrido et al., 2009; Rockland et al., 1999; Lachica and Casagrande, 1992; Carey et al., 1979). In a concurrent study, a modified rabies virus was used to retrogradely label cortical projections to the visual pulvinar (Moore et al., 2018). This set of retrograde tracer experiments

revealed that layer 6 pyramidal neurons have apical dendrites that can extend well into the most superficial layers of cortex. The processes labeled by our anterograde tracer injections could act in a modulatory fashion by synapsing on the apical dendrites of neurons like these that reside in cortical layers 3, 5, and 6. Unlike these projections ending in V1, the terminals observed in area 18 fall primarily within layer 4 and deep layer 3. Our results are in accord with other galago data that shows pulvinocortical targeting of layer 4 outside of area 17 (Marion et al., 2013). The described axonal termination patterns may generalize to all primates rather than just members of the strepsirrhine radiation as similar projections are seen in the squirrel monkey (Curcio and Harting, 1978) and macaque (Lim et al., 2009; Levitt et al., 1995; Livingstone and Hubel, 1982).

Confocal microscopy allowed us to examine the size and location of pulvinocortical projections in both V1 and V2.
All labeled boutons were then compared to previously gathered data on granular terminating LGN axons known to drive striate cortex (Marion et al., 2013). Bouton size is examined as it is correlated with both the number of synapses and post synaptic efficacy (Sherman and Guillery, 1996; Pierce and Lewin, 1994). The variance of bouton sizes could bias the results of the Wilcoxon rank-sum analysis used to make post-hoc pairwise comparisons, however, the laminar axon terminal size differences are so large that such bias will be negligible (Fagerland and Sandvik, 2009). Pulvinocortical boutons in superficial V1/V2 are, as expected, smaller than LGN's driving projections to granular V1 suggesting that these layer 1 projections may have lower synaptic efficacy, in turn, points to these synapses having a modulatory role. This anatomical finding is consistent with PL's known modulatory role gating V1's output signals to V2 (Purushothaman et al., 2012). PL boutons residing in granular area 18 are paradoxically large and comparable in size to neighboring driving projections from V1 (Marion et al., 2013).

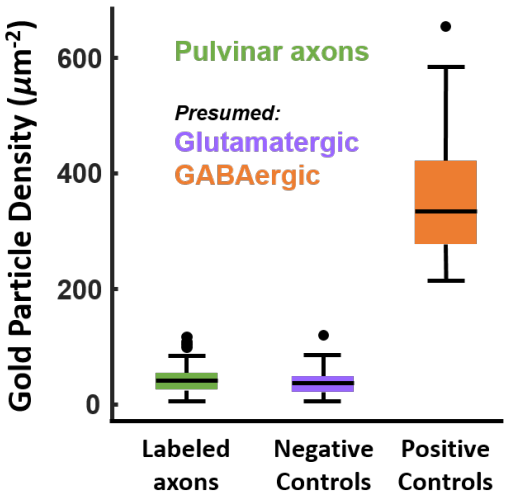

Figure 4.6: Visual pulvinar axons target non-GABAergic profiles in V1. Density distributions of gold particles immunostained for GABA in labeled pulvinar axons (green), negative controls (purple), and positive controls (orange). Positive (presumed GABAergic) and negative (presumed glutamatergic) controls consist of randomly chosen presynaptic profiles forming either symmetric or asymmetric synapses, respectively. Because of this, negative controls are presumed glutamatergic and positive controls are presumed GABAergic.

Close examination of visual cortex ultrastructure revealed that PL projections formed multiple synapses with adjacent profiles. A large number of presynaptic profiles were identified by having a dense vesicle presence. These profiles were classified as either a positive or negative control for GABA based on the respective presence of symmetric of asymmetric synapses. Symmetric synapses don't contain much of a postsynaptic density and are typically inhibitory while their often excitatory asymmetric counterparts have a prominent postsynaptic density that sets them apart (Peters Alan, Palay Sanford, 1976). Immunohistochemistry was used to label the presence of GABA with uniform microscopic gold particles allowing for the comparison of BDA labeled pulvinar processes with the aforementioned controls. Pulvinar axons in superficial V1 form synapses with non-GABAergic profiles which suggests that the visual pulvinar's previously demonstrated gating effects (Purushothaman et al., 2012) are not due to the recruitment of local interneuron networks as previously hypothesized. If networks of inhibitory neurons are not being used then how is the visual pulvinar able to gate V1's output? Glutamate uncaging that targets layer 1 causes deeper pyramidal cells to fire *in situ* (Dantzker and Callaway, 2000). Additionally, pyramidal neurons have the ability to initiate action potentials from their dendritic tufts (Larkum et al., 1999b,a; Schwindt and Crill, 1999; Schiller et al., 1997) which provides a plausible mechanism for which non-GABAergic pulvinocortical projections can gate V1 output.

References

Baldwin, M. K. L., Kaskan, P. M., Zhang, B., Chino, Y. M., and Kaas, J. H. (2012). Cortical and subcortical connections of V1 and V2 in early postnatal macaque monkeys. *The Journal of comparative neurology*, 520(3):544–69.

Boyd, J. D. and Matsubara, J. A. (1996). Laminar and columnar patterns of geniculocortical projections in the cat: Relationship to cytochrome oxidase. *Journal of Comparative Neurology*, 365(4):659–682.

Carey, R. G., Fitzpatrick, D., and Diamond, I. T. (1979). Layer I of striate cortex of Tupaia glis and Galago senegalensis: Projections from thalamus and claustrum revealed by retrograde transport of horseradish peroxidase. *Journal of Comparative Neurology*, 186(3):393–437.

Curcio, C. A. and Harting, J. K. (1978). Organization of pulvinar afferents to area 18 in the squirrel monkey: evidence for stripes. *Brain Research*, 143(1):155–161.

Dantzker, J. L. and Callaway, E. M. (2000). Laminar sources of synaptic input to cortical inhibitory interneurons and pyramidal neurons. *Nature neuroscience*, 3(7):701–7.

Fagerland, M. W. and Sandvik, L. (2009). The Wilcoxon-Mann-Whitney test under scrutiny. *Statistics in Medicine*, 28(10):1487–1497.

Felleman, D. J. and Van Essen, D. C. (1991). Distributed hierarchical processing in the primate cerebral cortex. *Cerebral cortex (New York, N.Y. : 1991)*, 1:1–47.

Ichida, J. M., Mavity-Hudson, J. A., and Casagrande, V. A. (2014). Distinct patterns of corticogeniculate feedback to different layers of the lateral geniculate nucleus. *Eye and brain*, 2014(6 Suppl 1):57–73.

Jones, E. G. (2007). *The Thalamus*. Cambridge University Press, Cambridge, UK, 2 edition.

Lachica, E. a. and Casagrande, V. a. (1992). Direct W-like geniculate projections to the cytochrome oxidase (CO) blobs in primate visual cortex: axon morphology. *The Journal of comparative neurology*, 319(1):141–58.

Larkum, M. E., Kaiser, K. M., and Sakmann, B. (1999a). Calcium electrogenesis in distal apical dendrites of layer 5 pyramidal cells at a critical frequency of back-propagating action potentials. *Proceedings of the National Academy of Sciences of the United States of America*, 96(25):14600–14604.

Larkum, M. E., Zhu, J. J., and Sakmann, B. (1999b). A new cellular mechanism for coupling inputs arriving at different cortical layers. *Nature*, 398(6725):338–341.

Levitt, J. B., Yoshioka, T., and Lund, J. S. (1995). Connections between the pulvinar complex and cytochrome oxidase-defined compartments in visual area V2 of macaque monkey. *Experimental brain research*, 104:419–430.

Li, K., Patel, J., Purushothaman, G., Marion, R. T., and Casagrande, V. A. (2013). Retinotopic maps in the pulvinar of bush baby (Otolemur garnettii). *Journal of Comparative Neurology*, 521(15):3432–3450.

Lim, H., Wang, Y., Xiao, Y., Hu, M., and Felleman, D. J. (2009). Organization of Hue Selectivity in Macaque V2 Thin Stripes. *Journal of Neurophysiology*, 102(5):2603–2615.

Livingstone, M. S. and Hubel, D. H. (1982). Thalamic inputs to cytochrome oxidase-rich regions in monkey visual cortex. *Proceedings of the National Academy of Sciences of the United States of America*, 79(19):6098–101.

Marion, R., Li, K., Purushothaman, G., Jiang, Y., and Casagrande, V. A. (2013). Morphological and neurochemical comparisons between pulvinar and V1 projections to V2. *Journal of Comparative Neurology*, 521(4):813–832.

Moore, B., Li, K., Kaas, J. H., Liao, C.-C., Boal, A. M., Mavity-Hudson, J., and Casagrande, V. (2018). Cortical projections to the two retinotopic maps of primate pulvinar are distinct. *Journal of Comparative Neurology*.

Ogren, M. P. and Hendrickson, a. E. (1977). The distribution of pulvinar terminals in visual areas 17 and 18 of the monkey. *Brain Research*, 137(2):343–350.

Peters Alan, Palay Sanford, W. H. (1976). *Fine Structure of the Nervous System: Neurons and Their Supporting Cells*. Oxford University Press, New York.

Pierce, J. P. and Lewin, G. R. (1994). An ultrastructural size principle. *Neuroscience*, 58(3):441–6.

Purushothaman, G., Marion, R., Li, K., and Casagrande, V. a. (2012). Gating and control of primary visual cortex by pulvinar. *Nature Neuroscience*, 15(6):905–912.

Rezak, M. and Benevento, L. A. (1979). A comparison of the organization of the projections of the dorsal lateral geniculate nucleus, the inferior pulvinar and adjacent lateral pulvinar to primary visual cortex (area 17) in the macaque monkey. *Brain Research*, 167(1):19–40.

Rockland, K. S., Andresen, J., Cowie, R. J., and Robinson, D. L. (1999). Single axon analysis of pulvinocortical connections to several visual areas in the macaque. *Journal of Comparative Neurology*, 406(2):221–250.

Rockland, K. S. and Pandya, D. N. (1979). Laminar origins and terminations of cortical connections of the occipital lobe in the rhesus monkey. *Brain Research*, 179(1):3–20.

Rubio-Garrido, P., Pérez-De-Manzo, F., Porrero, C., Galazo, M. J., and Clascá, F. (2009). Thalamic input to distal apical dendrites in neocortical layer 1 is massive and highly convergent. *Cerebral Cortex*, 19(10):2380–2395.

Schiller, J., Schiller, Y., Stuart, G., and Sakmann, B. (1997). Calcium action potentials restricted to distal apical dendrites of rat neocortical pyramidal neurons. *The Journal of physiology*, 505:605–16.

Schwindt, P. and Crill, W. (1999). Mechanisms underlying burst and regular spiking evoked by dendritic depolarization in layer 5 cortical pyramidal neurons. *Journal of neurophysiology*, 81(3):1341–1354.

Sherman, S. M. (2007). The thalamus is more than just a relay. *Current Opinion in Neurobiology*, 17(4):417–422.

Sherman, S. M. and Guillery, R. W. (1996). Functional organization of thalamocortical relays. *Journal of neurophysiology*, 76(3):1367–95.

Sherman, S. M. and Guillery, R. W. (1998). On the actions that one nerve cell can have on another: distinguishing "drivers" from "modulators". *Proceedings of the National Academy of Sciences of the United States of America*, 95(12):7121–7126.

Wong, P. and Kaas, J. H. (2010). Architectonic subdivisions of neocortex in the galago (Otolemur garnetti). *Anatomical Record*, 293(6):1033–1069.

CHAPTER 5
CONNECTION PATTERNS OF GALAGO ASSOCIATION PULVINAR

Most primate pulvinar studies focus on the visually driven subdivisions of this complex while the remaining nucei, collectively referred to as the association pulvinar, are comparatively unexamined. In the macaque, this group of nuclei include both medial pulvinar and the dorsomedial subdivision of lateral pulvinar. Monkey literature demonstrates dense projections from the association pulvinar to primarily three targets: frontal, posterior parietal, and superior temporal cortices. To test the possibility of strepsirrhine connective homology, four different retrograde tracers were placed in these suspected cortical targets across three galagos. Tracers placed in all three cortical locations labeled neurons within both medial and inferior pulvinar. Specifically, two mediolateral patches of neurons within medial pulvinar were found to project to either parietal or temporal cortices while only cells residing medially had frontal projections. Labeled cells within inferior pulvinar were sparser and lacked a clearly discernible pattern. This is in contrast to projections demonstrated in the macaque that originate primarily from only medial pulvinar and the dorsomedial subdivision of the lateral pulvinar.

Introduction

Research on the primate pulvinar's visually driven subdivisions are converging to a point where both anatomical and functional understanding are generally accepted (Baldwin et al., 2017, for review). While the visual pulvinar's architectonic and electrophysiological properties have been well examined (Kaas and Lyon, 2007; Cola et al., 2005; O'Brien et al., 2001; Adams et al., 2000; Stepniewska and Kaas, 1997), the complex's remaining nuclei consisting of the dorsomedial subdivision of lateral pulvinar (PL_{dm}) and medial pulvinar (PM) linger relatively unstudied. Although sparse compared to visual pulvinar research, the macaque literature demonstrates heavy projections from these pulvinar subdivisions to anterior superior temporal (Yeterian and Pandya, 1989; Markowitsch et al., 1985), frontal (Cappe et al., 2009; Asanuma et al., 1985; Baleydier and Mauguiere, 1985; Trojanowski and Jacobson, 1974), parietal (Matsuzaki et al., 2004; Cavada et al., 1995; Morecraft et al., 1993; Patrick Hardy and Lynch, 1992), and belt/parabelt cortices (Cappe et al., 2009; Hackett et al., 1998; Baleydier and Mauguiere, 1985). Given the functionality implied by these cortical targets, we refer collectively to these nuclei as the association pulvinar.

Although not considered part of the visual pulvinar, macaque PL_{dm} is heavily

involved with both ventral and dorsal visual processing streams (Lyon et al., 2010; Weller et al., 2002; Webster et al., 1993; Yeterian and Pandya, 1991) even exhibiting a capacity for face discrimination (Nguyen et al., 2013) and attentional modulation (Robinson et al., 1986; Robinson and Petersen, 1985). PM, however, is not visually driven and has known reciprocal connections with the auditory belt/parabelt, parietal, and frontal cortices (Cappe et al., 2009; Gutierrez et al., 2000; Trojanowski and Jacobson, 1974). While major features of association pulvinar organization may apply to all primates, how these features correspond with the pulvinar of the strepsirrhine radiation is unknown. Galagos, like other wet-nosed strepsirrhine primates, have brains that are more phylogenetically similar to those of early primate ancestors (Baldwin et al., 2017; Kaas and Lyon, 2007; Preuss et al., 1993; Preuss and Goldman-Rakic, 1991; Radinsky, 1975). The galago visual pulvinar's experimentally convenient dorsoventral retinotopy has made this species a popular comparative model (Moore et al., 2018; Baldwin et al., 2017; Li et al., 2013). Another prominent feature of the galago is its smooth brain which facilitates cortical injection studies. With these qualities in mind, we used retrograde tracers placed in cortical areas known in the macaque to receive projections from the association pulvinar: frontal, parietal, and anterior superior temporal cortices. Here we demonstrate a possible homology between the cortical targets of macaque and galago association pulvinar.

Materials and methods

Subjects

Three adult galagos (*Otolemur garnettii*) were used this study. These animals were cared for according to the National Institutes of Health Guide for the Care and Use of Laboratory Animals and according to a protocol approved by the Vanderbilt University Institutional Animal Care and Use Committee (IACUC). To reduce the number of these valuable primates used in experiments, some of the tissue from these animals was used in separate studies.

Surgery

Each of the following experiments shared a common surgical preparation (Liao et al., 2013). Ketamine was used as an initial anesthetic sedative (10-25 mg/kg), in order to allow for surgical preparation and intubations. Anesthesia was then maintained via inhaled isoflurane (1-2% mixed in O_2). While fully anesthetized, the galagos were placed in a stereotaxic frame. The surgery was performed under aseptic conditions, and vital signs including heart rate, respiration rate, blood pressure, and body temperature were regularly

monitored throughout the procedure. A unilateral craniotomy was made over either frontal or temporo-parietal cortices and the dura covering the exposed brain area was removed to allow for tracer injections.

Cortical injections

The organization of corticopulvinar connections was revealed by injecting neuroanatomical tracers into a combination of frontal, temporal, and parietal cortices (Figure 5.1). Four different retrograde tracers were used across our subjects: cholera toxin subunit B (CTB), diamidino yellow (DY), fast blue (FB), and 10kDA fluoro-ruby (FR). The tracers were stored frozen at -80°C and kept frozen on dry ice until just before injection to prevent degradation. Two cases received frontal lobe injections; both receiving 0.5μL 1% CTB with one having an additional rostral injection of 0.25μL 2% DY. Two galagos received injections posterior to the lateral fissure with a third receiving an injection just anterior to this sulcus. All of these subjects received 0.5μL 1% CTB with one having an additional medial injection of 0.2μL 3% FB. Finally, a single galago received an injection of 0.5μL 10% FR in posterior parietal cortex. All injections were made using a Hamilton syringe outfitted with glass pipettes drawn to a 30μm tip and staggered across depths between 1 and 1.5mm.

After each surgery, the galagos were treated with prophylactic antibiotics and analgesics after recovery from anesthesia. After a one-week survival time following the tracer injections, the galagos were euthanized via sodium pentobarbital overdose (>120 mg/kg), their blood was cleared with 0.1M PBS, and then they were perfused transcardially with 1.5 L of 4% paraformaldehyde.

Tissue preparation

For all experiments, the brain was stereotaxically blocked in the coronal plane, with a cut stereotaxically anterior to the thalamus. After blocking, the brain was removed from the skull. The brain was then cryoprotected in 30% sucrose in 0.1M phosphate buffer solution, frozen, and cut into 50μm slices using a freezing microtome. Sections were stored at -80°C in a 20% glycerol in Tris buffer solution. For cases in which a fluorescently tagged tracer (FR,FB, or DY) were used, every sixth section was mounted on glass slides, air dried, and coverslipped. These sections were used to visualize fluorescently labeled cells in the pulvinar. Adjacent sections were stained for cytochrome oxidase (CO) (Boyd and Matsubara, 1996), calbindin (CB) (Wong and Kaas, 2010) and, when applicable, CTB (Angelucci et al., 1996) before being mounted on glass slides, dried overnight, and coverslipped with DPX (Fisher). The CO and CB sections were used to reveal the

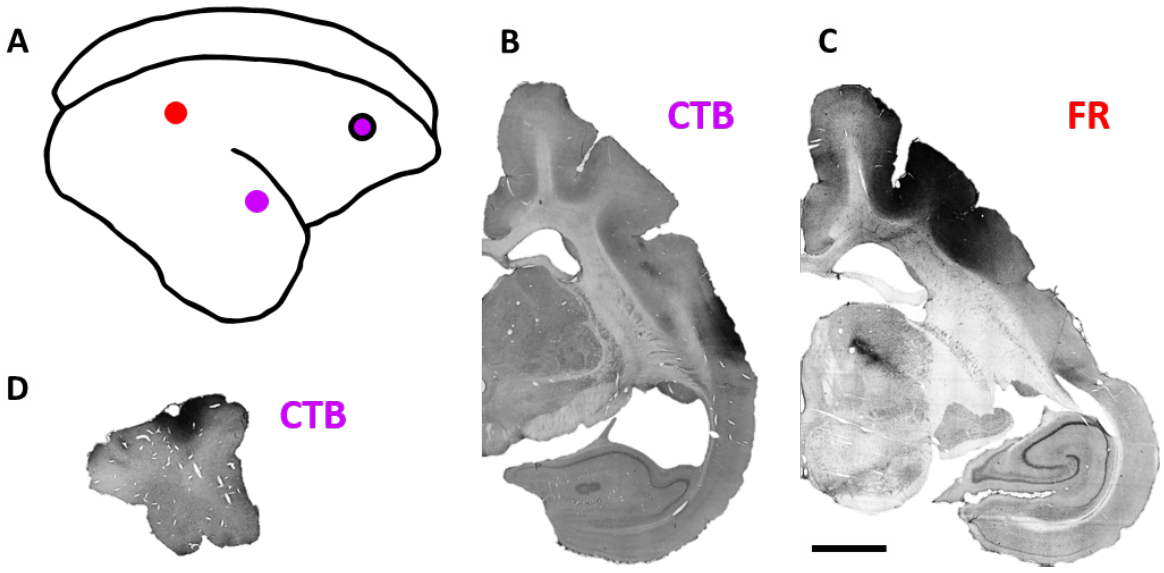

Figure 5.1: Temporal, parietal, and frontal tracer placement. Subject 18-12 received tracer placement in all three cortical targets of interest and is shown here to illustrate both the typical locations and spread of our retrograde tracer injections. A) An illustration of galago cortex where tracer injection locations are indicated by a colored dot. Purple refers to the use of CTB while red points to the use of FR. In this particular case, the frontal cortex site is located on the opposite hemisphere as indicated by its outline. B) Coronal section showing right temporal injection site. C) Right parietal FR injection site. Note the labeling that spreads along PM, PI, and SGN. D) CTB injection site in left frontal cortex. CTB = cholera toxin subunit B, FR = fluororuby, PI = inferior pulvinar, PL = lateral pulvinar, PM = medial pulvinar, SGN = suprageniculate nucleus. Scale bar is 1.5mm.

architectural boundaries in the thalamus (Figure 5.2) (Baldwin et al., 2012).

Antibody characterization

Anti-CB primary antibody: The rabbit polyclonal antibody (rabbit calbindin D28K antibody, Cat#PA1-931, Invitrogen, Carlsbad, CA) recognizes the vitamin D dependent 28kDa calcium-binding protein calbindin. This primary antibody was used at the concentration of 1:5000.

Anti-CTB primary antibody: The mouse monoclonal antibody (mouse cholera toxin beta antibody, Cat#MA1-21550, Invitrogen, Carlsbad, CA) recognizes transported CTB within a tissue sample. This primary antibody was used at the concentration of 1:4000.

Anti-tetramethylrhodamine: The rabbit polyclonal antibody (rabbit polyclonal TRITC antibody, Cat#A-6397, Invitrogen, Carlsbad, CA) recognizes transported FR within a tissue sample. This primary antibody was used at the concentration of 1:5000.

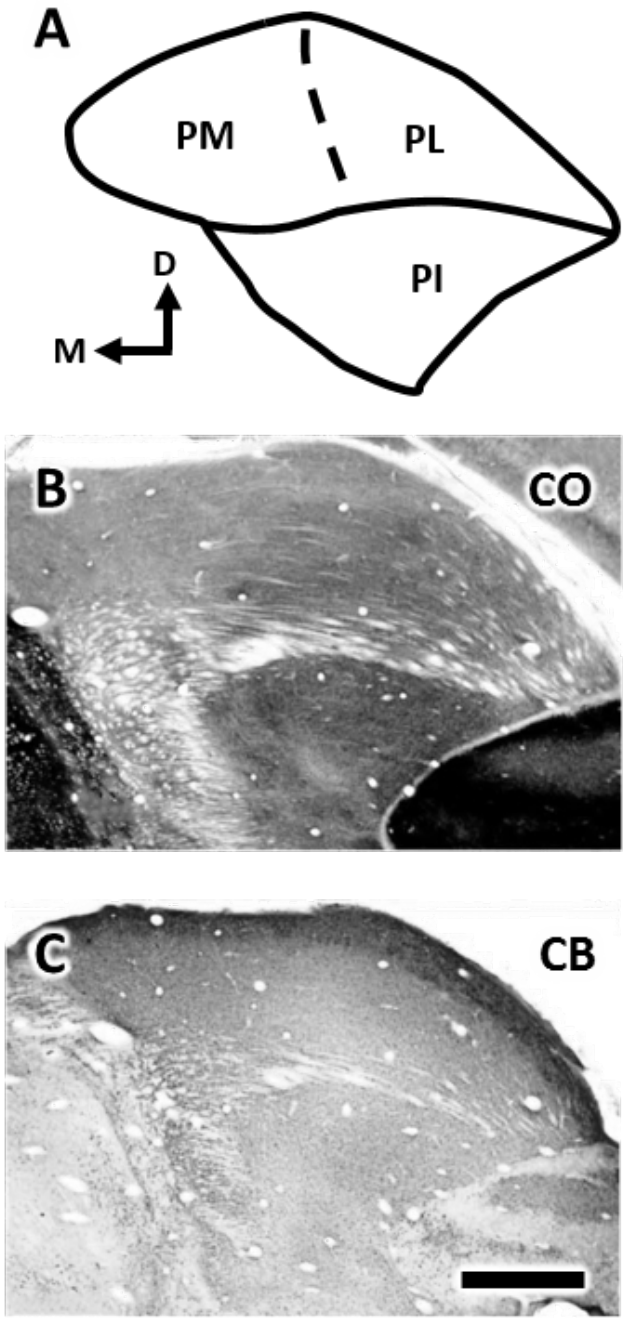

Figure 5.2: Cytoarchitechtonic staining reveals pulvinar subdivisions. A) An illustration of galago pulvinar subdivision. The vague border between PM and PL is indicated with a dashed line. B) A CO stained coronal section of galago pulvinar. PL is clearly separated from the darkly stained PI by the brSC. PM is stained slightly lighter than PL and can be properly differentiated when combined with other histological data. C) A CB stained coronal section of galago pulvinar. PM is stained slightly darker than PL and, when combined with CO data, can be used to accurately place the PL/PM border. CO = cytochrome oxidase, CB = calbindin, brSC = brachium of the superior colliculus, PI = inferior pulvinar, PL = lateral pulvinar, PM = medial pulvinar. Scale bar is 200μm.

Tissue imaging and analysis

Sections of pulvinar and cortex were observed using light or fluorescent microscopy (Zeiss M2 with an Axiocam MRC camera) where appropriate to confirm that: 1) injections were made successfully into the general locations of either frontal, temporal, or parietal cortices and 2) there was labeling of neurons in the thalamus. Locations of the labeled neurons within the thalamus were identified in adjacent brain sections processed for CO or CB. Photoshop 6.0 (Adobe, San Jose, CA) was used to count the number of labeled cells of each tracer in the pulvinar. This was accomplished by using Photoshop's "count" tool which keeps a running count of cells as they are plotted. These values were then transcribed into a spreadsheet for final analysis.

Results

The present study focused on characterizing galago association pulvinar's cortical projections. Injections of retrograde tracers into cortical sites known in the macaque to have reciprocal projections with association pulvinar (Cappe et al., 2009; Hackett et al., 1998; Huerta et al., 1986; Baleydier and Mauguiere, 1985; Trojanowski and Jacobson, 1974) revealed a partial homology between strepsirrhine and haplorhine anatomy. Frontal cortex injections reveal projections originating along the medial edge of association pulvinar spanning both PI and PM. Tracers in parietal cortex label cells that also span PI and PM, however, these neurons occur more medially. Finally, injections placed within temporal cortex reveal widespread projections originating from all three major chemoarchitectonic subdivisions of the pulvinar consistent with previous research (Moore et al., 2018). Those injections placed closer to the lateral sulcus, however, primarily labeled cells within medial PM and PI. This is in contrast to the macaque where frontal cortex receives projections only from the association pulvinar rather than having any PI projections (Morecraft et al., 1993; Trojanowski and Jacobson, 1976). Given the limited availability of galagos for these studies, our results are based on relatively few cases.

Parietal projections

Pulvinar neurons projecting to parietal cortex were identified by injecting a retrograde tracer into this cortical area. An injection of FR was placed in posterior parietal cortex and labeled 522 neurons within the pulvinar: 356 within PM, 147 in PI, and 19 in PL. Parietal projections mostly originated from both medial PM and PI. A more lateral patch of labeled PM neurons can also be observed just caudal to the aforementioned medially

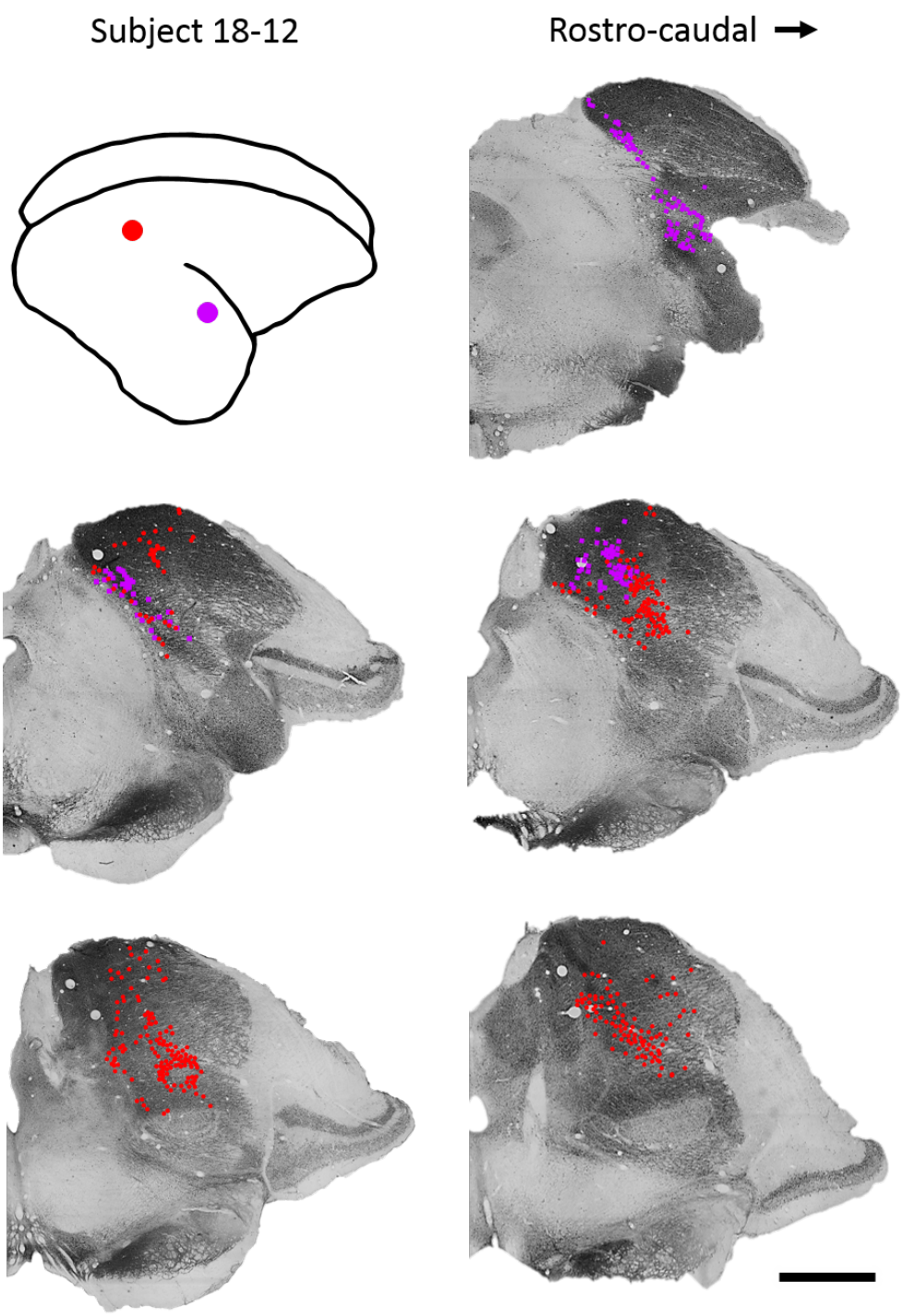

Figure 5.3: Temporal CTB and parietal FR injections label PM and PI. The illustrated galago brain indicates where temporally placed CTB (purple) and parietally injected FR (red) were located in subject 18-12. Each coronal section of pulvinar shown is 300μm apart and are in ascending rostro-caudal order. Labeled cells falling within SGN and MGN are not shown to emphasize pulvinar neurons. CTB = cholera toxin subunit B, FR = fluororuby, SGN = suprageniculate nucleus, MGN = medial geniculate nucleus. Scale bar is 200μm.

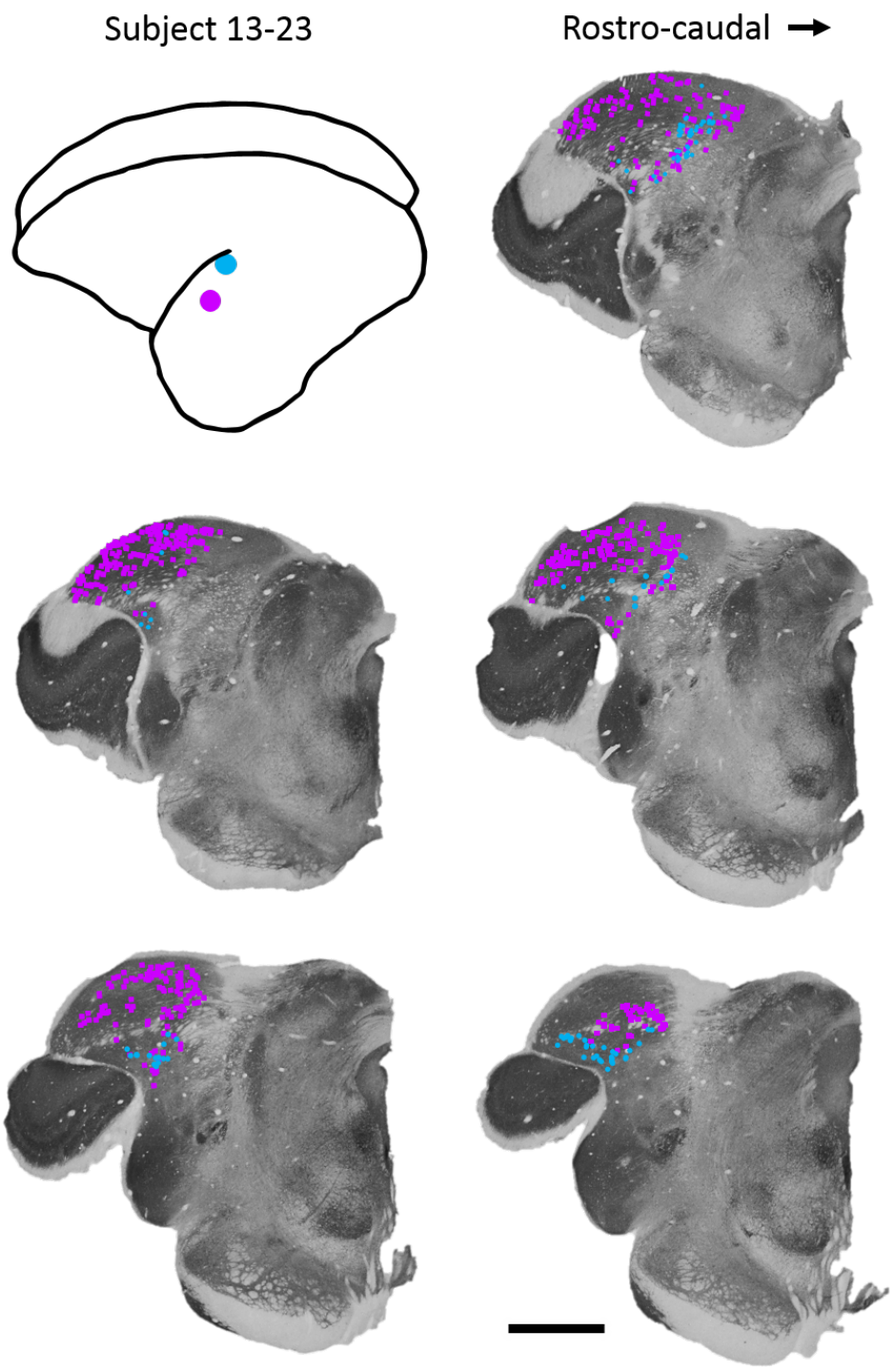

Figure 5.4: CTB and FB placed temporally labels PM, PL, and PI. The illustrated galago brain indicates where temporally placed CTB (purple) and FB (blue) were located in subject 13-23. Each coronal section of pulvinar shown is 300μm apart and are in ascending rostro-caudal order. Labeled cells falling within SGN and LGN are not shown to emphasize pulvinar neurons. CTB = cholera toxin subunit B, FB = fastblue, SGN = suprageniculate nucleus, LGN = lateral geniculate nucleus. Scale bar is 200μm.

residing cells. In rostral thalamic sections, a dense patch of labeled cells are also observed within the suprageniculate nucleus (SGN).

Temporal projections

Two subjects received retrograde tracer injections within temporal cortex. Case 18-12 received one CTB injection rostrolateral to the lateral sulcus' caudal end. This tracer labeled 207 cells within the pulvinar: 140 within PM and 67 in PI. Labeled pulvinar cells fall primarily with medial PM and PI with a small lateral patch in caudal PM (Figure 5.3). Small patches of labeled neurons were also observed within both MGN and SGN.

Case 13-23 received two tracer injections: an FB injection just lateral to the caudal edge of the lateral sulcus and a CTB injection rostrolateral to the FB placement site. These tracer injections resulted collectively in denser labeling than case 18-12 while the distribution of labeled neurons remained consistent (Figure 5.4). The FB injection labeled 107 pulvinar neurons: 36 within PM, 69 in PI, and 2 in PL. Of the over 500 cells labeled by CTB 260 reside within PM, 61 in PI, and 194 in PL. LGN exhibited extensive CTB labeling across both magnocellular and parvocellular layers. A small collection of CTB labeled cells were also observed within SGN.

Frontal projections

Two galagos received retrograde tracer injections within frontal cortex. Case 13-16 received two tracer injections: a DY injection in rostral frontal cortex and a CTB injection just caudolateral to the DY placement site. The DY injection labeled 223 pulvinar neurons: 126 within PM and 97 in PI. CTB labeling was less widespread but equally dense with 61 labeled neurons residing within PM and 46 in PI. The distribution of labeled pulvinar neurons coincides inversely with tracer placement such that CTB labeled cells are overtaken by those labeled with DY as sections advance rostrocaudally (Figure 5.5). A small group of cells labeled by both injections was also observed within SGN.

Case 18-12 only had one frontal cortex injection. Far fewer neurons were labeled in this case than in case 13-16 such that only 125 labeled cells were observed within PM. This is consistent with our other frontal cortex injections, however, the spread of labeled neurons was not as extensive as with other tracer placements in frontal cortex (Figure 5.6).

Discussion

In this study, we placed retrograde tracers into three cortical regions in the galago to explore the homologies between strepsirrhine and haplorhine pulvinocortical projection

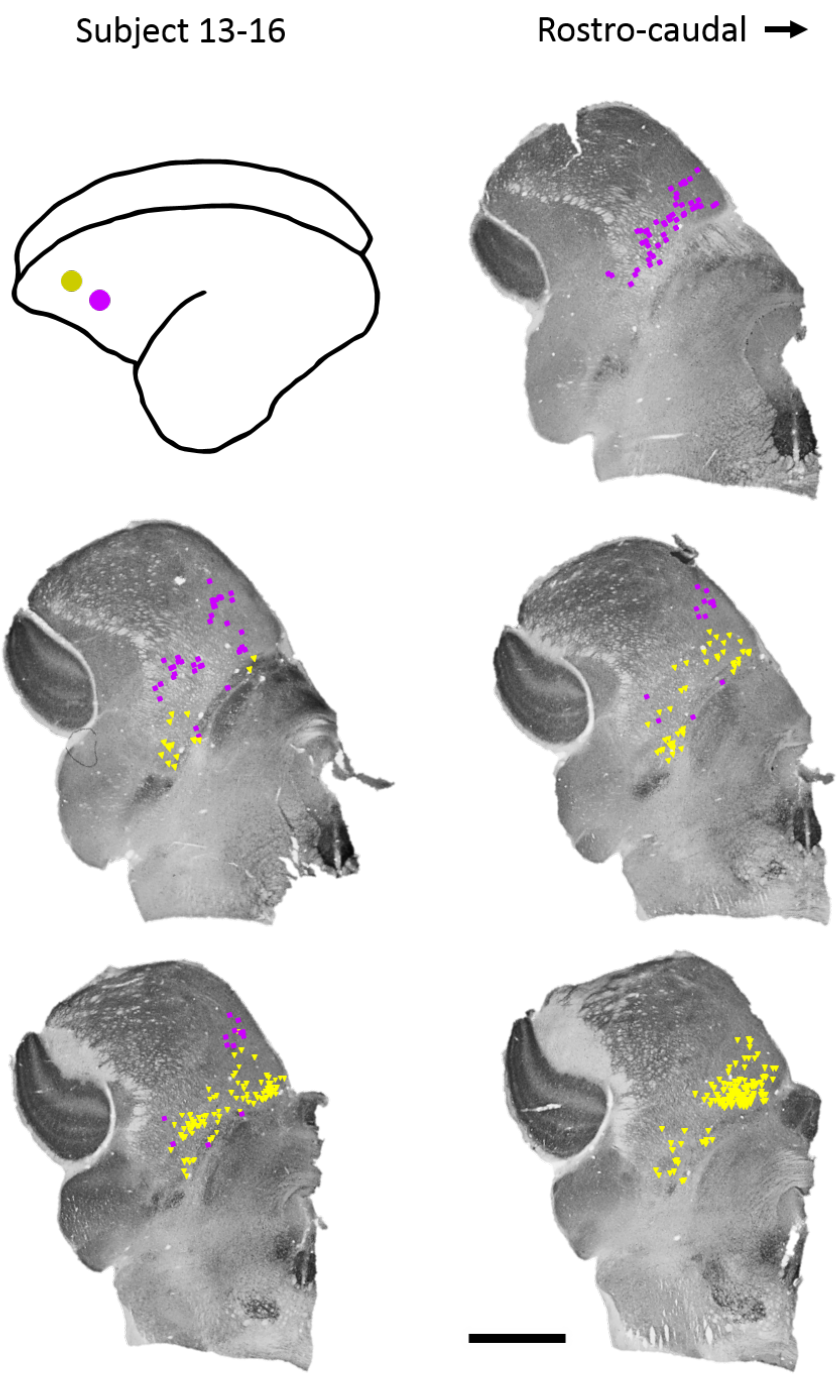

Figure 5.5: Tracers placed in frontal cortex label medial PM and PI. The illustrated galago brain indicates where rostrally placed CTB (purple) and DY (yellow) were located in subject 13-16. Each coronal section of pulvinar shown is 300μm apart and are in ascending rostro-caudal order. Labeled cells falling within SGN are not shown to emphasize pulvinar neurons. CTB = cholera toxin subunit B, DY = diamidino yellow, SGN = suprageniculate nucleus, LGN = lateral geniculate nucleus. Scale bar is 200μm.

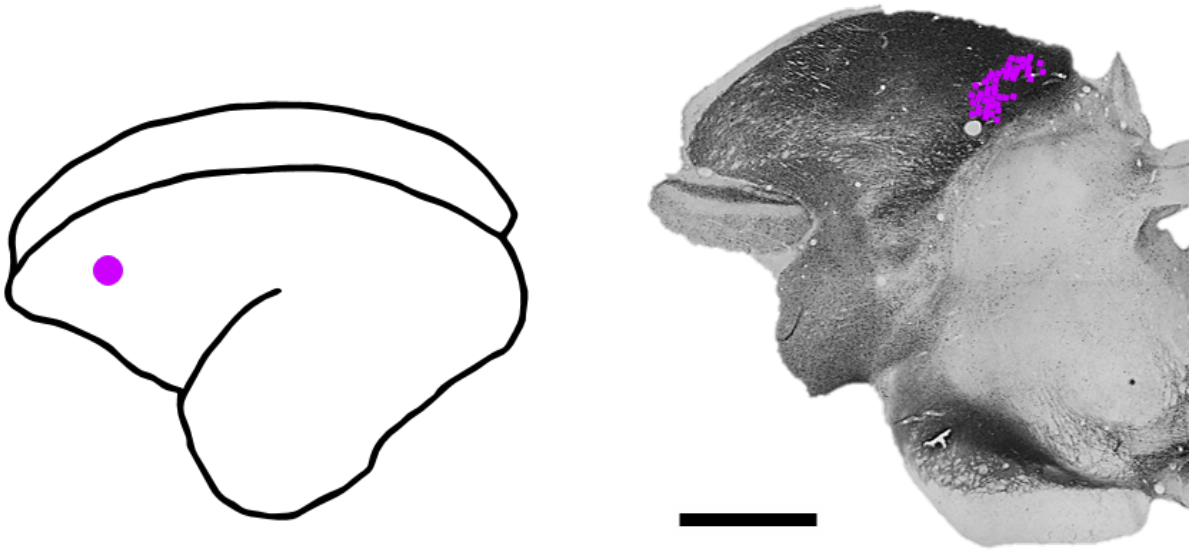

Figure 5.6: CTB in frontal cortex labels medial PM. The illustrated galago brain indicates where rostrally placed CTB (purple) was located in subject 18-12. Labeled cells falling within SGN are not shown to emphasize pulvinar neurons. CTB = cholera toxin subunit B, SGN = supragenicuIate nucleus. Scale bar is 200μm.

patterns. More specifically, we injected these tracers into cortical targets known in the macaque to receive projections from the association pulvinar. Macaque association pulvinar consists of PM and PL_{dm}. Although not typically considered a part of the visual pulvinar, PL_{dm} is involved with high level visual areas. Posterior PL_{dm} shares reciprocal projections with ventral visual stream areas in temporal cortex (Webster et al., 1993; Baizer et al., 1993; Yeterian and Pandya, 1991) and V4 (Lyon et al., 2010; Weller et al., 2002) while being functionally implicated in face perception (Nguyen et al., 2013). This portion of PL_{dm} is not just visually driven, however, as it also has suggested involvement in decision making (Komura et al., 2013). Anterior PL_{dm}, in contrast, reciprocally projects to parietal cortex, the frontal eye fields, and the auditory parabelt (Gutierrez et al., 2000; Yeterian and Pandya, 1985). This region also contains neurons with both covert attentional modulation and presaccadic activation (Robinson et al., 1986; Robinson and Petersen, 1985). PL_{dm} shares a poorly defined border with PM and lacks clear architectonic subdivisions. Medial PM is known to project within temporal cortex (especially auditory belt/parabelt) (Hackett et al., 1998; Romanski et al., 1997; Yeterian and Pandya, 1991) while more lateral PM projects reciprocally with parietal (Contini et al., 2010; Schmahmann and Pandya, 1990) and frontal cortices (Cavada et al., 1995; Trojanowski and Jacobson, 1977).

Galagos and the other members of the Strepsirrhine suborder more closely resemble the common primate ancestor and, as a result, have been a popular model organism for investigators interested in evolution (Jerison, 1979). The pulvinar of this species is bisected

into superior and inferior halves by the brSC with the superior portion of this complex being further subdivided into medial and lateral subdivisions such that galago pulvinar is an apparent caudo-ventral rotational shift of macaque pulvinar (Baldwin et al., 2013). Much like in the macaque, the border between galago PM and PL is often difficult to delineate (Li et al., 2013; Glendenning et al., 1975).

Tracers placed in parietal cortex during the present study revealed densely labeled patches of neurons in both PM and PI. Labeled cells primarily occurred along the medial border of both PM and PI, however, a second more lateral patch of cells were also observed. Additionally, this retrograde tracer injection labeled neurons in PL, albeit in a much sparser manner. This is similar to macaque PM which contains parietal projecting neurons in both medial (Baleydier and Mauguiere, 1985) and lateral patches of PM (Matsuzaki et al., 2004; Cavada et al., 1995; Baleydier and Mauguière, 1987), however, this is where these similarities end. Unlike our galago data, projections in the macaque are limited to originating in either PM or PL_{dm} with little evidence of comparable projections coming from the more visually driven PL_{cl} or PI (Matsuzaki et al., 2004).

Retrograde tracer injections placed approximately in the auditory belt/parabelt show that pulvinar cells targeting this partition of temporal cortex reside primarily along medial PM and medial PI. Within PM, a second smaller lateral patch of labeled neurons is also observed. Additionally, MGN contains a large number of labeled neurons confirming its known connections with the auditory belt/parabelt (Cappe et al., 2009; Hackett et al., 1998). Tracer placement made in the more visually driven inferior lateral temporal cortex resulted in dense labeling in PM, PI, and PL. LGN is also heavily labeled across its layers by these injections confirming previously reported thalamocortical connections (Moore et al., 2018; Li et al., 2013).

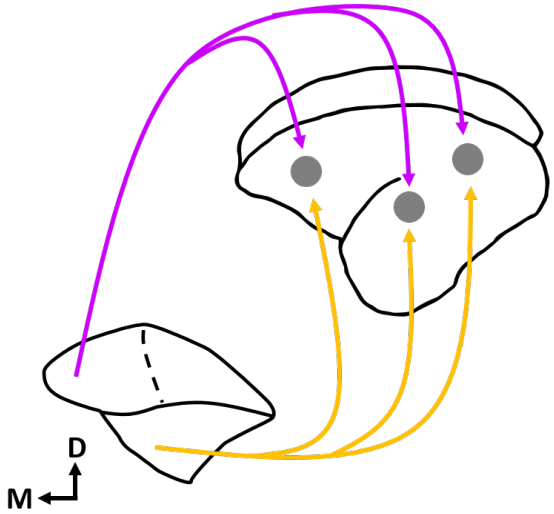

Figure 5.7: Galago association pulvinar. Illustration of galago association pulvinar output. Both PI and PM project to frontal, temporal, and parietal cortices.

The tracers placed in frontal cortex reveal labeled cells falling within both medial PM and PI. Those injections made in the frontal cortex of subject 13-16 demonstrate an interesting property in the distribution of labeled cells. The most rostral tracer injection

paradoxically labels cells falling caudal to neurons projecting to the other more caudal placement site. The macaque pulvinar is similar to that of the galago such that medial PM is known to project to frontal cortex (Cappe et al., 2009; Morecraft et al., 1993), however, frontal targeting PI neurons have not been observed.

The presence of either CB or PV reveals that macaque PI contains 4 clearly delineated subdivisions: a set of CB-rich but PV-poor posterior (PI_p) and central medial nuclei (PI_{cm}) interdigitated amongst the relatively CB-sparse but PV-dense medial (PI_m) and central lateral PI (PI_{cl}) that all extend ventrally from the edge of the SGN across the brSC forming a border abutting PM (Stepniewska and Kaas, 1997). These pulvinar nuclei are home to a series of retinotopic maps that were revealed through the use of both tracer injections (Ungerleider et al., 1984, 2014) and electrophysiology (Bender, 1981). Galago PI is also retinotopically organized, however, it lacks the histological delineations that are seen in the macaque (Moore et al., 2018; Li et al., 2013). Additionally, observed PI projection patterns suggest that this structure shares some functionality with the known association pulvinar subdivision, PM. It is possible that galago PI contains poorly differentiable cell populations that include a set of neurons acting in concert with PM similar to the role that PL_{dm} plays in the macaque. As such, experiments involving galago PI should involve a great deal of caution to avoid confusing visual and association pulvinar functionality. Despite the appearance of homology, similarity between macaque and galago association pulvinar should not be assumed without strong architectonic, connectivity, or electrophysiological evidence.

References

Adams, M. M., Hof, P. R., Gattass, R., Webster, M. J., and Ungerleider, L. G. (2000). Visual cortical projections and chemoarchitecture of macaque monkey pulvinar. *Journal of Comparative Neurology*, 419(3):377–393.

Angelucci, A., Clascá, F., and Sur, M. (1996). Anterograde axonal tracing with the subunit B of cholera toxin: A highly sensitive immunohistochemical protocol for revealing fine axonal morphology in adult and neonatal brains. *Journal of Neuroscience Methods*, 65(1):101–112.

Asanuma, C., Andersen, R. A., and Cowan, W. M. (1985). The thalamic relations of the caudal inferior parietal lobule and the lateral prefrontal cortex in monkeys: divergent cortical projections from cell clusters in the medial pulvinar nucleus. *The Journal of Comparative Neurology*, 241:357–81.

Baizer, J. S., Desimone, R., and Ungerleider, L. G. (1993). Comparison of subcortical connections of inferior temporal and posterior parietal cortex in monkeys. *Visual neuroscience*, 10(1):59–72.

Baldwin, M. K., Balaram, P., and Kaas, J. H. (2017). The evolution and functions of nuclei of the visual pulvinar in primates. *Journal of Comparative Neurology*, 525(15):3207–3226.

Baldwin, M. K. L., Balaram, P., and Kaas, J. H. (2013). Projections of the superior colliculus to the pulvinar in prosimian galagos (Otolemur garnettii) and VGLUT2 staining of the visual pulvinar. *Journal of Comparative Neurology*, 521(7):1664–1682.

Baldwin, M. K. L., Kaskan, P. M., Zhang, B., Chino, Y. M., and Kaas, J. H. (2012). Cortical and subcortical connections of V1 and V2 in early postnatal macaque monkeys. *The Journal of comparative neurology*, 520(3):544–69.

Baleydier, C. and Mauguiere, F. (1985). Anatomical evidence for medial pulvinar connections with the posterior cingulate cortex, the retrosplenial area, and the posterior parahippocampal gyrus in monkeys. *The Journal of comparative neurology*, 232(2):219–28.

Baleydier, C. and Mauguière, F. (1987). Network organization of the connectivity between parietal area 7, posterior cingulate cortex and medial pulvinar nucleus: a double fluorescent tracer study in monkey. *Experimental brain research*, 66(2):385–93.

Bender, D. B. (1981). Retinotopic organization of macaque pulvinar. *Journal of neurophysiology*, 46(3):672–693.

Boyd, J. D. and Matsubara, J. A. (1996). Laminar and columnar patterns of geniculocortical projections in the cat: Relationship to cytochrome oxidase. *Journal of Comparative Neurology*, 365(4):659–682.

Cappe, C., Morel, A., Barone, P., and Rouiller, E. M. (2009). The thalamocortical projection systems in primate: An anatomical support for multisensory and sensorimotor interplay. *Cerebral Cortex*, 19(9):2025–2037.

Cavada, C., Compañy, T., Hernández-González, A., and Reinoso-Suárez, F. (1995). Acetylcholinesterase histochemistry in the macaque thalamus reveals territories selectively connected to frontal, parietal and temporal association cortices. *Journal of Chemical Neuroanatomy*, 8(4):245–257.

Cola, M. G., Seltzer, B., Preuss, T. M., and Cusick, C. G. (2005). Neurochemical organization of chimpanzee inferior pulvinar complex. *Journal of Comparative Neurology*, 484(3):299–312.

Contini, M., Baccarini, M., Borra, E., Gerbella, M., Rozzi, S., and Luppino, G. (2010). Thalamic projections to the macaque caudal ventrolateral prefrontal areas 45A and 45B. *European Journal of Neuroscience*, 32(8):1337–1353.

Glendenning, K. K., Hall, J. A., Diamond, I. T., and Hall, W. C. (1975). The pulvinar nucleus of Galago senegalensis. *J Comp Neurol*, 161(3):419–458.

Gutierrez, C., Cola, M. G., Seltzer, B., and Cusick, C. (2000). Neurochemical and connectional organization of the dorsal pulvinar complex in monkeys. *Journal of Comparative Neurology*, 419(1):61–86.

Hackett, T. a., Stepniewska, I., and Kaas, J. H. (1998). Thalamocortical connections of the parabelt auditory cortex in macaque monkeys. *Journal of Comparative Neurology*, 400(January):271–286.

Huerta, M. F., Krubitzer, L. A., and Kaas, J. H. (1986). Frontal eye field as defined by intracortical microstimulation in squirrel monkeys, owl monkeys, and macaque monkeys: I. Subcortical connections. *The Journal of comparative neurology*, 253(4):415–39.

Jerison, H. J. (1979). Brain, body and encephalization in early primates. *Journal of Human Evolution*, 8(6):615–635.

Kaas, J. H. and Lyon, D. C. (2007). Pulvinar contributions to the dorsal and ventral streams of visual processing in primates. *Brain Research Reviews*, 55(2 SPEC. ISS.):285–296.

Komura, Y., Nikkuni, A., Hirashima, N., Uetake, T., and Miyamoto, A. (2013). Responses of pulvinar neurons reflect a subject's confidence in visual categorization. *Nature Neuroscience*, 16(6):749–55.

Li, K., Patel, J., Purushothaman, G., Marion, R. T., and Casagrande, V. A. (2013). Retinotopic maps in the pulvinar of bush baby (Otolemur garnettii). *Journal of Comparative Neurology*, 521(15):3432–3450.

Liao, C. C., Gharbawie, O. A., Qi, H., and Kaas, J. H. (2013). Cortical connections to single digit representations in area 3b of somatosensory cortex in squirrel monkeys and prosimian galagos. *Journal of Comparative Neurology*, 521(16):3768–3790.

Lyon, D. C., Nassi, J. J., and Callaway, E. M. (2010). A Disynaptic Relay from Superior Colliculus to Dorsal Stream Visual Cortex in Macaque Monkey. *Neuron*, 65(2):270–279.

Markowitsch, H. J., Emmans, D., Irle, E., Streicher, M., and Preilowski, B. (1985). Cortical and subcortical afferent connections of the primate's temporal pole: A study of rhesus monkeys, squirrel monkeys, and marmosets. *Journal of Comparative Neurology*, 242(3):425–458.

Matsuzaki, R., Kyuhou, S. I., Matsuura-Nakao, K., and Gemba, H. (2004). Thalamo-cortical projections to the posterior parietal cortex in the monkey. *Neuroscience Letters*, 355(1-2):113–116.

Moore, B., Li, K., Kaas, J. H., Liao, C.-C., Boal, A. M., Mavity-Hudson, J., and Casagrande, V. (2018). Cortical projections to the two retinotopic maps of primate pulvinar are distinct. *Journal of Comparative Neurology*.

Morecraft, R. J., Geula, C., and Mesulam, M. M. (1993). Architecture of Connectivity Within a Cingulo-Fronto-Parietal Neurocognitive Network for Directed Attention. *Archives of Neurology*, 50(3):279–284.

Nguyen, M. N., Hori, E., Matsumoto, J., Tran, A. H., Ono, T., and Nishijo, H. (2013). Neuronal responses to face-like stimuli in the monkey pulvinar. *European Journal of Neuroscience*, 37(1):35–51.

O'Brien, B. J., Abel, P. L., and Olavarria, J. F. (2001). The retinal input to calbindin-D28k-defined subdivisions in macaque inferior pulvinar. *Neuroscience Letters*, 312(3):145–148.

Patrick Hardy, S. G. and Lynch, J. C. (1992). The spatial distribution of pulvinar neurons that project to two subregions of the inferior parietal lobule in the macaque. *Cerebral Cortex*, 2(3):217–230.

Preuss, T. M., Beck, P. D., and Kaas, J. H. (1993). Areal, modular, and connectional organization of visual cortex in a prosimian primate, the slow loris (Nycticebus coucang). *Brain, behavior and evolution*, 42(6):321–335.

Preuss, T. M. and Goldman-Rakic, P. S. (1991). Architectonics of the parietal and temporal association cortex in the strepsirhine primate Galago compared to the anthropoid primate Macaca. *The Journal of comparative neurology*, 310(4):475–506.

Radinsky, L. (1975). Primate brain evolution. *American scientist*, 63(6):656–63.

Robinson, D. L. and Petersen, S. E. (1985). Responses of pulvinar neurons to real and self-induced stimulus movement. *Brain Research*, 338(2):392–394.

Robinson, D. L., Petersen, S. E., and Keys, W. (1986). Saccade-related and visual activities in the pulvinar nuclei of the behaving rhesus monkey. *Experimental Brain Research*, 62(3):625–634.

Romanski, L. M., Giguere, M., Bates, J. F., and Goldman-Rakic, P. S. (1997). Topographic organization of medial pulvinar connections with the prefrontal cortex in the rhesus monkey. *Journal of Comparative Neurology*, 379(June 1996):313–332.

Schmahmann, J. D. and Pandya, D. N. (1990). Anatomical investigation of projections from thalamus to posterior parietal cortex in the rhesus monkey: A WGA-HRP and fluorescent tracer study. *Journal of Comparative Neurology*, 295(2):299–326.

Stepniewska, I. and Kaas, J. H. (1997). Architectonic subdivisions of the inferior pulvinar in New World and Old World monkeys. *Vis Neurosci*, 14(6):1043–1060.

Trojanowski, J. Q. and Jacobson, S. (1974). Medial pulvinar afferents to frontal eye fields in rhesus monkey demonstrated by horseradish peroxidase. *Brain Research*, 80(3):395–411.

Trojanowski, J. Q. and Jacobson, S. (1976). Areal and laminar distribution of some pulvinar cortical efferents in rhesus monkey. *The Journal of comparative neurology*, 169:371–392.

Trojanowski, J. Q. and Jacobson, S. (1977). Brain The Morphology and Laminar Distribution of Cortico-Pulvinar Neurons in the Rhesus Monkey. *Experimental Brain Research*, 62(1-2):51–62.

Ungerleider, L. G., Desimone, R., Galkin, T. W., and Mishkin, M. (1984). Subcortical projections of area MT in the macaque. *The Journal of comparative neurology*, 223(3):368–386.

Ungerleider, L. G., Galkin, T. W., Desimone, R., and Gattass, R. (2014). Subcortical projections of area V2 in the macaque. *Journal of cognitive neuroscience*, 26(6):1220–33.

Webster, M. J., Bachevalier, J., and Ungerleider, L. G. (1993). Subcortical connections of inferior temporal areas TE and TEO in macaque monkeys. *The Journal of comparative neurology*, 335(1):73–91.

Weller, R. E., Steele, G. E., and Kaas, J. H. (2002). Pulvinar and other subcortical connections of dorsolateral visual cortex in monkeys. *Journal of Comparative Neurology*, 450(3):215–240.

Wong, P. and Kaas, J. H. (2010). Architectonic subdivisions of neocortex in the galago (Otolemur garnetti). *Anatomical Record*, 293(6):1033–1069.

Yeterian, E. H. and Pandya, D. N. (1985). Corticothalamic connections of the posterior parietal cortex in the rhesus monkey. *J. Comp. Neurol.*, 237(3):408–426.

Yeterian, E. H. and Pandya, D. N. (1989). Thalamic connections of the cortex of the superior temporal sulcus in the rhesus monkey. *The Journal of comparative neurology*, 282(November 1986):80–97.

Yeterian, E. H. and Pandya, D. N. (1991). Corticothalamic connections of the superior temporal sulcus in rhesus monkeys. *Experimental brain research*, 83(2):268–84.

CHAPTER 6
SUMMARY AND CONCLUSIONS

The experiments described in this volume are part of the greater effort to understand the pulvinar's structure and function. These experiments are a series of anatomical tract tracing studies performed in the northern greater galago (*Otolemur garnettii*). Although the majority of pulvinar research has been conducted in the macaque, galago studies provide a unique comparative perspective. Wet-nosed strepsirrhine primates, like galagos, are phylogenetically similar to early primate ancestors (Kaas and Lyon, 2007; Preuss et al., 1993; Preuss and Goldman-Rakic, 1991; Radinsky, 1975) which makes results from galago studies particularly relevant from a comparative perspective. The pulvinar is the largest component of the primate thalamus (Jones, 2007). This complex plays an important role in attention (Van Essen, 2005; Petersen et al., 1987) as well as being implicated in a large range of functionality spanning both visual (including visuomotor) and multisensory processing (Li et al., 2013; West et al., 2011; Purushothaman et al., 2012; Berman and Wurtz, 2011; Robinson et al., 1986), however, consensus on its functional subdivisions remains elusive with many different proposed organization schemes adding to the confusion (Baldwin et al., 2017; Lyon et al., 2010; Kaas and Lyon, 2007; Gutierrez et al., 2000).

In our review of the macaque pulvinar literature (Chapter 2), we propose that the this thalamic complex contains a sensory hierarchy similar to that observed along the progression of visually driven cortical areas. The visual pulvinar has an information flow that begins in the dual retinotopic maps of lateral pulvinar's ventrolateral subdivision (PL_{vl}) and inferior pulvinar's centrolateral nucleus (PI_{cl}) (Felleman and Van Essen, 1991). This information stream progresses from the pulvinar's ventrolateral to dorsomedial end much like the cortical visual hierarchy that runs from primary visual cortex (V1) before flowing in a caudorostral manner. As this cortical information flow progresses, it splits into ventral "what" and dorsal "where" processing streams. The pulvinar is suspected to exhibit a similar parallel organization with medial PI (PI_m sharing reciprocal connections with high level visual areas in temporal cortex while dorsomedial PL (PL_{dm}) is associated with the parietal "where " stream (Gutierrez et al., 2000; Adams et al., 2000; Rockland et al., 1999; Baleydier and Morel, 1992). This information flow ends with medial pulvinar (PM) functioning as a suspected multisensory integration area. A hierarchical model for pulvinar organization has been previously suggested for the visually responsive nuclei of this complex (Benevento and Davis, 1977), however, our theoretical framework takes into account modern anatomical borders (Kaas and Lyon, 2007) and includes the association

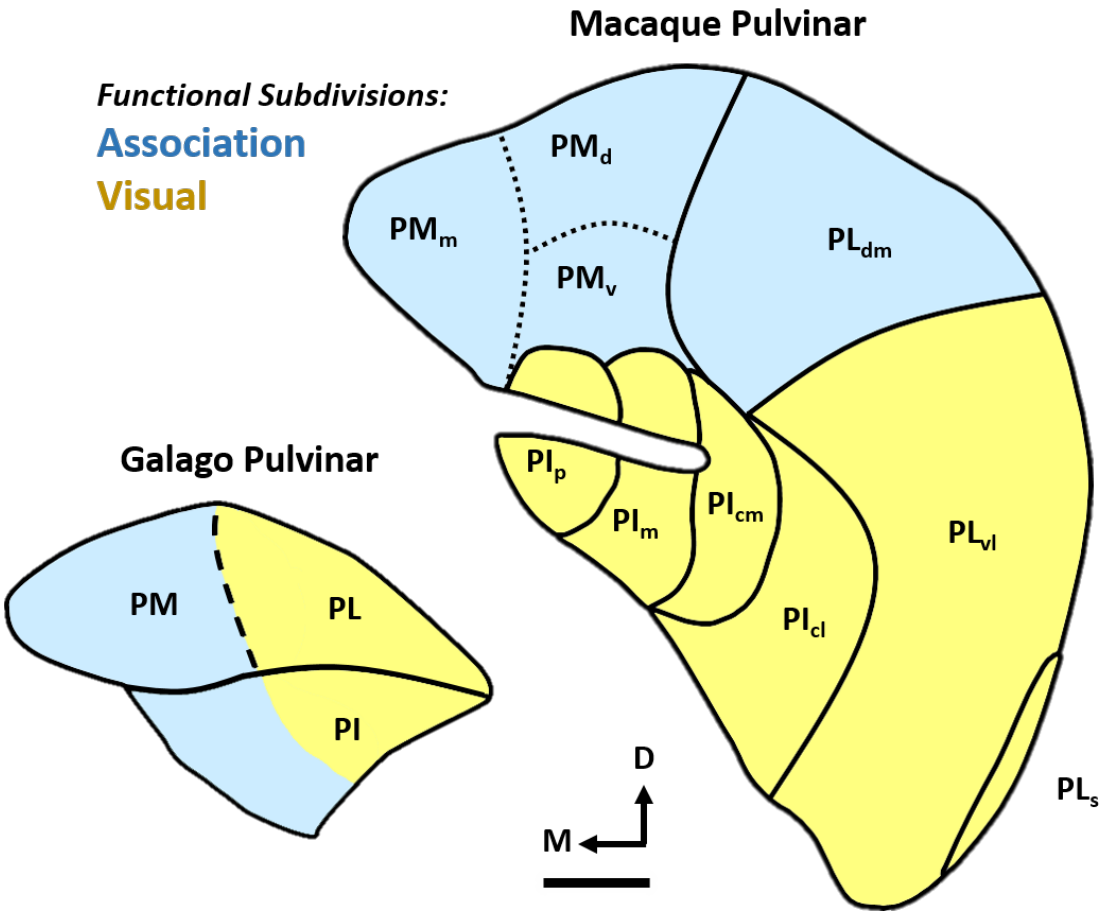

Figure 6.1: Comparison of galago and macaque pulvinar. Galago and macaque pulvinar with functional and architectonic labeled subdivisions. Visual and association pulvinar respectively shaded yellow or blue. Dotted lines in macaque PM indicate proposed subdivisions based on a series of anatomical tract tracing studies (Cappe et al., 2009; Gutierrez et al., 2000; Romanski et al., 1997; Cavada et al., 1995; Trojanowski and Jacobson, 1974). PI = inferior pulvinar, PL = lateral pulvinar, PM = medial pulvinar, PI = inferior pulvinar, PL = lateral pulvinar, PM_m = medial PM, PM_d = dorsal PM, PM_v = ventral PM, PL_{dm} = dorso-medial PL, PL_{vl} = ventro-lateral PL, PL_s = "shell" of PL, PI_p = posterior PI, PI_m = medial PI, PI_{cm} = centro-medial PI, PI_{cl} = centro-lateral PI. Scale bar is 1mm.

pulvinar nuclei.

Members of the Strepsirrhine suborder, including galagos, closely resemble the primate common ancestor and have been a popular model organism for investigators interested in evolution (Jerison, 1979). Galago pulvinar is an apparent caudoventral rotational shift of macaque pulvinar (Baldwin et al., 2013) (Figure 6.1) which means that the galago pulvinar's dual retinotopic maps fall into vertical alignment (Li et al., 2013) as opposed to the macaque where these maps exist along the mediolateral axis (Bender, 1981). The vertical alignment of these maps allowed for the first anatomical tract tracing study comparing retinotopically matched tracer injections placed within these two nuclei (Moore et al., 2018). This study (Chapter 3) used real-time electrophysiological data

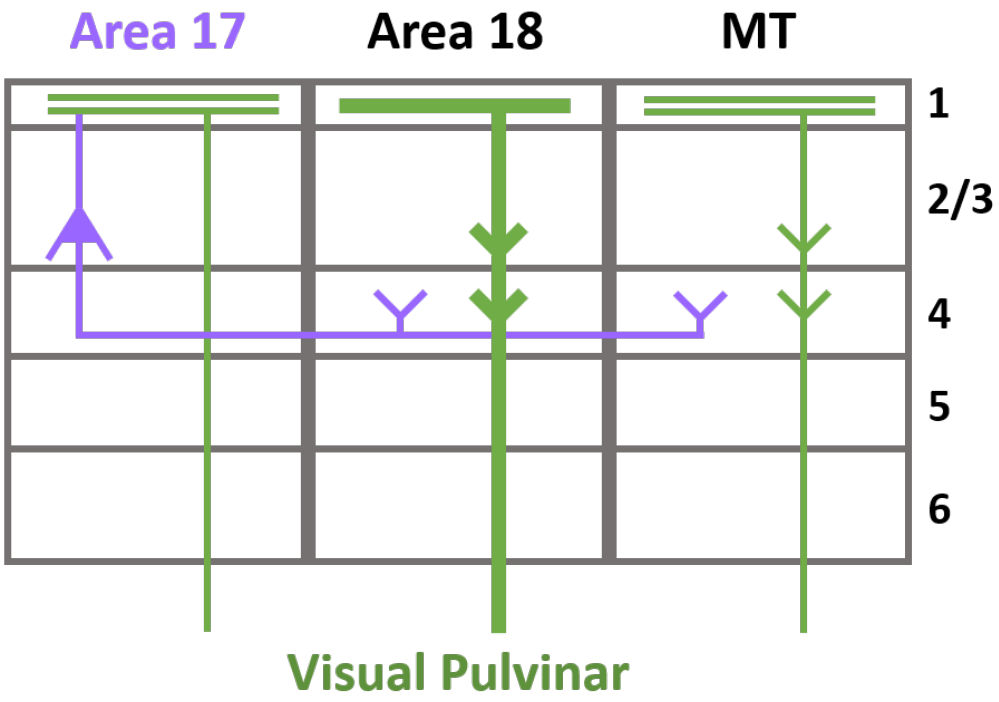

Figure 6.2: Summary of pulvinar projections to early visual cortices. The visual pulvinar projects to superficial V1 as well as granular V2 and MT. Purple indicates projections from V1 pyramidal neurons while green labels projections from the visual pulvinar. The thickness of V2 terminating projections reflects large bouton sizes.

collected with in-house manufactured injectrodes to guide tracer injections within the retinotopically mirrored dorsal and ventral maps of visual pulvinar. Retrograde tracer injections labeled populations of neurons extending over many cortical areas involved in vision (V1, V2, V3, MT, DL(V4), MST, IT). These projections originated primarily in layer 6 but a large population originated from layer 5 within the territories of V2 and V3. Neurons projecting to the dorsal and ventral retinotopic maps were from distinct but overlapping populations as reflected by the absence of double-labeled neurons in cortex.

To explore the extent of visual pulvinar output, a series of anterograde tracers were placed in galago PL and the ultrastructure of the pulvinar's synaptic targets in early visual cortices was examined with both confocal- and electron-microscopy (Chapter 4). Thalamocortical projections, like these from the pulvinar, can be classified as either driving a sensory signal or providing input that modifies such a signal (Sherman and Guillery, 1998). Although the driver/modulator designation is functionally defined, anatomical correlates of both types of thalamic output may be the foundation to a more complete understanding of the pulvinar's projections as well as providing information concerning the output of secondary thalamic nuclei in general. Anterograde tracers placed in PL revealed

projections terminating almost entirely within layer 1 of V1. This is consistent with macaque data (Rezak and Benevento, 1979; Ogren and Hendrickson, 1977). Observed arborizations spanned more than one cortical column, had boutons en passant, and sometimes formed collaterals in layers 2/3. These findings confirm similar results seen in both the galago (Lachica and Casagrande, 1992; Carey et al., 1979) and macaque literature (Rubio-Garrido et al., 2009; Rockland et al., 1999). The size and location of labeled pulvinocortical axon terminals in cortical layer 1 as well as the absence of GABA in postsynaptic profiles and previously reported gating functionality (Purushothaman et al., 2012) suggest that these projections may act in a modulatory fashion by synapsing on the apical dendrites of pyramidal neurons residing deeper in cortex. Projections targeting extrastriate areas primarily ended in layer 4 or deep layer 3 with V2 notably having boutons that were significantly larger than V1's known driving projections (Marion et al., 2013) suggesting that labeled processes are, in turn, cortical drivers (Figure 6.2). Taken together, this evidence suggests that galago visual pulvinar differentially drives and modulates cortex depending on the location of axonal termination.

The association pulvinar remains less studied than the visual pulvinar as this group of thalamic nuclei are responsive to more complex stimuli. The macaque literature demonstrates heavy projections from these pulvinar subdivisions to temporal (Yeterian and Pandya, 1989; Markowitsch et al., 1985), frontal (Cappe et al., 2009; Asanuma et al., 1985; Baleydier and Mauguiere, 1985; Trojanowski and Jacobson, 1974), parietal (Matsuzaki et al., 2004; Cavada et al., 1995; Morecraft et al., 1993; Patrick Hardy and Lynch, 1992), and belt/parabelt cortices (Cappe et al., 2009; Hackett et al., 1998; Baleydier and Mauguiere, 1985). A prominent feature of the galago is its smooth brain which makes it an extremely convenient species to perform comparative connection studies. One such study (Chapter 5) demonstrates a limited homology between the cortical targets of association pulvinar in the galago and the macaque. A series of retrograde tracers injected in temporal, frontal, and parietal cortices revealed projections originating from two mediolateral patches in PM and one running along medial PM and PI. The two adjacent PM cell patches differentially project to parietal and frontal/temporal cortices in a similar manner to what is seen in the macaque's dorsal and ventral PM subdivisions (Cappe et al., 2009; Hackett et al., 2007; Matsuzaki et al., 2004; Hackett et al., 1998; Cavada et al., 1995; Yeterian and Pandya, 1989; Baleydier and Mauguière, 1987; Asanuma et al., 1985; Baleydier and Mauguiere, 1985; Trojanowski and Jacobson, 1974). Projections to all three cortical injection sites were observed along the medial edge of PM and PI. Galago medial PI shows more similarity to macaque dorsomedial PL (PL_{dm}) than to macaque PI; a known component of the visual pulvinar (Figure 6.1). This study provides the first evidence that

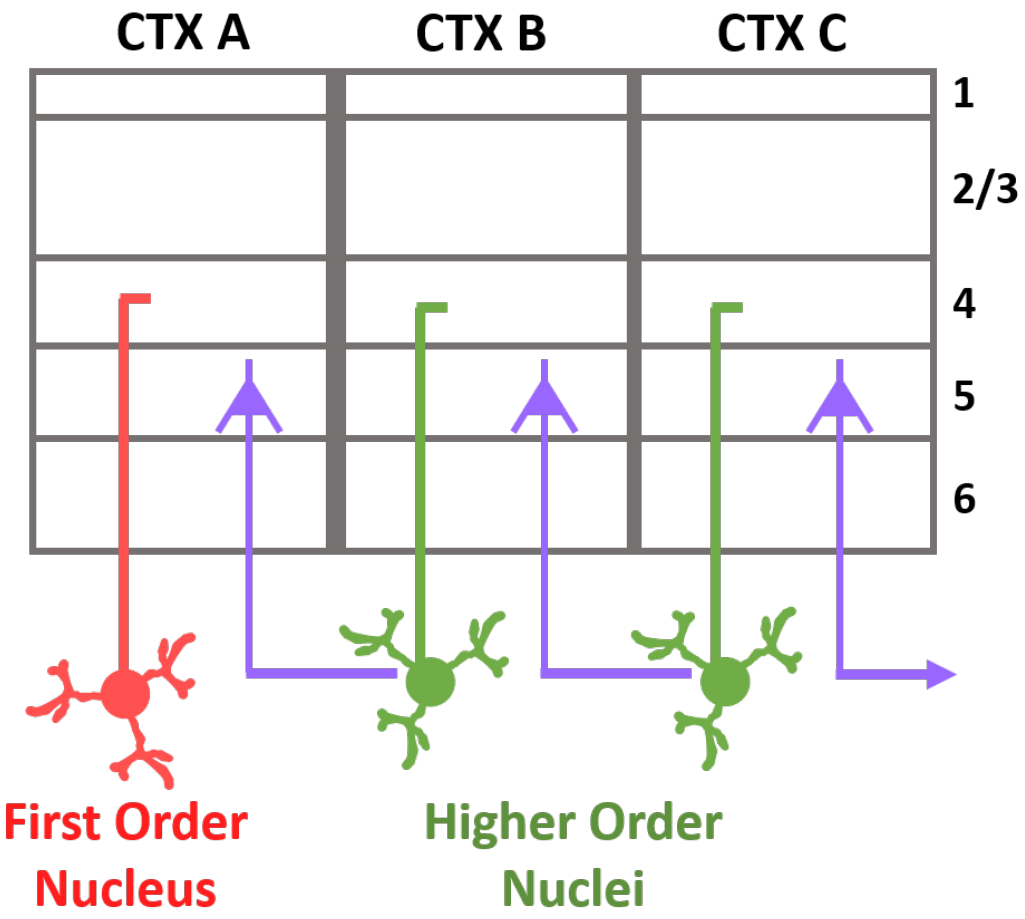

Figure 6.3: Schematic diagram of cortico-thalamo-cortical projections. Neurons in first order thalamic nuclei (red) project to cortical layer 4 and drive their cortical targets. In turn, neurons in this cortical area (purple) then drive a higher order thalamic nucleus (green) which propagates along a chain of cortico-thalamo-cortical feed-forward projections. In the context of early visual cortices, the first order nucleus would be the lateral geniculate nucleus (LGN) with the higher order nuclei residing within the pulvinar complex. Diagram adapted from Guillery (2005).

the association pulvinar's cortical projections are similar between macaques and their Strepsirrhine galago cousins.

The question of "What does the pulvinar do?" remains largely unanswered but progress has been made towards a more complete understanding of both this subcortical complex as well as second order thalamic nuclei in general. Higher order thalamic nuclei, like those that comprise the pulvinar complex, differ from first order nuclei in that they receive their driving input from cortical rather than subcortical sources. This difference allows for the propagation of feed-forward chains of cortico-thalamo-cortical projections (Figure 6.3). In the context of the visual system, the progression of driving projections begins with the LGN (a first order thalamic nucleus) which relays sensory signals from the

retina to V1. From here, layer 5 pyramidal neurons send driving projections to the visual pulvinar which, in turn, sends driving projections to granular V2. Theoretically such a feed-forward train of driving projections could extend throughout the visual system resulting in a processing stream that runs parallel to the traditionally held cortical visual hierarchy described by Felleman and Van Essen (1991). Much like how a primary thalamic nucleus relays a signal from the periphery to cortex, higher order nuclei like the pulvinar may relay signals between cortical areas.

The existence of parallel cortico-cortical and cortico-thalamo-cortical processing pathways may seem redundant at first, however, these dual pathways have one notable feature that cortico-cortical projections alone would lack. Projections from the cortex to higher order nuclei often branch to a number of extrathalamic subcortical targets including the midbrain and pons (Bourassa and Deschenes, 1995). Guillery (2006, 2005) suggests that information relayed to the midbrain through cortico-thalamo-cortical projections could be used to inform motor output along each stage of sensory processing. Microstimulation of striate cortex has been shown to evoke saccadic eye movements in just such a manner (Tehovnik et al., 2003). Its possible that other sensory modalities behave similarly.

This dissertation concludes with a word of caution that all eager neuroanatomists would be wise to heed. As always with the spectre of comparative research, any apparent homologies must not be assumed without further functional and architectonic evidence. To quote Oscar Wilde,"The truth is rarely pure and never simple." ✌

References

Adams, M. M., Hof, P. R., Gattass, R., Webster, M. J., and Ungerleider, L. G. (2000). Visual cortical projections and chemoarchitecture of macaque monkey pulvinar. *Journal of Comparative Neurology*, 419(3):377–393.

Asanuma, C., Andersen, R. A., and Cowan, W. M. (1985). The thalamic relations of the caudal inferior parietal lobule and the lateral prefrontal cortex in monkeys: divergent cortical projections from cell clusters in the medial pulvinar nucleus. *The Journal of Comparative Neurology*, 241:357–81.

Baldwin, M. K., Balaram, P., and Kaas, J. H. (2017). The evolution and functions of nuclei of the visual pulvinar in primates. *Journal of Comparative Neurology*, 525(15):3207–3226.

Baldwin, M. K. L., Balaram, P., and Kaas, J. H. (2013). Projections of the superior colliculus to the pulvinar in prosimian galagos (Otolemur garnettii) and VGLUT2 staining of the visual pulvinar. *Journal of Comparative Neurology*, 521(7):1664–1682.

Baleydier, C. and Mauguiere, F. (1985). Anatomical evidence for medial pulvinar connections with the posterior cingulate cortex, the retrosplenial area, and the posterior parahippocampal gyrus in monkeys. *The Journal of comparative neurology*, 232(2):219–28.

Baleydier, C. and Mauguière, F. (1987). Network organization of the connectivity between parietal area 7, posterior cingulate cortex and medial pulvinar nucleus: a double fluorescent tracer study in monkey. *Experimental brain research*, 66(2):385–93.

Baleydier, C. and Morel, A. (1992). Segregated thalamocortical pathways to inferior parietal and inferotemporal cortex in macaque monkey. *Visual neuroscience*, 8(5):391–405.

Bender, D. B. (1981). Retinotopic organization of macaque pulvinar. *Journal of neurophysiology*, 46(3):672–693.

Benevento, L. A. and Davis, B. (1977). Topographical projections of the prestriate cortex to the pulvinar nuclei in the macaque monkey: An autoradiographic study. *Experimental Brain Research*, 30(2-3):405–424.

Berman, R. A. and Wurtz, R. H. (2011). Signals conveyed in the pulvinar pathway from superior colliculus to cortical area MT. *The Journal of neuroscience : the official journal of the Society for Neuroscience*, 31(2):373–84.

Bourassa, J. and Deschenes, M. (1995). Corticothalamic projections from the primary visual cortex in rats: a single fiber study using biocytin as an anterograde tracer. *Neuroscience*, 66(2):253–263.

Cappe, C., Morel, A., Barone, P., and Rouiller, E. M. (2009). The thalamocortical projection systems in primate: An anatomical support for multisensory and sensorimotor interplay. *Cerebral Cortex*, 19(9):2025–2037.

Carey, R. G., Fitzpatrick, D., and Diamond, I. T. (1979). Layer I of striate cortex of Tupaia glis and Galago senegalensis: Projections from thalamus and claustrum revealed by retrograde transport of horseradish peroxidase. *Journal of Comparative Neurology*, 186(3):393–437.

Cavada, C., Compañy, T., Hernández-González, A., and Reinoso-Suárez, F. (1995). Acetylcholinesterase histochemistry in the macaque thalamus reveals territories selectively connected to frontal, parietal and temporal association cortices. *Journal of Chemical Neuroanatomy*, 8(4):245–257.

Felleman, D. J. and Van Essen, D. C. (1991). Distributed hierarchical processing in the primate cerebral cortex. *Cerebral cortex (New York, N.Y. : 1991)*, 1:1–47.

Guillery, R. W. (2005). Anatomical pathways that link perception and action. *Progress in Brain Research*, 149(1994):235–256.

Guillery, R. W. (2006). Branching Thalamic Afferents Link Action and Perception. *Journal of Neurophysiology*, 90(2):539–548.

Gutierrez, C., Cola, M. G., Seltzer, B., and Cusick, C. (2000). Neurochemical and connectional organization of the dorsal pulvinar complex in monkeys. *Journal of Comparative Neurology*, 419(1):61–86.

Hackett, T. A., De La Mothe, L. A., Ulbert, I., Karmos, G., Smiley, J., and Schroeder, C. E. (2007). Multisensory convergence in auditory cortex, II. Thalamocortical connections of the caudal superior temporal plane. *The Journal of comparative neurology*, 502(6):924–52.

Hackett, T. a., Stepniewska, I., and Kaas, J. H. (1998). Thalamocortical connections of the parabelt auditory cortex in macaque monkeys. *Journal of Comparative Neurology*, 400(January):271–286.

Jerison, H. J. (1979). Brain, body and encephalization in early primates. *Journal of Human Evolution*, 8(6):615–635.

Jones, E. G. (2007). *The Thalamus*. Cambridge University Press, Cambridge, UK, 2 edition.

Kaas, J. H. and Lyon, D. C. (2007). Pulvinar contributions to the dorsal and ventral streams of visual processing in primates. *Brain Research Reviews*, 55(2 SPEC. ISS.):285–296.

Lachica, E. a. and Casagrande, V. a. (1992). Direct W-like geniculate projections to the cytochrome oxidase (CO) blobs in primate visual cortex: axon morphology. *The Journal of comparative neurology*, 319(1):141–58.

Li, K., Patel, J., Purushothaman, G., Marion, R. T., and Casagrande, V. A. (2013). Retinotopic maps in the pulvinar of bush baby (Otolemur garnettii). *Journal of Comparative Neurology*, 521(15):3432–3450.

Lyon, D. C., Nassi, J. J., and Callaway, E. M. (2010). A Disynaptic Relay from Superior Colliculus to Dorsal Stream Visual Cortex in Macaque Monkey. *Neuron*, 65(2):270–279.

Marion, R., Li, K., Purushothaman, G., Jiang, Y., and Casagrande, V. A. (2013). Morphological and neurochemical comparisons between pulvinar and V1 projections to V2. *Journal of Comparative Neurology*, 521(4):813–832.

Markowitsch, H. J., Emmans, D., Irle, E., Streicher, M., and Preilowski, B. (1985). Cortical and subcortical afferent connections of the primate's temporal pole: A study of rhesus monkeys, squirrel monkeys, and marmosets. *Journal of Comparative Neurology*, 242(3):425–458.

Matsuzaki, R., Kyuhou, S. I., Matsuura-Nakao, K., and Gemba, H. (2004). Thalamo-cortical projections to the posterior parietal cortex in the monkey. *Neuroscience Letters*, 355(1-2):113–116.

Moore, B., Li, K., Kaas, J. H., Liao, C.-C., Boal, A. M., Mavity-Hudson, J., and Casagrande, V. (2018). Cortical projections to the two retinotopic maps of primate pulvinar are distinct. *Journal of Comparative Neurology*.

Morecraft, R. J., Geula, C., and Mesulam, M. M. (1993). Architecture of Connectivity Within a Cingulo-Fronto-Parietal Neurocognitive Network for Directed Attention. *Archives of Neurology*, 50(3):279–284.

Ogren, M. P. and Hendrickson, a. E. (1977). The distribution of pulvinar terminals in visual areas 17 and 18 of the monkey. *Brain Research*, 137(2):343–350.

Patrick Hardy, S. G. and Lynch, J. C. (1992). The spatial distribution of pulvinar neurons that project to two subregions of the inferior parietal lobule in the macaque. *Cerebral Cortex*, 2(3):217–230.

Petersen, S. E., Robinson, D. L., and Morris, J. D. (1987). Contributions of the pulvinar to visual spatial attention. *Neuropsychologia*, 25(1 PART 1):97–105.

Preuss, T. M., Beck, P. D., and Kaas, J. H. (1993). Areal, modular, and connectional organization of visual cortex in a prosimian primate, the slow loris (Nycticebus coucang). *Brain, behavior and evolution*, 42(6):321–335.

Preuss, T. M. and Goldman-Rakic, P. S. (1991). Architectonics of the parietal and temporal association cortex in the strepsirhine primate Galago compared to the anthropoid primate Macaca. *The Journal of comparative neurology*, 310(4):475–506.

Purushothaman, G., Marion, R., Li, K., and Casagrande, V. a. (2012). Gating and control of primary visual cortex by pulvinar. *Nature Neuroscience*, 15(6):905–912.

Radinsky, L. (1975). Primate brain evolution. *American scientist*, 63(6):656–63.

Rezak, M. and Benevento, L. A. (1979). A comparison of the organization of the projections of the dorsal lateral geniculate nucleus, the inferior pulvinar and adjacent lateral pulvinar to primary visual cortex (area 17) in the macaque monkey. *Brain Research*, 167(1):19–40.

Robinson, D. L., Petersen, S. E., and Keys, W. (1986). Saccade-related and visual activities in the pulvinar nuclei of the behaving rhesus monkey. *Experimental Brain Research*, 62(3):625–634.

Rockland, K. S., Andresen, J., Cowie, R. J., and Robinson, D. L. (1999). Single axon analysis of pulvinocortical connections to several visual areas in the macaque. *Journal of Comparative Neurology*, 406(2):221–250.

Romanski, L. M., Giguere, M., Bates, J. F., and Goldman-Rakic, P. S. (1997). Topographic organization of medial pulvinar connections with the prefrontal cortex in the rhesus monkey. *Journal of Comparative Neurology*, 379(June 1996):313–332.

Rubio-Garrido, P., Pérez-De-Manzo, F., Porrero, C., Galazo, M. J., and Clascá, F. (2009). Thalamic input to distal apical dendrites in neocortical layer 1 is massive and highly convergent. *Cerebral Cortex*, 19(10):2380–2395.

Sherman, S. M. and Guillery, R. W. (1998). On the actions that one nerve cell can have on another: distinguishing "drivers" from "modulators". *Proceedings of the National Academy of Sciences of the United States of America*, 95(12):7121–7126.

Tehovnik, E. J., Slocum, W. M., and Schiller, P. H. (2003). Saccadic eye movements evoked by microstimulation of striate cortex. *European Journal of Neuroscience*, 17(4):870–878.

Trojanowski, J. Q. and Jacobson, S. (1974). Medial pulvinar afferents to frontal eye fields in rhesus monkey demonstrated by horseradish peroxidase. *Brain Research*, 80(3):395–411.

Van Essen, D. C. (2005). Corticocortical and thalamocortical information flow in the primate visual system. *Progress in Brain Research*, 149(4):173–185.

West, G. L., Al-Aidroos, N., Susskind, J., and Pratt, J. (2011). Emotion and action: The effect of fear on saccadic performance. *Experimental Brain Research*, 209(1):153–158.

Yeterian, E. H. and Pandya, D. N. (1989). Thalamic connections of the cortex of the superior temporal sulcus in the rhesus monkey. *The Journal of comparative neurology*, 282(November 1986):80–97.

APPENDIX A
ELECTROPHYSIOLOGICAL ATLAS OF GALAGO VISUAL THALAMUS

To accurately map receptive fields, a modified version of Bishop's plotting method was utilized (Bishop et al., 1971). The optic disk and retinal blood vessels are back reflected off the galago's tapetum lucidum with a fiber-optic light source and plotted on a screen 57 cm in front of the eyes of the subject. These retinal landmarks are used to locate the area centralis which subsequently serves as the origin for reported retinotopic coordinates. A simple light stimulus consisting of either a drifting bar or dot was used to map neurons in LGN and visual pulvinar. Horsley-Clarke stereotactic coordinates are reported for each penetration location. All data in this electrophysiological atlas have been included in previously published studies (Moore et al., 2018; Li et al., 2013; Marion et al., 2013).

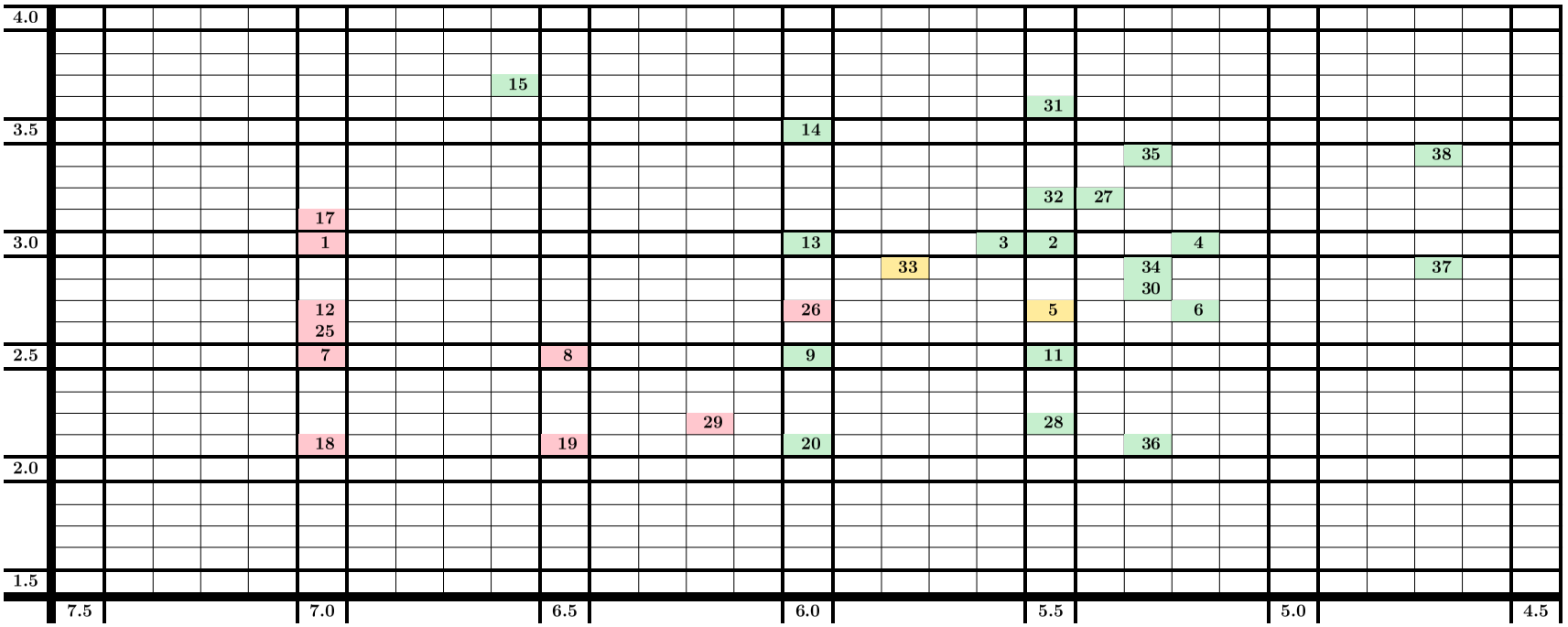

Table A.1: Galago visual thalamus penetration map. The vertical axis represents the rotrocaudal dimension while the horizontal axis runs mediolaterally. Horsley-Clarke stereotactic coordinates are reported for each penetration location. Recording column containing LGN (red), pulvinar (green), or both (yellow).

Table A.2: Retinotopic mapping of galago LGN. Recording site numbers correspond to those in Table A.1. The area centralis is used as the origin for both polar (θ, r) and Cartesian (X,Y) coordiate systems. Horsley-Clarke stereotactic coordinates are reported for each penetration location in mm.

Site	Subject	AP	ML	Depth	θ	r	X	Y	Ocularity
1	1021	3	7	9.3	41.5	11.3	8.46	1.66	contralateral
1	1021	3	7	9.5	31	14.2	12.17	2.99	contralateral
1	1021	3	7	9.8	49.5	11.1	7.21	1.39	ipsilateral
1	1105	3	7	9.6	-2	10.2	10.19	1.81	contralateral
1	1105	3	7	9.8	-7	12.9	12.8	2.86	
1	1105	3	7	10	-5	9.5	9.46	1.56	ipsilateral
1	1105	3	7	10.1	-9.5	11	10.85	2.07	ipsilateral
1	1105	3	7	10.1	-15	12.6	12.17	2.65	ipsilateral
1	1107	3	7	8.8	2.5	59.5	59.44	51.22	
1	1107	3	7	9	-0.5	35.1	35.1	20.18	
1	1107	3	7	9.2	-12	24.5	23.96	9.94	ipsilateral
1	1107	3	7	9.4	10.5	17.5	17.21	5.17	
1	1107	3	7	9.7	24	25.5	23.3	10.03	
1	1107	3	7	10.2	29	12.9	11.28	2.52	
1	1107	3	7	10.2	-125	3	-1.72	-0.09	contralateral
1	1107	3	7	10.3	-51.5	0.7	0.44	0.01	contralateral
7	1105	2.5	7	9.3	12.5	9	8.79	1.37	contralateral
7	1105	2.5	7	10.1	-9	14.9	14.72	3.78	ipsilateral
8	1105	2.5	6.5	7.9	18	32.5	30.91	16.61	contralateral
8	1105	2.5	6.5	8	8	23.8	23.57	9.51	contralateral
8	1105	2.5	6.5	8.6	3.5	17.7	17.67	5.37	
8	1105	2.5	6.5	8.7	31.5	9.3	7.93	1.28	ipsilateral
8	1105	2.5	6.5	9	3	9.6	9.59	1.6	contralateral
8	1105	2.5	6.5	10.3	-177	2.4	-2.4	-0.1	ipsilateral
8	1105	2.5	6.5	10.4	-104	2.8	-0.68	-0.03	ipsilateral
8	1109	2.5	6.5	9.4	157	24.2	-22.28	-9.13	
8	1109	2.5	6.5	9.8	162.5	54.3	-51.79	-42.06	
8	1109	2.5	6.5	10.1	121	1.1	-0.57	-0.01	contralateral
8	1109	2.5	6.5	10.4	160	2.8	-2.63	-0.13	contralateral
8	1109	2.5	6.5	10.6	-79.5	0.7	0.13	0	ipsilateral
12	1107	2.72	7	9.1	142.5	16.8	-13.33	-3.85	contralateral

Site	Subject	AP	ML	Depth	θ	r	X	Y	Ocularity
12	1107	2.72	7	9.3	185.5	9	-8.96	-1.4	
12	1107	2.72	7	9.4	125.5	7.6	-4.41	-0.58	ipsilateral
12	1107	2.72	7	9.5	107.5	8.5	-2.56	-0.38	ipsilateral
12	1107	2.72	7	9.6	137.5	10.2	-7.52	-1.33	
12	1107	2.72	7	9.7	107	14.1	-4.12	-1	ipsilateral
12	1107	2.72	7	9.8	116.5	30.8	-13.74	-7.04	
12	1107	2.72	7	9.9	91.5	3.5	-0.09	-0.01	contralateral
12	1107	2.72	7	9.1	157.5	8.3	-7.67	-1.11	
12	1107	2.72	7	9.2	132	9	-6.02	-0.94	
12	1107	2.72	7	9.3	121.5	12.4	-6.48	-1.39	
12	1107	2.72	7	9.7	127	8.1	-4.87	-0.69	
12	1107	2.72	7	9.9	113.5	14.8	-5.9	-1.51	
12	1107	2.7	7	8.1	31	16.2	13.89	3.87	
12	1107	2.7	7	8.3	27	14.2	12.65	3.1	
12	1107	2.7	7	8.5	29	14.3	12.51	3.09	
12	1107	2.7	7	8.8	31.5	13.5	11.51	2.69	
12	1107	2.7	7	8.9	31	16.2	13.89	3.87	contralateral
12	1107	2.7	7	9.4	47	13.8	9.41	2.24	
12	1107	2.7	7	10	51	16.2	10.19	2.84	
12	1107	2.7	7	9.9	61	15	7.27	1.88	
12	1107	2.7	7	10.1	31	15.7	13.46	3.64	ipsilateral
12	1107	2.7	7	10.3	37	11.6	9.26	1.86	
12	1107	2.7	7	10.5	73	11	3.22	0.61	
12	1109	2.7	7	10.5	45	13	9.19	2.07	contralateral
12	1109	2.7	7	11.1	27.5	15.6	13.84	3.72	ipsilateral
17	1108	3.1	7	7.3	29	48.8	42.68	32.11	
17	1108	3.1	7	9	25	10.1	9.15	1.61	contralateral
17	1108	3.1	7	9.8	-27	11.6	10.34	2.08	contralateral
17	1108	3.1	7	9.9	-29	14.2	12.42	3.05	
17	1108	3.1	7	10.1	-27.5	16.3	14.46	4.06	ipsilateral
18	1108	2.1	7	8	48	20	13.38	4.58	
18	1108	2.1	7	8.1	7	9.6	9.53	1.59	
18	1108	2.1	7	8.2	-34	19.2	15.92	5.23	
18	1108	2.1	7	8.3	85	27.4	2.39	1.1	ipsilateral

Site	Subject	AP	ML	Depth	θ	r	X	Y	Ocularity
18	1108	2.1	7	8.6	85	20.9	1.82	0.65	ipsilateral
18	1108	2.1	7	8.7	71	27.4	8.92	4.11	
18	1108	2.1	7	8.8	82	28.9	4.02	1.94	
18	1108	2.1	7	9.2	-70.5	2.7	0.9	0.04	contralateral
19	1108	2.1	6.5	8.1	85	5.5	0.48	0.05	
19	1108	2.1	6.5	8.5	85	13.2	1.15	0.26	
19	1108	2.1	6.5	8	-81	3.6	0.56	0.04	contralateral
25	1108	2.65	7	7.5	15.5	20.9	20.14	7.18	
25	1108	2.65	7	8.3	30.5	12.6	10.86	2.37	
25	1108	2.65	7	8.7	130	10.1	-6.49	-1.14	
25	1108	2.65	7	8.8	-31	64.6	55.37	50.02	
25	1108	2.65	7	9.1	8	11.5	11.39	2.27	contralateral
25	1108	2.65	7	9.2	-2	12.4	12.39	2.66	
25	1108	2.65	7	9.4	-29.5	9.5	8.27	1.36	ipsilateral
25	1108	2.65	7	9.6	-29.5	12.5	10.88	2.35	ipsilateral
25	1109	2.65	7	9.4	61.5	2	0.95	0.03	contralateral
25	1109	2.65	7	9.8	17.5	4.5	4.29	0.34	ipsilateral
26	1108	2.7	6	8.6	50	32.2	20.7	11.03	
26	1108	2.7	6	8.7	13	51.7	50.37	39.53	
26	1108	2.7	6	8.9	3	34.6	34.55	19.62	
26	1108	2.7	6	9.2	-8	30.2	29.91	15.04	
26	1108	2.7	6	9.7	15	40.2	38.83	25.06	
26	1108	2.7	6	10	59.5	8.7	4.42	0.67	
26	1108	2.7	6	10.2	-65.5	5.7	2.36	0.23	contralateral
26	1108	2.7	6	10.3	-81	5.5	0.86	0.08	contralateral
26	1108	2.7	6	10.4	-93	5.8	-0.3	-0.03	contralateral
26	1108	2.7	6	10.5	-86	6.7	0.47	0.05	contralateral
26	1108	2.7	6	10.9	-83.5	7.5	0.85	0.11	ipsilateral
26	1108	2.7	6	11	-80	8.3	1.44	0.21	ipsilateral
29	1109	2.2	6.24	9.6	4	34.2	34.12	19.18	
29	1109	2.2	6.24	10.3	87.5	8.9	0.39	0.06	contralateral
29	1109	2.2	6.24	10.4	78	9.7	2.02	0.34	ipsilateral
29	1109	2.2	6.24	10.9	72.5	9.8	2.95	0.5	ipsilateral
29	1109	2.2	6.24	11	80.5	8.9	1.47	0.23	contralateral

Table A.3: Retinotopic mapping of galago visual pulvinar. Recording site numbers correspond to those in Table A.1. The area centralis is used as the origin for both polar (θ, r) and Cartesian (X,Y) coordiate systems. Horsley-Clarke stereotactic coordinates are reported for each penetration location in mm.

Site	Subject	AP	ML	Depth	θ	r	X	Y
2	1021	3	5.5	7.5	12.5	42.7	41.69	28.27
2	1021	3	5.5	7.6	-20.5	17.8	16.67	5.1
2	1021	3	5.5	7.8	-32	16.1	13.65	3.79
2	1021	3	5.5	8	-8.5	5	4.95	0.43
2	1021	3	5.5	8.4	-13.5	3.9	3.79	0.26
2	1021	3	5.5	8.6	0	4.8	4.8	0.4
2	1021	3	5.5	9.6	-21	11.7	10.92	2.22
2	1021	3	5.5	9.9	-59	26.9	13.85	6.27
2	1021	3	5.5	10	-59	50.2	25.85	19.86
2	1021	3	5.5	10.2	4.5	39.4	39.28	24.93
2	1105	3	5.5	9.8	-43.5	30.4	22.05	11.16
2	1107	3	5.5	9.2	-96	10	-1.05	-0.18
2	1107	3	5.5	9.3	-76	6.1	1.48	0.16
2	1107	3	5.5	9.8	-86.5	2.3	0.14	0.01
2	1107	3	5.5	10.6	-17.5	15.2	14.5	3.8
2	1107	3	5.5	10.8	-150	14	-12.12	-2.93
3	1021	3	5.75	7.9	37	76.2	60.86	59.1
3	1021	3	5.75	8.3	8	26.8	26.54	11.97
3	1021	3	5.75	8.7	0	11.3	11.3	2.21
3	1021	3	5.75	8.8	-4	12.6	12.57	2.74
3	1021	3	5.75	9	-28.5	7.2	6.33	0.79
3	1021	3	5.75	10	29.5	6.4	5.57	0.62
3	1021	3	5.75	10.3	1.5	7.4	7.4	0.95
3	1021	3	5.75	10.6	-40	17.5	13.41	4.03
3	1021	3	5.75	10.9	-52.5	35.1	21.37	12.29
3	1021	3	5.75	11.1	18.5	40.9	38.79	25.4
4	1021	3	5.2	7.4	49	28.5	18.7	8.92
4	1021	3	5.2	7.8	-30.5	14.1	12.15	2.96
4	1021	3	5.2	7.9	28	6.8	6	0.71
4	1021	3	5.2	8	-28.5	7.2	6.33	0.79
4	1021	3	5.2	8.1	-9	5.4	5.33	0.5

Site	Subject	AP	ML	Depth	θ	r	X	Y
4	1021	3	5.2	8.3	3	5.9	5.89	0.61
4	1021	3	5.2	8.7	1.5	5.2	5.2	0.47
4	1021	3	5.2	9.7	-65.5	12.3	5.1	1.09
4	1021	3	5.2	9.8	-75	25.7	6.65	2.88
4	1021	3	5.2	9.9	-77	32.7	7.36	3.97
6	1021	2.7	5.2	9.6	-12.5	1.3	1.27	0.03
6	1021	2.7	5.2	9.8	-37.5	4.5	3.57	0.28
6	1021	2.7	5.2	9.9	-57	14.4	7.84	1.95
9	1105	2.5	6	7.5	32	80	67.84	66.81
9	1105	2.5	6	7.9	26.5	40	35.8	23.01
9	1105	2.5	6	8.2	1	19.4	19.4	6.44
9	1105	2.5	6	8.3	-9	13.5	13.33	3.11
9	1105	2.5	6	8.8	-22.5	8.5	7.85	1.16
9	1105	2.5	6	9	-3	6	5.99	0.63
9	1105	2.5	6	9.7	-46	3.3	2.29	0.13
9	1105	2.5	6	10	-53.5	7.4	4.4	0.57
9	1105	2.5	6	10.1	-42	21.8	16.2	6.02
9	1107	2.5	6	7.7	-154.5	7.9	-7.13	-0.98
9	1107	2.5	6	8.7	-101.5	3.2	-0.64	-0.04
9	1107	2.5	6	9.1	-37	41.7	33.3	22.15
11	1105	2.5	5.5	10.9	-39	4.5	3.5	0.27
11	1105	2.5	5.5	11.6	-79	21	4.01	1.44
13	1107	3	6	8.4	169.5	7.2	-7.08	-0.89
13	1107	3	6	8.5	184	5.9	-5.89	-0.6
13	1107	3	6	8.6	181	4.7	-4.7	-0.39
13	1107	3	6	8.7	243.5	5	-2.23	-0.19
13	1107	3	6	8.9	228	4	-2.68	-0.19
13	1107	3	6	9.1	168.5	3.6	-3.53	-0.22
13	1107	3	6	9.2	264	2.7	-0.28	-0.01
13	1107	3	6	9.3	204	2.1	-1.92	-0.07
13	1107	3	6	9.5	139.5	6.9	-5.25	-0.63
13	1107	3	6	9.6	177.5	8.2	-8.19	-1.17
13	1107	3	6	9.7	191	13	-12.76	-2.87
13	1107	3	6	9.8	187.5	14.4	-14.28	-3.55

Site	Subject	AP	ML	Depth	θ	r	X	Y
13	1107	3	6	9.9	198	26.6	-25.3	-11.33
13	1107	3	6	10	201	40.1	-37.44	-24.11
13	1107	3	6	8.7	201	10.2	-9.52	-1.69
13	1107	3	6	7.4	31	54.9	47.06	38.5
13	1107	3	6	8	-23.5	28.9	26.5	12.81
13	1107	3	6	8.5	-39.5	11.2	8.64	1.68
13	1107	3	6	8.7	-51.5	8.3	5.17	0.75
13	1107	3	6	8.9	-89	7.7	0.13	0.02
13	1107	3	6	9.1	-101	4.4	-0.84	-0.06
13	1107	3	6	9.5	-54	1	0.59	0.01
13	1107	3	6	9.7	-81	4	0.63	0.04
13	1107	3	6	10.2	-96	3	-0.31	-0.02
13	1107	3	6	10.4	-51.5	8.3	5.17	0.75
13	1107	3	6	10.5	-52	15.6	9.6	2.58
14	1107	3.5	6	9.2	-52.5	24.8	15.1	6.33
14	1107	3.5	6	11	-65	13.5	5.71	1.33
14	1107	3.5	6	11	-65	44.1	18.64	12.97
14	1107	3.5	6	11	-50	59.9	38.5	33.31
14	1107	3.5	6	11.1	-36	72.6	58.73	56.05
15	1107	3.7	6.58	9	16.5	9.8	9.4	1.6
15	1107	3.7	6.58	11	-6.5	17.5	17.39	5.23
15	1107	3.7	6.58	11.3	36	56.5	45.71	38.12
15	1107	3.7	6.58	11.7	-96	4.7	-0.49	-0.04
20	1108	2.1	6	8.1	-9	10.2	10.07	1.78
20	1108	2.1	6	8.1	20.5	51.4	48.14	37.63
20	1108	2.1	6	8.3	5.5	58.6	58.33	49.79
20	1108	2.1	6	8.7	-24.5	18.1	16.47	5.12
20	1108	2.1	6	8.9	-6.5	20.1	19.97	6.86
20	1108	2.1	6	9.1	-2	13.2	13.19	3.01
27	1108	3.2	5.41	7.6	-134	15.5	-10.77	-2.88
27	1108	3.2	5.41	8.1	-58.5	9.9	5.17	0.89
27	1108	3.2	5.41	8.3	10	16.1	15.86	4.4
27	1108	3.2	5.41	8.6	-15.5	20.4	19.66	6.85
27	1108	3.2	5.41	9	-24	43.2	39.47	27.02

Site	Subject	AP	ML	Depth	θ	r	X	Y
27	1108	3.2	5.41	9.1	-35.5	44.9	36.55	25.8
27	1108	3.2	5.41	9.2	-40.5	41.4	31.48	20.82
27	1108	3.2	5.41	9.3	-48.5	35.7	23.66	13.8
27	1108	3.2	5.41	9.4	-39	34.2	26.58	14.94
27	1108	3.2	5.41	9.6	-40.5	29.7	22.58	11.19
27	1108	3.2	5.41	9.8	-36	36.6	29.61	17.65
27	1108	3.2	5.41	9.9	-36	42.1	34.06	22.83
27	1108	3.2	5.41	10	-27.5	53.2	47.19	37.79
28	1109	2.2	5.53	9	3.5	9.2	9.18	1.47
30	1109	2.8	5.3	7.7	-120	27.8	-13.9	-6.48
30	1109	2.8	5.3	7.9	-102.5	18.7	-4.05	-1.3
30	1109	2.8	5.3	8.1	-140	9.6	-7.35	-1.23
30	1109	2.8	5.3	8.5	-107	7.4	-2.16	-0.28
30	1109	2.8	5.3	8.6	-105	11.1	-2.87	-0.55
30	1109	2.8	5.3	8.7	-112	7.5	-2.81	-0.37
30	1109	2.8	5.3	8.8	-97	2.9	-0.35	-0.02
30	1109	2.8	5.3	8.9	-119.5	3.7	-1.82	-0.12
30	1109	2.8	5.3	9	-105	7.2	-1.86	-0.23
30	1109	2.8	5.3	9.2	-98	9.9	-1.38	-0.24
30	1109	2.8	5.3	9.3	-101	14.5	-2.77	-0.69
30	1109	2.8	5.3	9.6	-115.5	23	-9.9	-3.87
30	1109	2.8	5.3	8.7	-98	9	-1.25	-0.2
30	1109	2.8	5.3	8.9	-150	6.5	-5.63	-0.64
30	1109	2.8	5.3	9	180	3.5	-3.5	-0.21
30	1109	2.8	5.3	9.4	-120	15	-7.5	-1.94
30	1109	2.8	5.3	9.7	-111	15.5	-5.55	-1.48
30	1109	2.8	5.3	9.8	-133	38.6	-26.33	-16.42
31	1109	3.6	5.5	8.5	-137	37.7	-27.57	-16.86
31	1109	3.6	5.5	10.9	-104.5	33.3	-8.34	-4.58
32	1109	3.2	5.5	8.2	-92	43.5	-1.52	-1.05
32	1109	3.2	5.5	8.3	-103	34.1	-7.67	-4.3
32	1109	3.2	5.5	8.4	-103	34.1	-7.67	-4.3
32	1109	3.2	5.5	8.6	-115	28	-11.83	-5.56
32	1109	3.2	5.5	8.7	-114	23	-9.35	-3.66

Site	Subject	AP	ML	Depth	θ	r	X	Y
32	1109	3.2	5.5	9	126	35.2	-20.69	-11.93
32	1109	3.2	5.5	8.5	-91.5	45	-1.18	-0.83
32	1109	3.2	5.5	8.7	-101	37.4	-7.14	-4.33
32	1109	3.2	5.5	8.8	-101	30	-5.72	-2.86
32	1109	3.2	5.5	8.9	-111	28	-10.03	-4.71
32	1109	3.2	5.5	9	-115	28	-11.83	-5.56
32	1109	3.2	5.5	9.1	-125	15.3	-8.78	-2.32
34	1109	2.9	5.3	7.7	2	31.5	31.48	16.45
34	1109	2.9	5.3	8.2	-27	14.8	13.19	3.37
34	1109	2.9	5.3	8.4	-24	11.1	10.14	1.95
34	1109	2.9	5.3	8.5	-22	6.4	5.93	0.66
34	1109	2.9	5.3	8.6	20	2.2	2.07	0.08
34	1109	2.9	5.3	9.2	-3	3.7	3.69	0.24
34	1109	2.9	5.3	9.4	-24	11.1	10.14	1.95
34	1109	2.9	5.3	9.7	-16.5	9.7	9.3	1.57
34	1109	2.9	5.3	9.8	-48	20	13.38	4.58
34	1109	2.9	5.3	10.1	-61.5	32.5	15.51	8.33
35	1109	3.4	5.3	7	22.5	67.5	62.36	57.61
35	1109	3.4	5.3	7.2	13	58.4	56.9	48.47
35	1109	3.4	5.3	7.4	6.5	37.3	37.06	22.46
35	1109	3.4	5.3	7.9	-27	30.2	26.91	13.54
35	1109	3.4	5.3	8.1	-36	19.9	16.1	5.48
35	1109	3.4	5.3	8.2	-71.5	11.6	3.68	0.74
35	1109	3.4	5.3	8.4	-25.5	11.2	10.11	1.96
35	1109	3.4	5.3	9	-24	6	5.48	0.57
35	1109	3.4	5.3	9.3	-25.5	10	9.03	1.57
35	1109	3.4	5.3	9.5	-58	15.4	8.16	2.17
35	1109	3.4	5.3	9.8	-55.5	23.5	13.31	5.31
35	1109	3.4	5.3	10.1	-63.5	37.5	16.73	10.19
36	1109	2.1	5.3	7.6	11	32.2	31.61	16.84
36	1109	2.1	5.3	7.8	-30	19.9	17.23	5.87
36	1109	2.1	5.3	8.1	71	12.4	4.04	0.87
36	1109	2.1	5.3	8.4	56.5	5.3	2.93	0.27
36	1109	2.1	5.3	9.1	-22	7	6.49	0.79

Site	Subject	AP	ML	Depth	θ	r	X	Y
36	1109	2.1	5.3	9.3	-42.5	16.3	12.02	3.37
36	1109	2.1	5.3	9.4	-32	32.9	27.9	15.15
36	1109	2.1	5.3	9.5	-34	48.9	40.54	30.55
37	1109	2.9	4.7	7.9	-19	6.7	6.33	0.74
37	1109	2.9	4.7	8	59	6.2	3.19	0.34
37	1109	2.9	4.7	8.1	18	7.5	7.13	0.93
37	1109	2.9	4.7	8.3	-32	11.1	9.41	1.81
37	1109	2.9	4.7	8.6	-38	6.9	5.44	0.65
37	1109	2.9	4.7	9.5	-35	1.5	1.23	0.03
37	1109	2.9	4.7	9.6	-32	4.2	3.56	0.26
37	1109	2.9	4.7	9.8	-42.5	6.1	4.5	0.48
37	1109	2.9	4.7	9.9	-45	8.7	6.15	0.93
37	1109	2.9	4.7	10	-18	17.7	16.83	5.12
37	1109	2.9	4.7	10.1	-11.5	18.3	17.93	5.63
37	1109	2.9	4.7	10.3	-7.5	27.7	27.46	12.77
38	1109	3.4	4.7	7.1	-12	14	13.69	3.31
38	1109	3.4	4.7	7.4	-41.5	20.7	15.5	5.48
38	1109	3.4	4.7	7.5	-60	13.6	6.8	1.6
38	1109	3.4	4.7	7.7	-86	5.8	0.4	0.04
38	1109	3.4	4.7	8.3	-55.5	3.7	2.1	0.14
38	1109	3.4	4.7	8.5	-48	3.4	2.28	0.13
38	1109	3.4	4.7	8.9	-53.5	5.4	3.21	0.3
38	1109	3.4	4.7	9	-78	9.4	1.95	0.32
38	1109	3.4	4.7	9.1	-84.5	12.3	1.18	0.25
38	1109	3.4	4.7	9.5	9.5	12.2	12.03	2.54

Table A.4: Retinotopic mapping of penetration sites with both LGN and pulvinar. Recording site numbers correspond to those in Table A.1. The area centralis is used as the origin for both polar (θ, r) and Cartesian (X,Y) coordiate systems. Horsley-Clarke stereotactic coordinates are reported for each penetration location in mm.

Site	Subject	AP	ML	Depth	θ	r	X	Y	Ocularity
5	1021	2.7	5.5	8.8	-2	12.2	12.19	2.58	
5	1021	2.7	5.5	9.8	29.5	2.6	2.26	0.1	
5	1021	2.7	5.5	10.2	-15.5	5.1	4.91	0.44	
5	1021	2.7	5.5	10.4	-59.5	30.4	15.43	7.81	contralateral
5	1021	2.7	5.5	10.6	-60	47.5	23.75	17.51	contralateral
5	1108	2.7	5.5	8.4	104.5	15.9	-3.98	-1.09	
5	1108	2.7	5.5	8.6	-30	66	57.16	52.22	
5	1108	2.7	5.5	8.7	-43	56.3	41.18	34.26	
5	1108	2.7	5.5	8.8	-41	45	33.96	24.01	
5	1108	2.7	5.5	9	-51	38.5	24.23	15.08	
5	1108	2.7	5.5	9.1	-61.5	28.1	13.41	6.32	
5	1108	2.7	5.5	9.2	-58	24.9	13.19	5.56	
5	1108	2.7	5.5	9.3	-72	21.1	6.52	2.35	
5	1108	2.7	5.5	9.5	-62	19.2	9.01	2.96	contralateral
5	1108	2.7	5.5	9.6	-49.5	20.1	13.05	4.49	
5	1108	2.7	5.5	10.1	-53	19.5	11.74	3.92	
5	1108	2.7	5.5	10.2	-41.5	26.7	20	8.99	
5	1108	2.7	5.5	10.3	-37	32.4	25.88	13.86	
5	1108	2.7	5.5	10.5	-32.5	50.2	42.34	32.53	
5	1109	2.7	5.5	8.3	-10	38.5	37.92	23.6	
5	1109	2.7	5.5	9.6	6	9	8.95	1.4	
5	1109	2.7	5.5	9.7	2.5	11.4	11.39	2.25	
5	1109	2.7	5.5	10.5	-110	1	-0.34	-0.01	contralateral
5	1109	2.7	5.5	10.8	-110	1	-0.34	-0.01	ipsilateral
33	1109	2.9	5.8	7.5	-2.5	57.1	57.05	47.9	contralateral
33	1109	2.9	5.8	7.6	-15	39	37.67	23.71	contralateral
33	1109	2.9	5.8	7.7	-19.5	37.6	35.44	21.63	
33	1109	2.9	5.8	7.8	-31	30.5	26.14	13.27	
33	1109	2.9	5.8	8	-37	26.7	21.32	9.58	
33	1109	2.9	5.8	8.4	-31.5	15	12.79	3.31	

Site	Subject	AP	ML	Depth	θ	r	X	Y	Ocularity
33	1109	2.9	5.8	8.9	-18	10.1	9.61	1.68	
33	1109	2.9	5.8	9.3	-5	6.1	6.08	0.65	
33	1109	2.9	5.8	9.5	-18	10.1	9.61	1.68	
33	1109	2.9	5.8	9.8	-31	14.5	12.43	3.11	
33	1109	2.9	5.8	9.9	-39	20.6	16.01	5.63	
33	1109	2.9	5.8	10	-33.5	34.1	28.44	15.94	
33	1109	2.9	5.8	10.2	-34	60.5	50.16	43.65	

References

Bishop, P. O., Henry, G. H., and Smith, C. J. (1971). Binocular interaction fields of single units in the cat striate cortex. *The Journal of physiology*, 216(1):39–68.

Li, K., Patel, J., Purushothaman, G., Marion, R. T., and Casagrande, V. A. (2013). Retinotopic maps in the pulvinar of bush baby (Otolemur garnettii). *Journal of Comparative Neurology*, 521(15):3432–3450.

Marion, R., Li, K., Purushothaman, G., Jiang, Y., and Casagrande, V. A. (2013). Morphological and neurochemical comparisons between pulvinar and V1 projections to V2. *Journal of Comparative Neurology*, 521(4):813–832.

Moore, B., Li, K., Kaas, J. H., Liao, C.-C., Boal, A. M., Mavity-Hudson, J., and Casagrande, V. (2018). Cortical projections to the two retinotopic maps of primate pulvinar are distinct. *Journal of Comparative Neurology*.